NUREG/CR-5176
UCID-21425

— 1988 —

Seismic Failure and Cask Drop Analyses of the Spent Fuel Pools at Two Representative Nuclear Power Plants

Prepared by P. G. Prassinos, C. Y. Kimura, D. B. McCallen, R. C. Murray/LLNL
M. K. Ravindra, R. D. Campbell, P. S. Hashimoto, A. M. Nafday, W. H. Tong/EQE

Lawrence Livermore National Laboratory

EQE Engineering, Inc.

Prepared for
U.S. Nuclear Regulatory Commission

NUREG/CR-5176
UCID-21425
R4, 9H

Seismic Failure and Cask Drop Analyses of the Spent Fuel Pools at Two Representative Nuclear Power Plants

Manuscript Completed: June 1988
Date Published: January 1989

Prepared by
P. G. Prassinos, C. Y. Kimura, D. B. McCallen, R. C. Murray, Lawrence Livermore National Laboratory
M. K. Ravindra, R. D. Campbell, P. S. Hashimoto, A. M. Nafday, W. H. Tong, EQE Engineering, Inc.

Lawrence Livermore National Laboratory
7000 East Avenue
Livermore, CA 94550

Subcontractor:
EQE Engineering, Inc.
3150 Bristol, Suite 350
Costa Mesa, CA 92626

Prepared for
Division of Safety Issue Resolution
Office of Nuclear Regulatory Research
U.S. Nuclear Regulatory Commission
Washington, DC 20555
NRC FIN A0814

ABSTRACT

This report discusses work done in support of the resolution of Generic Issue-82, "Beyond Design Basis Accidents in Spent Fuel Pools". Specifically the probability of spent fuel pool failure due to earthquakes was determined for the pools at the Vermont Yankee Nuclear Power Station (BWR) and the H. B. Robinson S.E. Plant, Unit 2 (PWR). The dominant failure mode for each pool was gross structural failure caused by seismic motion resulting in the loss of pool liner integrity. The resulting sudden loss of water was then assumed to lead to a self-propagating cladding failure and fission product inventory release from the spent fuel elements in the pool. The mean annual frequency of failure due to this failure mode was found to be 6.7E-06 at Vermont Yankee and 1.8E-06 at H. B. Robinson. Other earthquake induced failure modes studied but found to be less important were loss of pool cooling and make-up capability, fuel rack damage and loss of liner integrity due to a cask drop accident.

TABLE OF CONTENTS

LIST OF TABLES

LIST OF FIGURES

ACKNOWLEDGEMENT

This project was performed in cooperation with the U.S. Nuclear Regulatory Commission. We greatly appreciate the support and guidance by Ed Throm, Office of Nuclear Regulatory Research, Division of Reactor and Plant Systems. This assistance was essential to the completion of this project.

We wish to thank the utility participants for their cooperation in providing information on their plants.

EXECUTIVE SUMMARY

Previous work [Sailor, et al., January 1987] in support of the resolution of Generic Issue-82, "Beyond Design Basis Accidents in Spent Fuel Pools", indicated that the risk due to seismic induced failure of nuclear power plant spent fuel pools (SFP) may be significant and dominates the total risk resulting from SFP failure. This result was based on use of generic seismic hazard and fragility data and resulted in calculated risk numbers with wide uncertainty ranges. To test the result, Lawrence Livermore National Laboratory was asked to determine seismically induced spent fuel pool failure probabilities for two specific plants, the Vermont Yankee Nuclear Power Station, a boiling water reactor, and the H. B. Robinson S.E. Plant, Unit 2, a pressurized water reactor. Plant specific seismic hazard and fragility information was used for each site. The results of this work is presented in the report which follows.

The major concern about accidents in SFP's is the loss of water inventory and its capability to cool the radioactive fuel. Without sufficient water, some theoretical models suggest that the fuel's zircaloy cladding may initiate and sustain rapid oxidation (fire) that can spread to adjacent fuel assemblies (self-propagating) with the potential of releasing significant amounts of long-lived radioactive isotopes. Although these isotopes may not present a significant acute health hazard, their release could cause contamination of surrounding property comparable or larger than would occur from a reactor core melt accident.

The failure modes considered in this study were: (1) loss of liner integrity precipitated by gross structural failure of the SFP, (2) loss of function of the fuel pool support system (pool cooling and make-up) resulting in loss of water inventory, (3) damage to fuel racks, and (4) loss of liner integrity due to a cask drop accident. The first failure mode turned out to be the dominant contributor to risk. The second failure mode, loss of pool cooling and make-up capability, was discounted since 3 to 7 days would be available to find alternate water sources before fuel damage could occur. The third failure mode was discounted after analysis showed that crushing of the fuel in the fuel racks could not result in a criticality accident. The fourth failure mode was discounted because the probability of a cask drop is believed low (<1.0E-08/RY) as reported in the Sailor study. If this is not the case, the cask drop accidents would be important since a dropped cask probably would result in loss of liner integrity.

The first failure mode, gross structural failure of the pool, was analyzed by first identifying the potential locations and issues for gross failure. In the Vermont Yankee pool the out-of-plane shear failure of the pool slab controlled. In the H. B. Robinson pool the out-of-plane bending of the pool was wall controlled. It was found that the median acceleration capacity was 1.4g and 2.0g at each pool respectively. The High Confidence of Low Probability of Failure capacity (5% chance of failure with 95% confidence) was 0.50g and 0.65g respectively. Since the Safe Shutdown Earthquake at each plant is 0.14g and 0.20g respectively, it can be seen that there is a large safety margin inherent in each pool design. The mean annual frequency of failure was calculated as 6.7E-06 for Vermont Yankee and 1.8E-06 for H. B. Robinson. This compares with values of 2.2E-05 for a BWR and 1.6-05 for a PWR found in the Sailor study.

1. INTRODUCTION

Increasing amounts of spent fuel are being stored at nuclear power plants rather than being shipped to reprocessing facilities or disposal repositories. This increasing amount of on-site spent fuel storage has resulted in much larger inventories in spent fuel storage pools than previously anticipated. While the radioactive material inventory of the spent fuel will be less than an active core, there is a potential for accidents in spent fuel pools involving the equivalent of several cores of spent fuel bundles.

The major concern is for the spent fuel pool to lose its water inventory and thus its capability to cool the spent fuel inventory. Without sufficient water inventory, a theoretical model suggested that the zircaloy cladding material of recently discharged spent fuel rods can initiate and sustain a rapid oxidation (fire) that can spread to adjacent fuel assemblies with the potential of releasing significant amounts of long-lived radioactive isotopes.

The overall objective of this report is to present the results of probabilistic analyses of the seismic failure of two specific spent fuel pools. The spent fuel pools considered are at the Vermont Yankee Nuclear Power Station, a General Electric Boiling Water Reactor (BWR) located near Vernon, Vermont, and the H. B. Robinson S. E. Plant, Unit 2, a Westinghouse Pressurized Water Reactor (PWR), located in Hartsville, South Carolina.

1.1 Background

An analysis of the risk associated with spent fuel storage was performed in the Reactor Safety Study (RSS) [USNRC, 1975]. This analysis indicated that the risk associated with spent fuel pool accidents was small compared to the risk from accidents involving the reactor core with failure probabilities in the range of 10^{-6} (denoted E-6) per reactor-year. The RSS analysis included external initiating events and heavy load drops. Release estimates were based on accidents involving one-third of a core of spent fuel. The overall conclusion in the RSS was that loss of the spent fuel pool water inventory, and radioactivity release was unlikely based on design and operational features.

Subsequently, because of the increased storage of spent fuel at nuclear power plants and the possibility of zircaloy fire ignition and propagation, the NRC sponsored a study of Generic Safety Issue 82, "Beyond Design Basis Accidents in Spent Fuel Pools" [Sailor, et al., January 1987]. This study revisited the RSS analysis to see if there was a possibility for new events or more severe consequences. The study involved a probabilistic analysis of the risk associated with spent fuel pool failures initiated by random system failures, seismic events and the dropping of heavy loads, primarily a spent fuel shipping cask, on the pool wall. The analysis considered initiating event frequencies, spent fuel pool systems response, accident phenomenology such as cladding fires, and consequences such as radioactivity release, transport, deposition and health effects.

The accident initiating events that were considered in the BNL study included:

- pool heat-up due to loss of cooling water inventory and circulation capability,
- structural failure of the pool due to seismic events or missiles,
- partial drain down of the pool due to pneumatic seal failure, and
- structural failure of the pool due to heavy load drop.

Data and information from several plant sites including Ginna, Millstone 1, Zion and Oyster Creek were used in the spent fuel pool analyses. These plants were chosen specifically for their perceived vulnerability, being designed to less restrictive requirements than presently employed, in particular to seismic events.

Estimates of spent fuel pool cooling system failure by BNL were derived from previous probabilistic analyses for "trained" (parallel) systems, and included component failures, and unavailabilities. Consideration was also given for the capability of several alternative systems to supply makeup water to the pool. The frequency for failure of fuel pool cooling leading to uncovering the spent fuel and to radioactivity release was estimated to be about E-6 per reactor-year for both PWRs and BWRs.

The BNL analysis of the spent fuel pool structural failure utilized the seismic hazard representation for the Millstone site taken from the EUS Seismic Hazard Characterization Study [Bernrueter, et al., 1985, 1987]. Since no published seismic hazard study existed for the Ginna site, the Millstone seismic hazard curves were scaled by the Ginna SSE peak ground acceleration at 200, 1,000, and 4,000 year return periods. The analysis for Millstone also used seismic hazard curves at the same return periods. For the Millstone analysis, four hazard curves (best estimate, median, 15% and 85% confidence curves) were used. For the Ginna analysis, only one hazard curve was used.

In the BNL study [Sailor, January 1987], the seismic fragility of pool structures was assigned by comparing with published PRAs. Since Millstone 1 is a BWR, the seismic fragility developed for the Oyster Creek reactor building was judged appropriate for the Millstone 1 spent fuel pool. For the Ginna spent fuel pool, the fragility of the Zion plant auxiliary building shear walls was used.

Use of these representative fragilities and the assigned hazard curves, resulted in a large range of values for seismically induced spent fuel pool structural failure. For a PWR plant, the annual frequency of seismically induced gross structural failure was given as 1.6E-11 to 2.6E-4 per reactor year. For a BWR plant, this range was given as 4.5E-11 to 6.5E-4 per reactor year. The mean frequency was estimated by BNL to be 2.2 E-5 per reactor year for a BWR and 1.6 E-5 per reactor year for a PWR.

The structural failure of the spent fuel pool due to dropping of a spent fuel transfer cask has been considered by the NRC as an Unresolved Safety Issue - TAP A-36, "Control of Heavy Loads at Nuclear Power Plants". The NRC has concluded in Generic Letter 85-11, that all licensees meet A-36 criteria "such that the risk associated with potential heavy load drops is acceptably small", with consideration for:

- o single failure cranes,
- o appropriate handling procedures and training, and
- o analysis of heavy load structural and mechanical capacities.

The BNL study also considered spent fuel pool structural failure due to dropping of a spent fuel shipping cask. This analysis considered the anticipated frequency of spent fuel shipment when a repository becomes available, the time the cask would be over the pool wall, crane failure, and human error in properly rigging, lifting and moving the spent fuel shipping cask. In addition, it was assumed that the conditional probability of structure failure of the spent fuel pool wall given a cask drop has a value of 0.1 with an uncertainty range of 0.01 to 1. The results of this analysis indicates that failure of the spent fuel pool due to cask drop accidents has a range of 3.E-12 to 3.E-5 per reactor year.

It was concluded from the BNL study that the dominant contributors to risk are structural failures resulting from beyond design basis seismic events and from heavy load drops. Large uncertainties were associated with both these events. The uncertainty in the seismic failure of the pool resulted from uncertainties in the seismic hazard curves and spent fuel pool fragilities, and the use of generic information and data. The uncertainty in pool failure from heavy load drops resulted from uncertainties in human error rates and the conditional probability of pool structural failure from shipping cask impact.

The estimate of the overall risk due to beyond design basis accidents in spent fuel pools for seismic events at the PWR surrogate plant ranges from 600 person-rem/Ry to a negligible value with an estimated mean value of about 50 person-rem/Ry in the BNL study. The estimates for the BWR surrogate plant were about a factor of three less. The overall risk due to a heavy load drop event was estimated to range from 70 person-rem/Ry to a negligible value for the PWR surrogate plant and also a factor of about three less for the BWR surrogate plant. The unique character of spent fuel pool accidents (potentially large release of long-lived isotopes) makes it difficult to compare directly to reactor core melt accidents. There are no early health effects associated with spent fuel pool accidents. Land interdiction area is postulated to be larger for spent fuel pool accidents, as compared to reactor core melt accidents.

The large uncertainties and the use of generic information and data (seismic hazards, fragilities and systems descriptions) in the previous analyses has

provided the impetus for performing this present study of specific spent fuel pools. This study, while providing results for specific plants, is being performed to gain insight into representative values for the probability of spent fuel pool failure.

1.2 Objective of this Study

The purpose of this effort is to provide technical assistance to the NRC concerning Generic Issue-82, "Beyond Design Basis Accidents in Spent Fuel Pools". The overall objective is to estimate the realistic seismic capacity of spent fuel pool structures and systems, and to assess the seismic contribution to risk from accidents in spent fuel pools. This objective is accomplished by using plant specific analyses of actual spent fuel pools and site specific hazard analyses. This effort includes:

1. Establish an appropriate definition of spent fuel pool failure.
2. Evaluate the seismic capacity of a typical BWR and PWR spent fuel pool, and determine their seismic fragility and failure probability.
3. Evaluate the effect of dropping a spent fuel shipping cask on the pool wall.

1.3 Report Organization

The remainder of this report is organized into six chapters. Chapter 2 present a discussion of the methodology utilized in the spent fuel pool analysis followed by the fragility analysis of the spent fuel pool structure and equipment presented in Chapter 3. The systems analysis of the spent fuel pool cooling and make-up water systems is provided in Chapter 4, and Chapter 5 presents the equipment fragilities. The result of probabilistic evaluation are presented in Chapter 6. Chapter 7 presents the analysis of the cask drop, and the summary and conclusions are presented in Chapter 8.

2. SEISMIC RISK ANALYSIS METHODOLOGY

2.1 Introduction

Seismic risk analysis methodology for reactor core damage accidents has now been well established, with its application to over 25 nuclear power plants and standardized by NUREG/CR-2300 [USNRC, 1983]. The objectives of such an overall probabilistic risk assessment are to estimate the frequencies of occurrence of severe core damage, serious radiological releases, and consequences in terms of early fatalities, long term adverse health effects and property damage, and to identify significant contributors to plant risks. The key elements of such an analysis are:

1. Seismic hazard analysis - estimation of the frequency of various levels of seismic ground motion (acceleration) occurring at the site.

2. Seismic fragility evaluation - estimation of the conditional probabilities of structural or equipment failure for given levels of ground acceleration.

3. Systems/accident sequence analysis - modeling of the various combinations of structural and equipment failures that could initiate and propagate a seismic core damage accident sequence.

4. Evaluation of core damage frequency and public risk - assembly of the results of the seismic hazard, fragility, and systems analyses to estimate the frequencies of core damage and plant damage states. Assessment of the impact of seismic events on the containment and consequence analyses, and integration of these results with the core damage analysis to obtain estimates of seismic risk in terms of effects on public health.

This methodological sequence is modified by the use of a screening approach based on component capacity to address the specific issue at hand, which is estimating the failure frequency of spent fuel pools initiated by earthquake events. It is described in the subsequent sections.

2.2 Seismic Hazard Analysis

Seismic hazard is usually expressed in terms of the frequency distribution of the peak value of a ground-motion parameter (e.g., peak ground acceleration) during a specified time interval. The different steps of this analysis are as follows:

1. Identification of the sources of earthquakes, such as faults and seismotectonic provinces.

2. Evaluation of the earthquake history of the region to assess the frequencies of occurrence of earthquakes of different magnitudes or epicentral intensities.

3. Development of attenuation relationships to estimate the intensity of earthquake-induced ground motion (e.g., peak ground acceleration) at the site.

4. Integration of the above information to estimate the frequency of exceedance for selected ground motion parameters.

The hazard estimate depends on uncertain estimates of attenuation, upperbound magnitudes, and the geometry of the postulated sources. Such uncertainties are included in the hazard analysis by assigning probabilities to alternative hypotheses about these parameters. A probability distribution for the frequency of occurrence is thereby developed. The annual frequencies for exceeding specified values of the ground motion parameter are displayed as a family of curves with different probabilities. Sample hazard curves are shown in Figure 2-1.

2.3 Seismic Fragility Evaluation

Seismic fragility evaluation has been described in the PRA Procedures Guide [USNRC, 1983] and by [Kennedy and Ravindra, 1984]. The seismic fragility of a spent fuel pool is the conditional probability of its failure for a given peak ground acceleration. In the seismic probabilistic risk assessment studies, the seismic fragility is expressed in terms of the peak ground acceleration capacity. Typically, seismic fragility is characterized by means of a family of curves, each curve showing the conditional probability of failure as a function of the peak ground acceleration. The family of curves is necessary to represent the uncertainties in the failure modes and model parameters. Usually a subjective probability or weight is assigned to each curve to reflect the degree of belief associated with each hypothesis (i.e., a set of model parameters).

In the seismic PRAs, the entire family of fragility curves for a structure or equipment is developed by means of a simple fragility model wherein the capacity is represented by means of three fragility parameters: median acceleration capacity, A_m, and the logarithmic standard deviations β_R and β_U representing, respectively, the random variability and the uncertainty in median capacity. These parameters are estimated using the margins and variabilities existing in the nuclear power plant seismic design and qualification procedures. Figure 2-2 shows the seismic fragility curves for a structure where the middle one is the median fragility curve and the outer two show the fragility at 95% and 5% confidence.

A useful indicator of the seismic capacity presently being used in seismic margin studies is the High Confidence Low Probability of Failure (HCLPF) capacity of the structure which is defined as the acceleration value at which we can state with 95% confidence that the conditional probability of failure will not exceed 5%. The example in Figure 2-2 shows the median capacity of the structure as 0.90g, the HCLPF capacity as 0.30g and the safe shutdown earthquake as 0.17g. Therefore, the HCLPF capacity may be taken as the maximum

ground level motion that the structure could survive with a high degree of confidence.

The starting point in estimating the fragility of a spent fuel pool structure is to define what is considered to be failures and to identify the critical failure modes. Guidance on the relevant failure modes is obtained by USNRC and ANS standards [USNRC 1981; ANS 1976], although the failure of the structures and equipment beyond the design basis earthquake is of concern here. For each failure mode, the fragility or equivalently the ground acceleration capacity is estimated. The structure is modeled to fail if any one of the failure modes occur and the fragility of the structure is obtained as the conditional probability of occurrence of the union of these failure modes. The failure modes of the spent fuel pool are discussed later in this report.

For each failure mode, the ground acceleration capacity is expressed as the product of the SSE acceleration times an overall factor of safety. The overall factor of safety is further modeled as a product of the factors reflecting the conservatisms and uncertainties in different variables such as spectral shape, damping, mode combination, earthquake component combination, material strength and ductility. Each factor is represented by its median value, A_m, β_R and β_U. Using the lognormal model, the parameters of the overall factor and of the ground acceleration capacity are calculated knowing the parameters of the individual factors. The HCLPF capacity is expressed as

$$\text{HCLPF Capacity} = A_m \exp\left[-1.64\ (\beta_R + \beta_U)\right]$$

This fragility model and development of fragility parameters have been utilized in over 25 seismic PRAs. For further details, the reader is referred to [Kennedy and Ravindra 1984] and [Ravindra et. al 1987].

2.3.1 Failure Criteria for Spent Fuel Pools

Before the seismic fragility of a structure or equipment is estimated, the potential failure criteria need to be established.

There are several different spent fuel pool designs and fuel rack designs. The fuel rack designs depend on the vintage, fabricator and pool configuration.

In analyzing the failure of the spent fuel pool structures and systems, we considered the following:

- Loss of liner integrity precipitated by structural failure of the spent fuel pool
- Loss of function of the fuel pool support systems (e.g., pool cooling and make-up water capacity) resulting in loss of water inventory through boil-off or drainage

- o Damage to fuel racks caused by fuel rack motion.

The loss of spent fuel pool water inventory either through a structural failure or a failure in the support systems can result in degradation to stored spent fuel and possibly zircaloy cladding fires. For the purpose of this analysis, spent fuel pool failure and its probability of occurrence (risk) is considered when;

- o Spent fuel is uncovered long enough for a self-sustaining zircaloy cladding oxidation initiation (~1650 deg. F), or

- o Spent fuel is uncovered long enough for the zircaloy cladding to be damaged (breached) and releases some or all of its gaseous and volatile fission inventory. Sufficient fission products are released to exceed 10 CFR 20 guidelines at the site exclusion zone boundary.

In the following sections we describe the different structures and equipment comprising these systems and discuss the more credible failure modes under earthquakes.

2.3.1.1 Spent Fuel Pool Structures

2.3.1.1.1 BWR Mark I & Mark II Plant Fuel Storage Pool

In BWR Mark I and Mark II containment system, the spent fuel storage pool is located at the operating floor level (100'-150' above grade). The fuel storage pool is typically ~80' long x 40' wide x 44' deep. The thickness of the pool floor and walls is on the order of 4'-6'. The horizontal and vertical loads from the pool floor are transmitted to the two longitudinal walls which are designed as deep girders supported at the peripheral wall of the reactor building. The pool floor and walls are designed for dead and live loads, hydrostatic pressure loads, seismic loads, hydrodynamic loads, thermal loads and loads resulting from accidental drop of casks or heavy objects.

The critical locations for the design of the pool floor are at the mid span of the floor for bending moments and at the intersection of pool floor and wall for negative bending moment and shear loads. The critical locations for the design of the pool walls are the intersection of pool walls, intersection of the pool wall and floor and mid span of the walls.
Typical loads for the design of the fuel storage pool are:

Pool Floor = 9 kips/sq. ft.
Pool Walls = 100 kips/ft.

Failure mechanisms that need to be considered are given below:

1. The failure mode for the pool floor is that of a slab fixed at four edges. Figure 2-3 shows the yield lines for the floor. Figure 2-4 shows the yield lines for the out of plane failure of the pool wall. The girders supporting the pool are in reality long walls

acting as deep girders and are supported by the peripheral walls of the reactor building.

2. Compressive and shear stresses at the reaction points of the girders (onto the reactor building walls) for transmitting vertical and horizontal seismic loads from the fuel storage pool to the foundation should be investigated for structural adequacy.

3. Due to large concentrated loads (50 kips to 70 kips) at each foot of the storage rack, bearing and punching shear stress in the pool floor should also be investigated.

4. For laterally braced high density fuel storage racks, large concentrated loads are transmitted to the pool wall at either the base level or at the base and the upper seismic bracing level. The effect of concentrated load should be investigated.

Although the thermal loads are important in the design of the fuel pools, their influence on the fragility of the pool is judged not significant because the thermal loads are self-relieving.

2.3.1.1.2 PWR and BWR Mark III Fuel Storage Pools

The fuel storage pools for the PWR and BWR Mark III plants are located typically at the ground level. Due to lower elevation, the seismic response is relatively low. The vertical and horizontal loads from the pool floor are transmitted to the ground for the case of free standing or floor mounted fuel storage racks. For the case of laterally braced racks, the horizontal seismic loads from the fuel storage racks are transmitted to the pool wall at either the base level or at the base and the upper seismic bracing level.

Failure modes for the pool floor are:

1. Punching shear stress due to concentrated loads at the foot of the storage racks.

2. Foundation settlements for soil; soil settlement may only be an issue for piping relative displacements.

Failure modes for the walls are similar to that described for Mark I and Mark II BWR's.

2.3.1.1.3 Failure Modes of Liner Plate

The fuel storage pool floor and walls are lined with 1/8" to 1/4" thick stainless steel leak tight liner plate. The liner plates are welded to each other by seam welds. Under the seam welds, leak detection (control) channels are provided. Possible failure modes for the liner plates are:

1. Tearing of the liner plate or seam welds at the leak channels due to

vertical/horizontal loads from fuel storage racks; this is of concern only if the rack slides and the foot bears on leak channels.

2. Tearing of the liner plate due to sliding of the rack over any local floor depression or wrinkles in the liner plate.

3. For a laterally braced rack, puncturing of the liner plate at the knuckle in the vicinity of pool floor/walls intersection.

2.3.1.2 Fuel Racks

2.3.1.2.1 Types of Racks:

1. Low Density Racks (Cell Pitches 20" to 30") Subcritical configuration is achieved by the physical separation of fuel assemblies in an open-frame aluminum or steel structure. Structurally the racks can be laterally braced at the upper and lower levels or they could be bolted to the floor at four corners with upper and lower grids connected by cross bracing.

2. Medium Density Racks (Cell Pitches 9" (BWR) to 13" (PWR)) Subcritical configuration is achieved by the flux trap principle. The fuel assemblies are surrounded by stainless steel cans or cells which prevent the neutrons in the water region between the cells from returning to the fuel assemblies. The typical cell wall thickness is 1/8". Structurally the racks can be laterally braced at the upper and lower grid levels, bolted to the pool floor at four corners with upper and lower grids connected by cross-bracing, or they can be cantilever cells (2 x 2 or 4 x 4 modules to reduce flexibility) welded to a base structure.

3. High Density Fuel Racks (Cell Pitches 6" (BWR) 9" (PWR)) Subcriticality is achieved by addition of neutron absorbing poison material between fuel assemblies. Poison is in the form of boron containing material such as boron-carbide, borated stainless steel, or borated aluminum. Storage cell walls have poison containing pockets. Structurally the racks are mostly free standing or laterally braced at the lower level. The honeycomb construction provides structural integrity. The cell walls are typically 0.09" in thickness. The cells are attached to each other by fusion or spot welds.

4. Consolidated Fuel Racks - The fuel assembly is disassembled and stored in a fuel canister. The canister is then stored in high density storage racks. The consolidated ratio can be 2 to 1.

2.3.1.2.2 Failure Modes of Free Standing High Density Fuel Storage Racks

There are various types of fuel rack designs depending on the time (vintage), fabricator and pool configuration. The design analysis of the fuel storage

racks is a complex task. There are non-linearities associated with gaps between the fuel and cell wall, and friction at the base of rack. With a low coefficient of friction, the racks could slide on the pool floor. With a high coefficient of friction, the rack could lift up and fall back during a seismic event. Due to the presence of water there is hydrodynamic coupling between the fuel and racks, between adjacent fuel racks and between fuel racks and pool walls [Habedank, et al., 1979; Dong, 1978].

The design analysis of the fuel storage racks is based on the requirements of Appendix D to Standard Review Plan 3.8.4. The load combination and acceptance criteria of SRP 3.8.4 Appendix D are based on subsection NF of ASME Code Section III. Most of the high density fuel storage racks are of cold-form construction. The design analysis procedure and acceptance criteria of cold-form construction should be based on the AISI Cold Form Stainless Steel code which is much more conservative (lower allowable stress limits and severe weld spacing requirements) than the subsection NF of ASME Code Section III. Such differences in the code criteria are taken into account in the fragility analysis.

Due to multiplicity of storage rack designs, and fabricator/vendor(s), the uncertainties in the design/analysis procedures and fabrication methods are fairly large.

2.3.1.2.2.1 Free Standing/sliding Rack

A typical high density fuel storage rack consists of a welded assembly of individual storage cells in a staggered checkerboard array. The storage cells are comprised of double wall Type 304L stainless steel boxes welded to each other with corner angles to maintain the desired pitch (6" for BWR & 8" for PWR). Poison sheets in the form of boron containing materials such as borated stainless steel, or boron carbide are placed between the pockets formed by cell wall (0.08" to 0.1" thick) and poison retainer sheet (0.05") (See Figures 2-5 and 2-6). The unitized (honeycombed) construction of the racks provides the structural strength to withstand vertical dead and live loads as well as seismic loads.

The bottom of the storage cells sits on and is welded to the rack base plate or base support structure. The base plate provides level support for each fuel assembly and contains a cooling flow orifice for each cell. Each rack module typically consists of a 15 x 18 array of fuel storage locations for a BWR rack or a 10 x 10 array of storage locations for a PWR rack (Figures 2-7 and 2-8). These rack modules are supported by adjustable swivel feet. Each support foot contains a remotely adjustable jack screw to permit the rack to be leveled following wet installation. The support pad (feet) raise the rack above the pool floor to the height required to provide an adequately sized cooling water supply plenum.

The storage racks are positioned on the pool floor so that adequate clearances are provided between racks and between pool structures to avoid impacting of the racks during a design basis seismic event. The vertical dead weight and

seismic loads are transmitted directly to the pool floor by the support feet. The only horizontal seismic loads transmitted from the rack structure to the pool floor are those associated with friction between the rack structure and the pool liner. The high density, free standing/sliding fuel storage racks are popular with the utilities because they offer substantial increase in storage capacity and they can be easily installed in an existing contaminated wet pool.

2.3.1.2.2.2 Failure Modes of Free Standing/Sliding Racks

There are various types of design for free standing/sliding racks depending upon the vendor (fabricator) and the time they were fabricated. The critically stressed regions are the foot, storage cell wall in the vicinity of the foot and the spot welds (fusion weld) with which the honeycomb structure was built. Failure modes will vary depending upon the design feature of the racks. The most likely failure mode however, will be the fallback impact load in a seismic event. The storage cell wall above the foot weldment will buckle and the fusion spot welds will open up resulting in the failure of the rack.

2.3.1.2.2.3 Laterally Braced High Density Fuel Racks

In the laterally braced storage racks, the storage racks are placed next to each other without any gap between them. Seismic bracing is provided around the periphery of the storage racks arrangement to transmit horizontal seismic load to the storage pool walls. The seismic lateral bracing are provided at the lower base level and sometimes at the lower base level and upper grid level of the storage rack (See Figures 2-9 and 2-10). The vertical dead weight and vertical seismic load are transmitted by the individual racks to the pool floor through the support foot. The horizontal seismic load is transmitted from the storage racks to the peripheral seismic bracing and then to the fuel pool walls. In order to account for variable distance between the peripheral racks and the fuel pool walls, seismic bracing with rack screws at their end are provided for easy field adjustment. The seismic bracings around the periphery are very heavily loaded. Therefore, the most likely failure mode for the laterally braced racks is the compression buckling failure of the periphery seismic bracing. Once the bracing fails, the storage rack will become the free standing/sliding type. As the load paths and design of a free standing rack configuration is quite different from that of a laterally braced design, the laterally braced racks without seismic bracing could fail. The failure mode for the storage rack will be same as that of freestanding fuel racks. Due to fallback impact load in a seismic event, the foot weldment may break or the storage cell wall above the foot weldment will buckle and the spot weld (fusion weld) between storage cells will open up, resulting in failure of the storage racks.

2.3.1.2.3 Consequence of Rack Failure

Various failure modes for different rack systems were described above. The exact nature of the damage to the pool system by seismically induced failure of racks has to be assessed by the nuclear systems engineers. The rack

failure under examination is not expected to lead to a sudden drainage of the pool. The loadings introduced by different rack systems during a seismic event will be considered in the structural failure mode evaluation of the pool.

2.3.1.3 Pool Support Systems

Equipment failures in the systems that provide the spent fuel pool cooling and make-up water functions could also result in the loss of pool water inventory through leakage and water boil-off. The components in these systems such as the piping, valves, pumps, heat exchangers, tanks, and electrical distribution systems are reviewed and the impact of their seismic failures on the spent fuel pool behavior is examined. Seismic fragilities of these components are developed using the failure modes and procedures described in the PRA Procedures Guide [USNRC, 1983] and [Ravindra et al., 1987]. The HCLPF capacities of components and systems are derived using the seismic fragilities of components and the Boolean expressions for the system failures. This analysis is very specific to the particular spent fuel pool configuration. For the two representative pools analyzed, the support systems are reviewed and the seismic fragilities and HCLPF capacities estimated.

To determine the component included in the systems analysis, a screening approach was utilized based on seismic capacity. This approach was developed under the NRC Seismic Design Margins Program [Budnitz, et al., 1985, and Prassinos et al., 1985] and uses an extensive table of generic seismic HCLPF capacities for various components. Based on results of the Seismic Design Margins Program HCLPF capacity of 0.3g was used as the screening value for this analysis. It is judged that the components with HCLPF capacities larger than 0.3g pga have no significant contribution to the failure of spent fuel pools.

The systems that provide and support the cooling and make-up water functions for the spent fuel pools examined were reviewed and inspected by performing a plant walkdown. Those components within these system that were not found to have any characteristics that would reduce their seismic capacity, and were adequately supported and anchored such that their HCLPF capacity was larger than 0.3g were screened out from further consideration. Components with HCLPF capacity less than the screening value remained in the analysis.

2.4 Analysis of Systems and Accident Sequences

The analysis of systems behavior is performed by combining plant logic models with component fragilities and seismic hazard estimates. Event and fault trees are constructed to identify the accident sequences and systems failures that may lead to loss of water inventory in the pool and possible spent fuel degradation.

Plant systems and sequence analyses used in seismic PRAs are based on the PRA Procedures Guide [USNRC, 1983]. The analysis used in this study follows the screening approach given in [Budnitz, et al., 1985] and is summarized as follows:

1. Event trees were constructed reflecting the sequence of systems successes and failures that will lead to loss of spent fuel pool water inventory.

2. Fault trees were constructed reflecting the combination of component failures that could lead to the systems failure identified in the event tree sequences. Only those component that were not screened out of the analysis based on capacity were used in the fault trees construction. Care was taken to include, however, all the failure paths that could lead to system failure.

3. The Boolean expressions for the systems failures derived from the fault trees were then substituted into the accident sequences developed from the event trees to obtain a Boolean expression for each accident sequence. The logical summation of all the accident sequences resulted in an overall Boolean expression that described the loss of water inventory from the spent fuel pool. The first, second and third order cut sets of this Boolean expression were obtained for further analysis.

4. The fragility of each component identified in the cut sets was then estimated and those cut sets that had a component whose HCLPF capacity was greater than the screening value (0.3g) were then eliminated from further consideration.

5. The overall fragility for loss of spent fuel pool water inventory due to systems failure was then determined by aggregating the fragilities of the individual components as given in the overall Boolean expression.

As an example, the Boolean expression for seismic core damage at a representative plant could be:

$$M_S = 4 + 8 + 10 + 14 + 17 + 21 + (12 + 22 + 26) * 9$$

The numbers represent components for which seismic fragilities have been developed, as described earlier. The symbols "+" and "*" indicate "OR" and "AND" operations, respectively. This Boolean expression represent the combination of the Boolean expression for all accident sequences that lead to seismic core damage. A plant level fragility curve can then be obtained by aggregating the fragilities of the individual components using either Monte Carlo simulation or numerical integration. The plant level fragility represents the conditional probability of severe core damage for a given peak ground acceleration at the site. The uncertainty in plant level fragility is displayed by developing a family of fragility curves and assigning weights (probability) to each curve derived from the fragility curves of components appearing in the specific plant accident sequence.

2.5 Evaluation of Accident Frequency

The frequency of seismic induced accidents is evaluated by convolving the seismic hazard distribution with the overall seismic fragility. If the seismic hazard and the fragility are known, there will be a single hazard curve and a single fragility curve, and the result of the convolution will be a single value for the annual frequency of the accident.

However, there is uncertainty in the seismic hazard, this uncertainty is represented by either a probability distribution (annual frequency of exceedance) or a discrete set of values of the frequency of exceedance along with attached subjective weights at each specific peak ground or spectral acceleration. Therefore, the uncertainty in the seismic hazard may be represented by a family of curves with subjective weights attached to them or by a family of curves at different confidence values (subjective probabilities of non-exceedance). Similarly, the uncertainty in the seismic fragility can be expressed by means of a family of fragility curves with subjective weights assigned to them.

For the seismic hazard, the subjective weights are assigned by a hazard expert for each hypothesis or seismic model that yielded the hazard curve. In the seismic fragility evaluation, the subjective weight for each fragility curve is obtained by discretizing the uncertainty distribution which is also assigned by a fragility analyst.

The convolution is performed by taking one hazard curve and one fragility curve at a time, and the resulting frequency of the accident carries a subjective weight equal to the product of the subjective weights assigned to the specific hazard and fragility curves involved. The result of the convolution of both families of curves (hazard and fragility) is a subjective probability distribution for the annual frequency of the seismic induced accident. The convolution process can be accomplished by numerical integration using the Discrete Probability Distribution method (DPD) [Kaplan, 1981] or by simulation. The numerical integration procedure is described below.

Each discrete hazard curve may actually represent the output of one seismic hazard model (by one hazard expert with subjective weight attached to the curve); hence a large number of hazard curves may have to be convolved with the fragility curve. Experience has shown that the use of five fragility curves would be sufficiently accurate in representing the uncertainty in the fragilities of components [Ravindra, et al., 1984].

The uncertainty in seismic hazard is represented by a family of hazard curves at different confidence values and an uncertainty distribution was used to develop a new set of discrete curves. Five hazard curves (probability of exceedance vs peak ground acceleration) with subjective cumulative probabilities of 5%, 15%, 50%, 85% and 95% were provided by [Bernreuter, et al., 1987, Table 2-1]. A lognormal distribution was assumed for the

distribution of the uncertainty in probability of exceedance at each acceleration value; the parameters of the lognormal distribution (i.e., median and logarithmic standard deviation) were calculated by using the 50th and 95th percentile values. If X is the hazard value at any acceleration, the median of this distribution is X_{50} and the logarithmic standard deviation of the uncertainty is $\beta = (1/1.64) \ln (X_{95}/X_{50})$. However, since the tail of the lognormal distribution extends to infinity, one might get values of variates (probabilities of exceedance) greater than 1.0. A possible way to avoid this problem is to modify the lognormal distribution by truncating at the variate value of 1.0. Another option is to truncate the distribution at a selected value of the variate (other than 1.0). In the present study, after examining the truncations at 99th, 98th and 97th percentile values, it was judged that the distribution could be truncated at X_{99}, the 99th percentile value (i.e., 99% of the area of the uncertainty distribution is covered by the lognormal distribution) where X_{99} is given by $X_{50} \exp (2.33 \beta)$. The lognormal distribution was normalized to get a new distribution with cutoff at X_{99}. The sensitivity of this assumption was tested by running the case studies 1 (a), (b), (c) and (d) for the pool structure failure and the results are shown in Table 6.2. The range of the hazard represented by this truncated (lognormal) distribution at any acceleration was discretized into eleven discrete values of the hazard (i.e., annual probability of exceedance) with subjective probabilities of 0.03, 0.05, 0.07, 0.12, 0.15, 0.16, 0.15, 0.12, 0.07, 0.05 and 0.03. By repeating this procedure at other accelerations, a family of hazard curves is obtained.

Table 2-1

Annual Probability of Exceedance at
Different Acceleration Levels

Plant	Peak Ground Acceleration (g)	Cumulative Subjective Probability				
		5%	15%	50%	85%	95%
Vermont Yankee	0.050	.1127E-03	.3192E-03	.2594E-02	.2902E-01	.8137E-01
	0.075	.3970E-04	.1478E-03	.1111E-02	.1416E-01	.4217E-01
	0.125	.8001E-05	.4473E-04	.3544E-03	.5219E-02	.1572E-01
	0.200	.1501E-05	.1298E-04	.1132E-03	.1742E-02	.5554E-02
	0.250	.6306E-06	.5792E-05	.6117E-04	.9989E-03	.3308E-02
	0.400	.8267E-07	.8172E-06	.1439E-04	.2703E-03	.1032E-02
	0.560	.1291E-07	.1455E-06	.4383E-05	.1005E-03	.4153E-03
	0.610	.7213E-08	.8548E-07	.3204E-05	.7759E-04	.3190E-03
	0.760	.1144E-08	.1992E-07	.1319E-05	.3676E-04	.1680E-03
	1.000	.1790E-10	.2601E-08	.3914E-06	.1448E-04	.7848E-04
Robinson Unit 2	0.050	.8451E-04	.2548E-03	.2196E-02	.1647E-01	.6474E-01
	0.075	.3747E-04	.1072E-03	.8943E-03	.7708E-02	.3211E-01
	0.125	.1063E-04	.3355E-04	.2871E-03	.2746E-02	.1247E-01
	0.200	.2418E-05	.8655E-05	.8762E-04	.9079E-03	.4640E-02
	0.250	.9409E-06	.4223E-05	.4682E-04	.5118E-03	.2726E-02
	0.400	.9607E-07	.6552E-06	.1120E-04	.1465E-03	.7376E-03
	0.560	.1067E-07	.1250E-06	.3330E-05	.5414E-04	.2739E-03
	0.610	.4826E-08	.7736E-07	.2395E-05	.4108E-04	.2078E-03
	0.760	.6465E-09	.1967E-07	.1013E-05	.1937E-04	.1045E-03
	1.000	.2234E-10	.3157E-08	.2982E-06	.7717E-05	.4173E-04

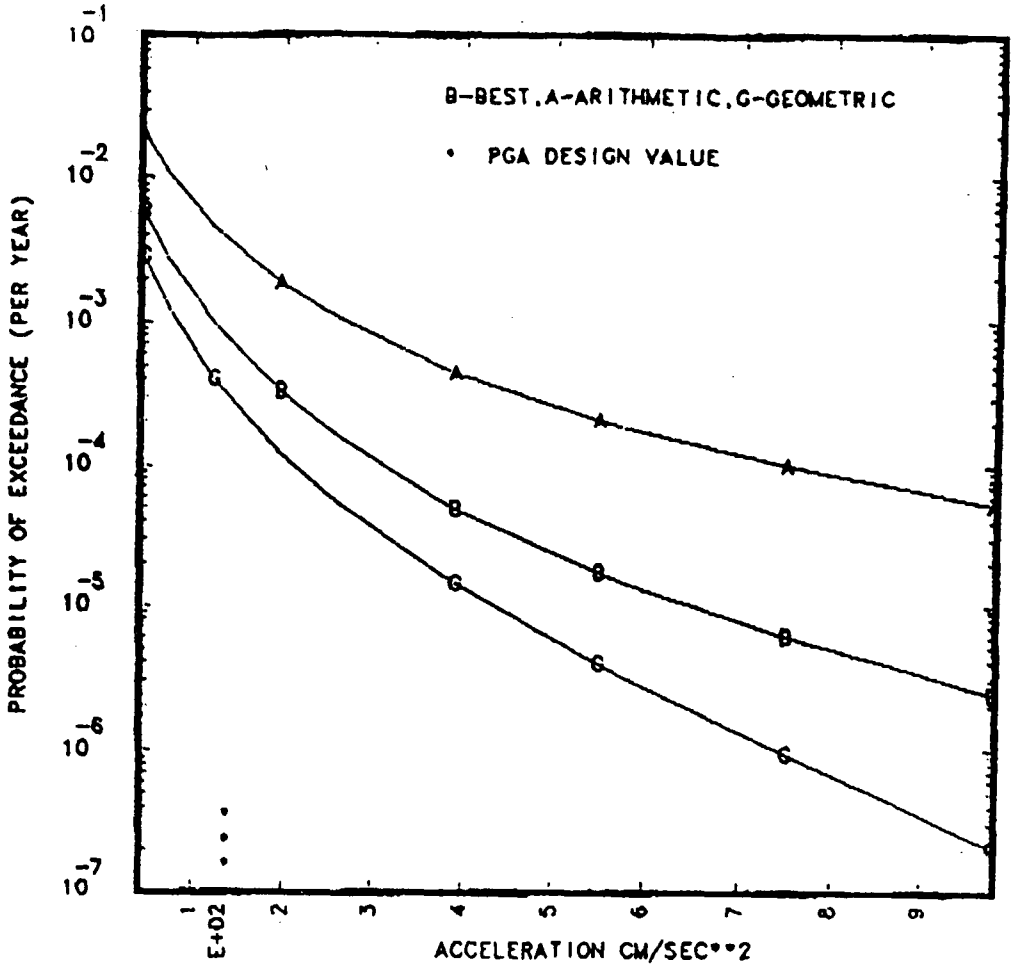

Figure 2-1: Sample Seismic Hazard Curves

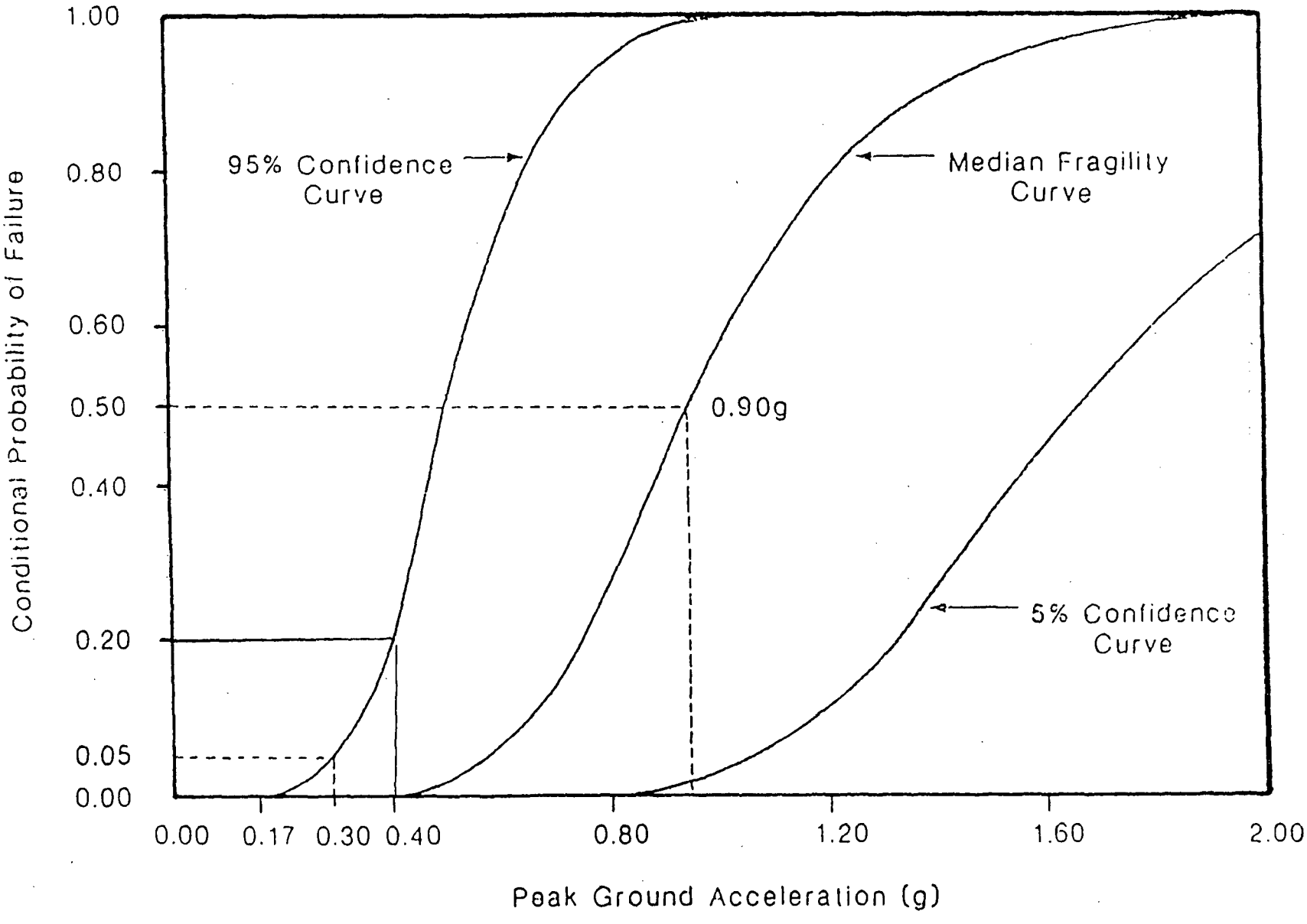

Figure 2-2: Example Fragility Curves for a Structure

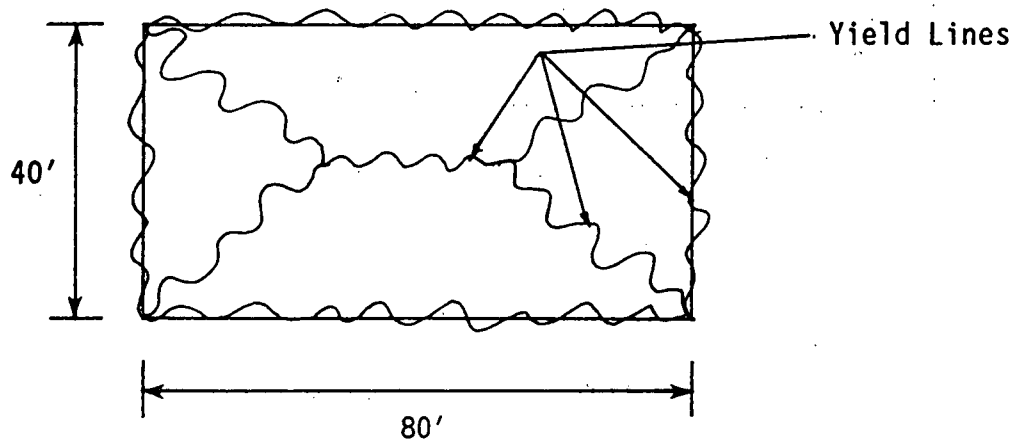

Figure 2-3: Failure Mechanism for the Pool Floor

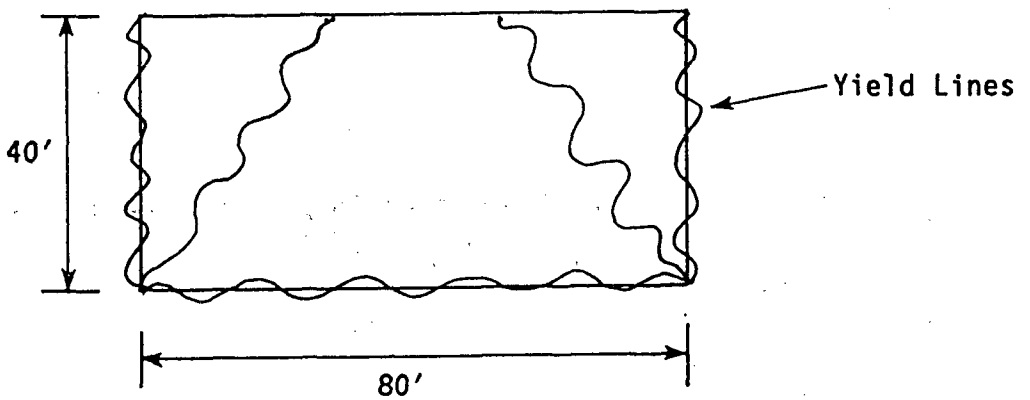

Figure 2-4: Failure Mechanism for the Pool Wall

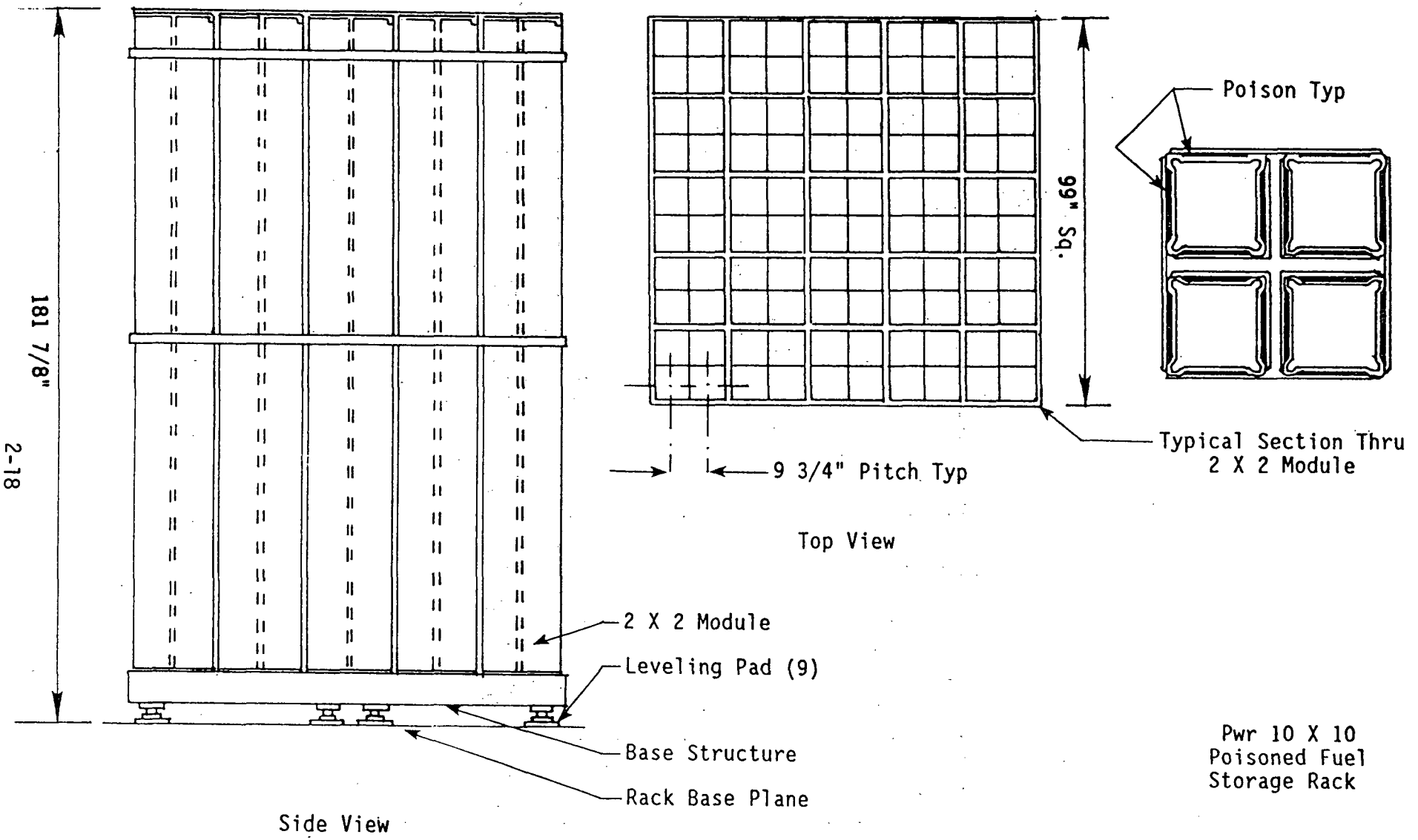

Figure 2-5: Spent Fuel Storage Rack Schematic (10 x 10)

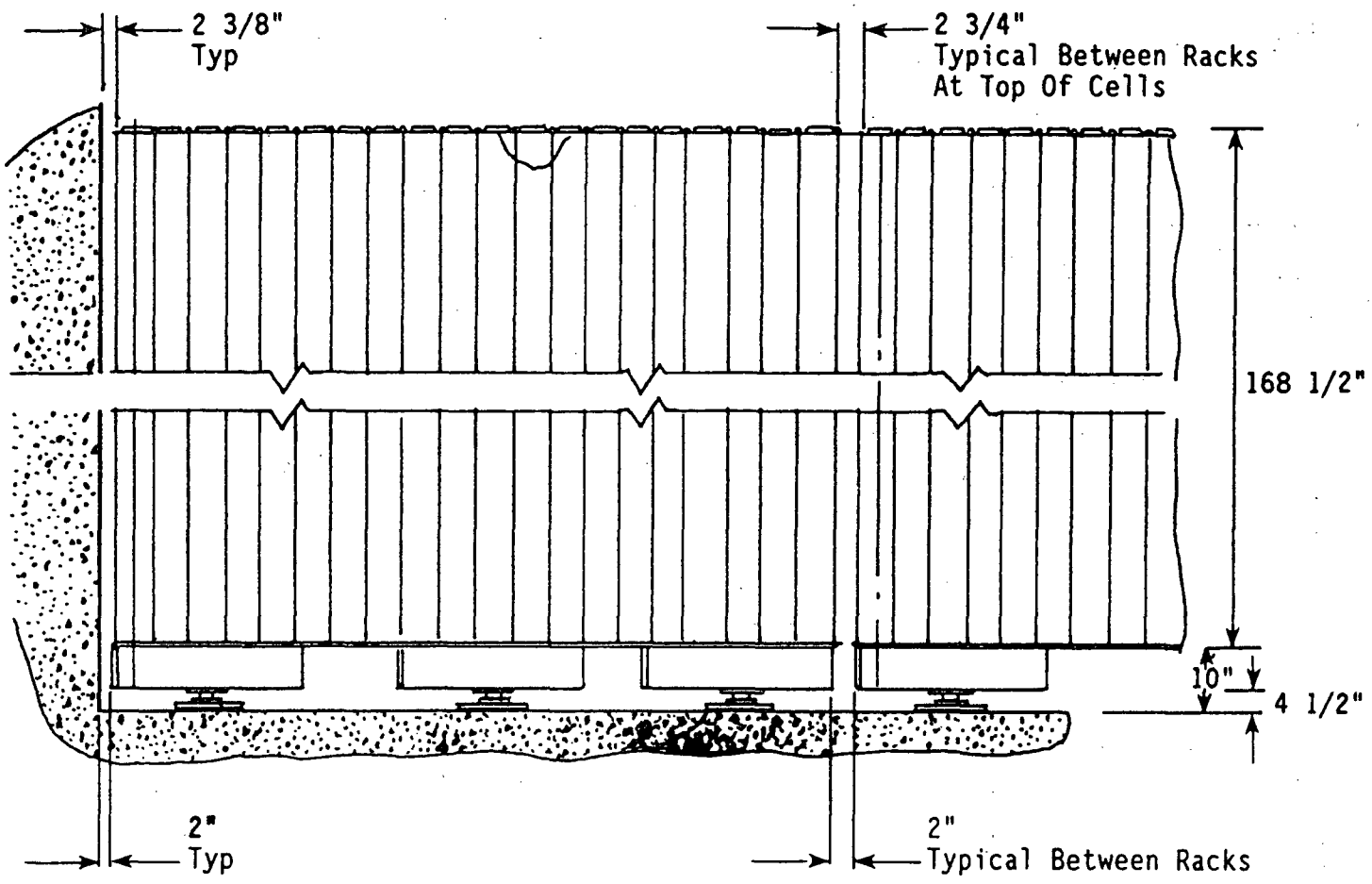

Figure 2-6: Typical Rack Elevation View

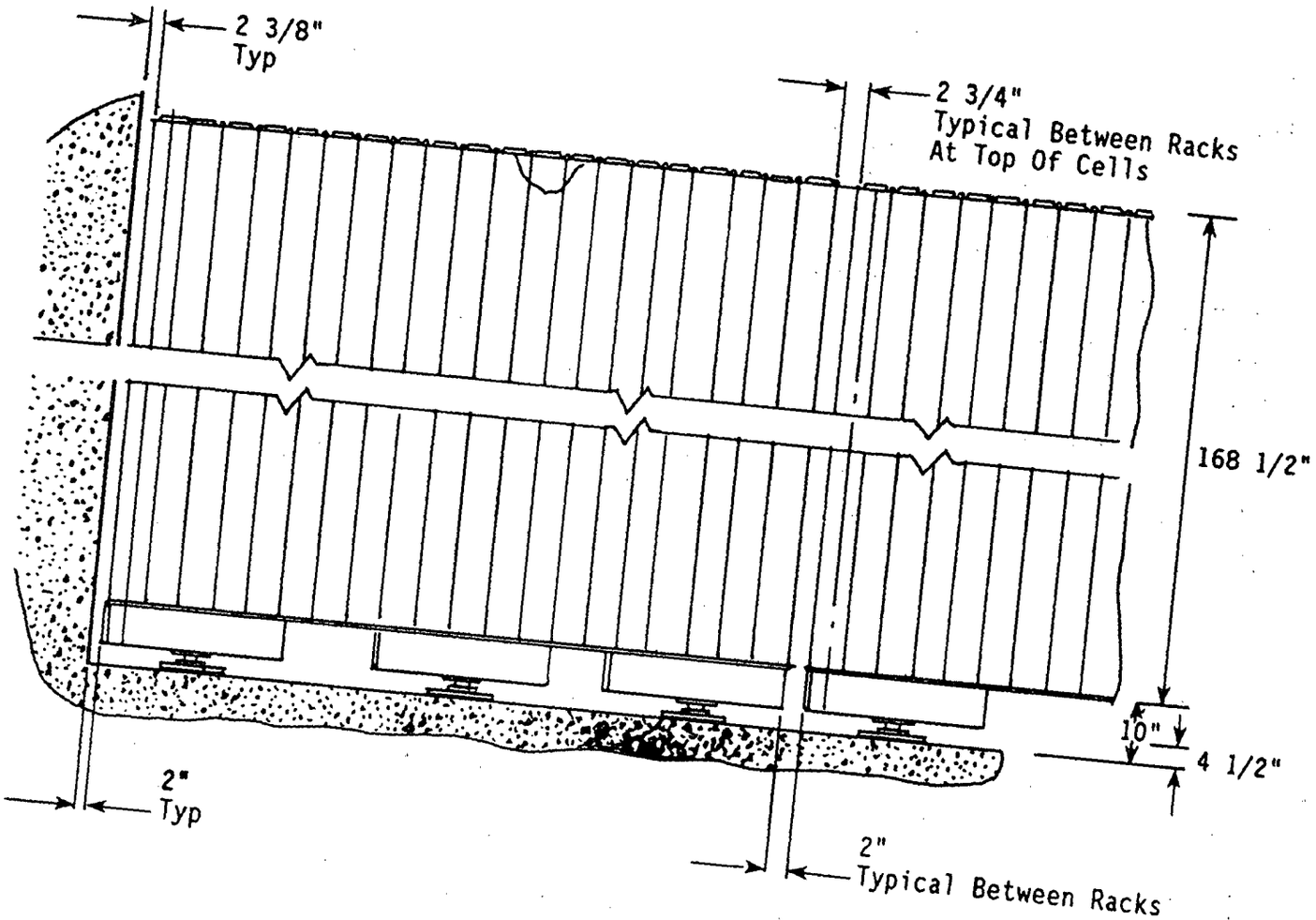

Figure 2-6: Typical Rack Elevation View

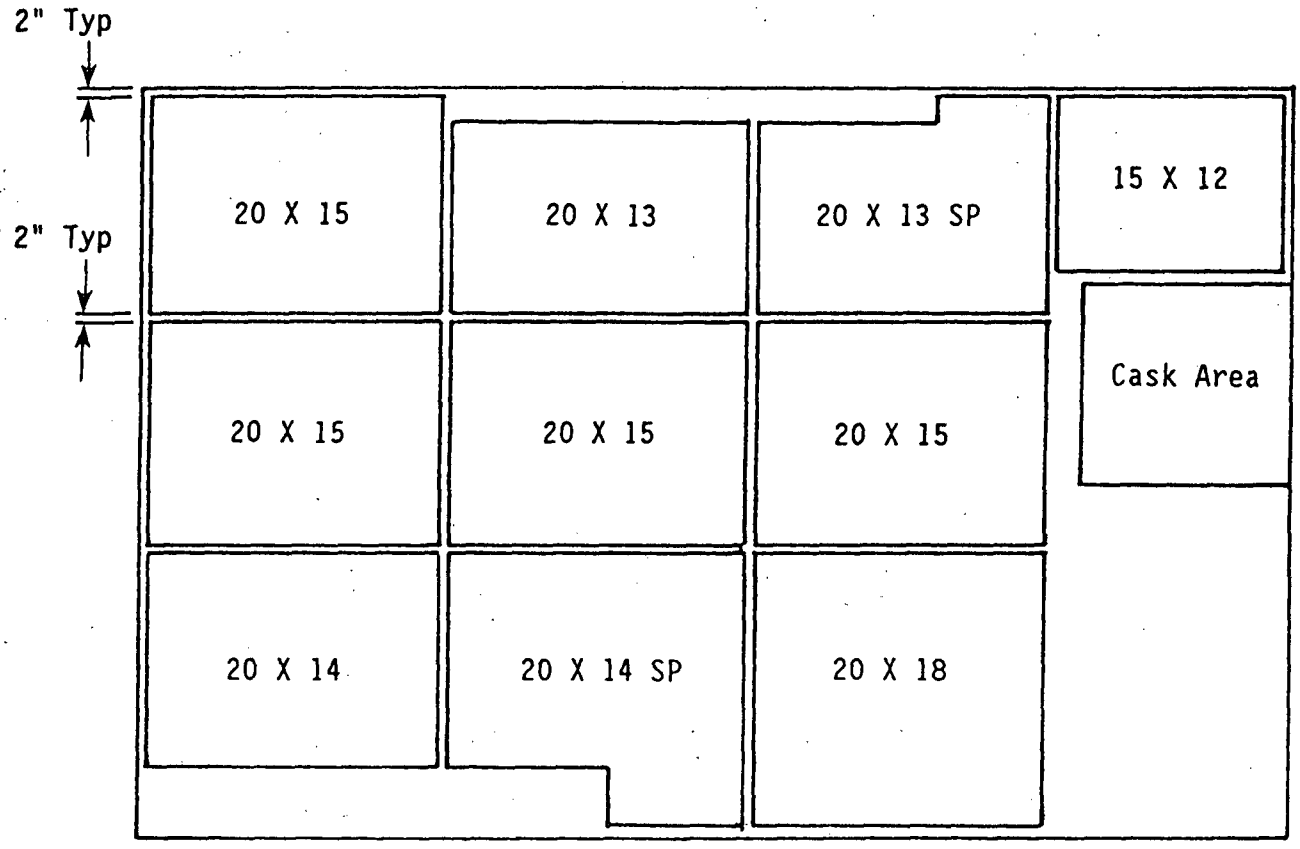

Figure 2-7: Pool Layout

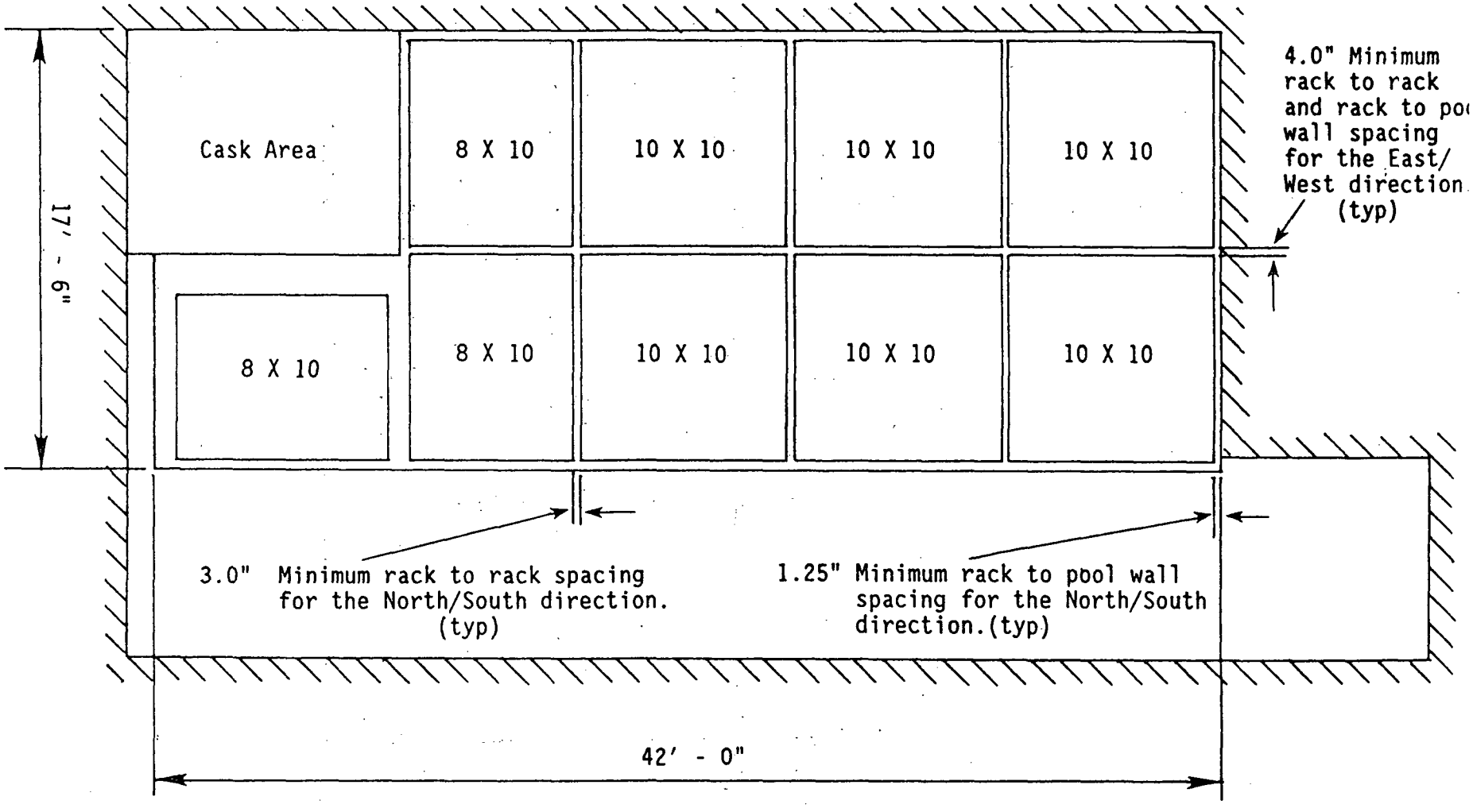

Figure 2-8: Plan Fuel Storage Rack Arrangement

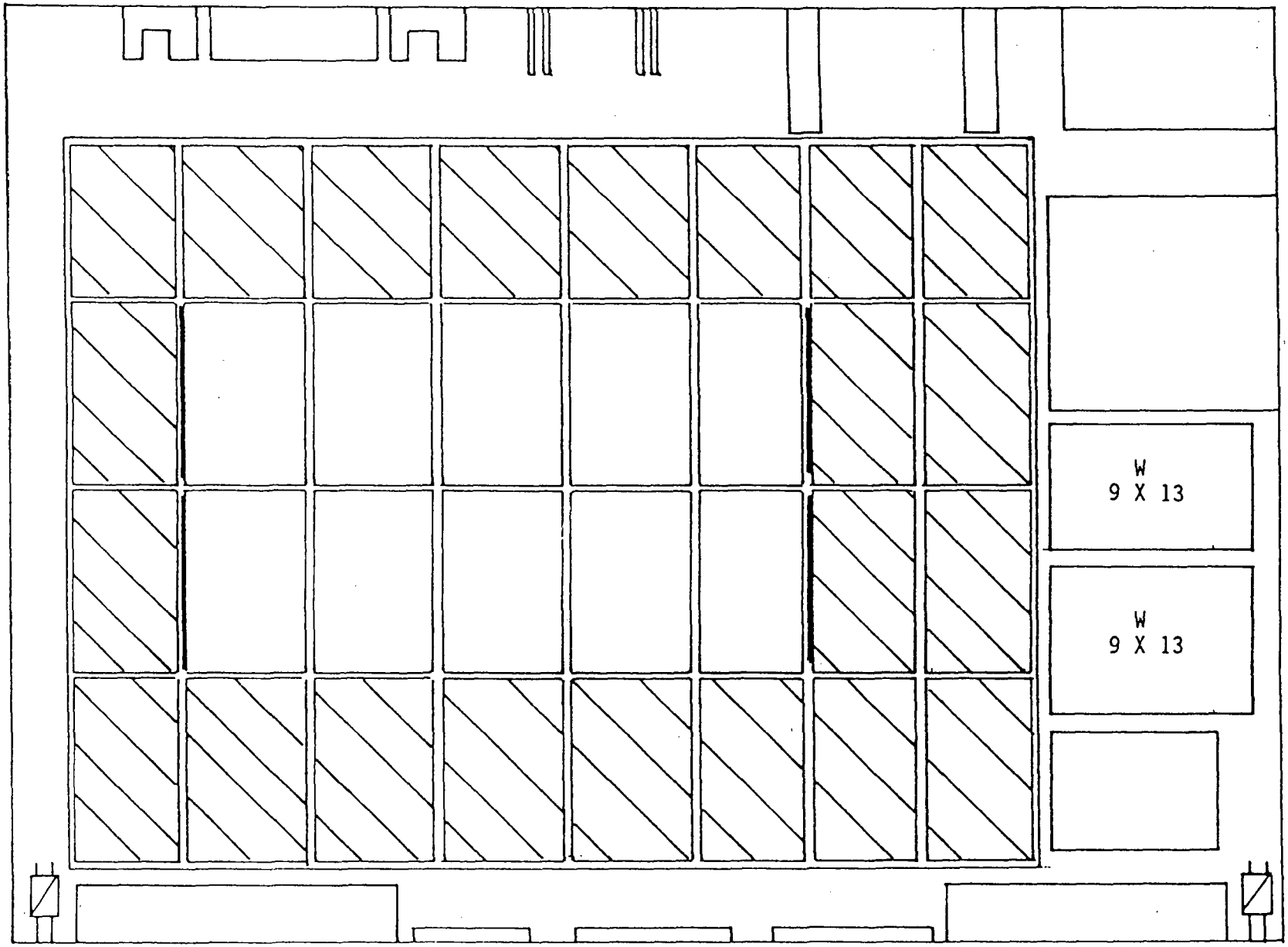

Key: Crosshatched = Consolidated Region (1436 Avail. Cells)
Bordered = Intact Cells (982 Avail. Cells)

Figure 2-9: Fuel Pool Arrangement for Laterally Braced High Density Fuel Racks

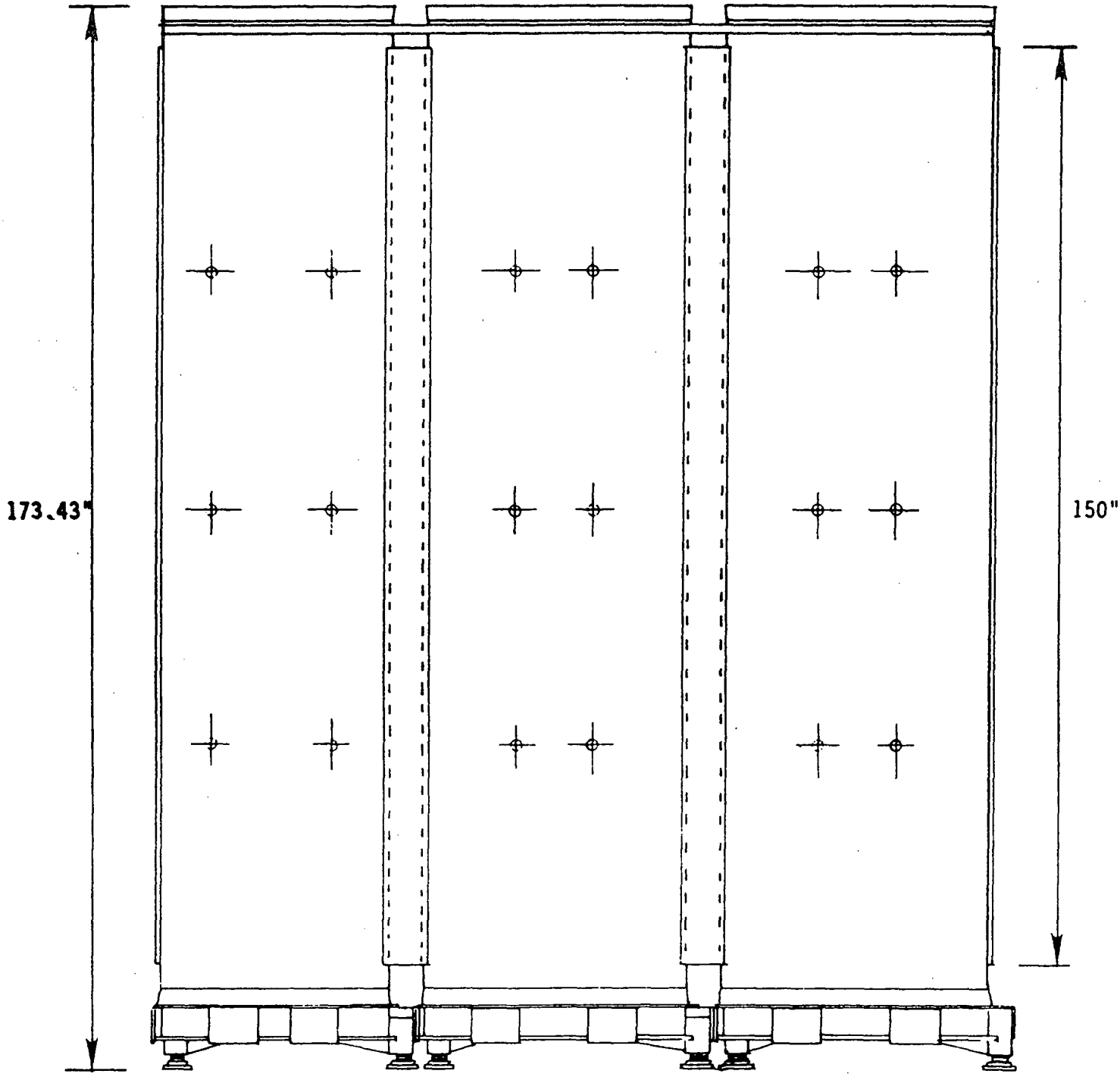

Figure 2-10: Typical Elevation - All Groups

3. SEISMIC FRAGILITY OF POOL STRUCTURES

3.1 Introduction

The evaluation described below was performed to determine the seismic capacity of spent fuel pool structures. Failure of the spent fuel pool structure for this study is defined to be a gross, rapid loss of the fluid which provides cooling for the spent fuel rods. Minor leakage is not considered to constitute failure. The investigation was limited to the structural components forming the spent fuel pool.

3.2 Vermont (VYNPS) Spent Fuel Pool (SFP)

3.2.1 VYNPS SFP Structure Description

The Vermont Yankee spent fuel pool structure is an integral part of the reactor building, and was designed as a Seismic Category I structure, SSE=0.14g. It is situated at the south side of the reactor building, with the top of the spent fuel pool located at the operating floor which is about 140 feet above the building foundation. The spent fuel pool is twenty six feet wide in the north-south direction and forty feet wide in the east-west direction. It is normally filled with water to a depth of 35.75 feet above the bottom of the pool which is located at Elevation 306'-5".

The spent fuel pool structure is shown in Figures 3-1 and 3-2. It is built of reinforced concrete. The floor slab is 4'-1" thick with an eleven inch thick grout topping. The walls at the south, east, and west sides are from 4'-6" to 6'-0" thick. The drywell shield wall bounds the spent fuel pool on the north side. The spent fuel pool structure is constructed integral with the reactor building floors at Elevations 303'-0", 318'-8", and 345'2". The interior of the spent fuel pool is lined with stainless steel plate anchored to the walls and floor slab.

3.2.2 VYNPS SFP Structure Evaluation

A detailed evaluation of the Vermont Yankee spent fuel pool structure was based on the maximum loading condition when the high density storage racks are filled to their total storage capacity. The following plant specific information formed the basis for this evaluation:

- Structural drawings
- Final Safety Analysis Report (FSAR)
- "Vermont Yankee Spent Fuel Storage Rack Replacement Report" (1986).

A number of potential failure modes of the spent fuel pool structure were analyzed, including the following:

- Out of plane shear failure of the pool floor slab
- Out of plane bending failure of the pool floor slab

- o Punching shear failure of the pool floor slab under the fuel rack support pad
- o Out of plane bending failure of the south pool wall
- o Bending and shear failure of the girder under the south pool wall
- o Bending and shear failure of the girder under the east pool wall
- o Overall transfer of N-S and E-W inertial loads to the reactor building

Of these, the controlling failure mode with the lowest seismic capacity was determined to be out of plane shear failure of the pool floor slab.

The spent fuel pool floor slab is 4'-1" thick with clear spans of 24'6" and 40'-0" in the north-south and east-west directions, respectively. It is reinforced by steel bars in the two horizontal directions, but shear reinforcement was not provided. The pool floor slab behaves as a two way member spanning between the girders and drywell shield wall at the boundaries.

The spent fuel pool concrete was specified to have a minimum compressive strength of 4000 psi. The results of non-destructive concrete strength testing, believed to be Windsor probe, from four locations at the bottom face of the pool slab are reported in [Vermont Yankee 1986]. These tests indicate an average concrete compressive strength of 7000 psi. Because this test method is reportedly very accurate, the median concrete compressive strength was taken to be this value. A coefficient of variation of 0.15 was estimated. This median strength and variability are within the range of values used in previous fragility evaluations of nuclear plant structures with 4000 psi concrete.

Reinforcement for the spent fuel pool was specified to be Grade 40. Reinforcement strength test data was not available. A median yield strength of 48,000 psi and coefficient of variation of 0.10 were estimated based upon past nuclear plant fragility evaluations.

The slab was evaluated for out-of-plane loading resulting from dead load plus seismic load. Sources of dead load are the weights of the slab, grout, water, fuel racks, and attached equipment. Sources of seismic load are:

- o Vertical seismic response of the slab and attached masses
- o Fluid impulsive and convective mode responses induced by horizontal seismic excitation
- o Horizontal seismic response of the spent fuel racks

Thermal gradients across the walls and slab can introduce significant stresses at elastic levels. However, these stresses are stiffness dependent and diminish as the structure stiffness decreases. Under increased transverse slab loads, the concrete will crack and crush and the reinforcement will yield, with resulting reduction in stiffness. The slab stiffness approaches zero asymptotically as the slab is loaded to failure. This evaluation is performed to assess structure failure capacity. Because the slab stiffness is small when its failure capacity is reached, thermal stresses at this load level are small and can be neglected.

Maximum dead load shear at the slab supports due to uniform transverse loadings from the weight of slab, grout, water, and attached equipment was determined by modeling the slab as a one way member. Although the slab actually develops two way action, this approximation is sufficiently accurate since the difference is minor for the slab aspect ratio.

Seismic response of the slab was derived from the reactor building floor spectra, shown in Figures 3-3 to 3-5, from [Vermont Yankee 1986]. These floor spectra were reportedly generated from a seismic analysis using the N 69' W component of the 1952 Taft earthquake normalized to 0.07g for the operating basis earthquake (OBE). Five percent damping was assigned to the structure. Safe shutdown earthquake (SSE) input was taken to be twice the OBE. An actual plot of the ground spectra corresponding to the Taft time history is not available. They were therefore assumed to be consistent with the spectra shown in Figure B-2a of [Kennedy et al., 1985].

For the fragility evaluation, design seismic input to the spent fuel pool were factored to reflect input that would result from the use of median centered seismic response parameters. The factors used vary depending on the response considered as discussed below. Median site specific ground spectra are not currently available for Vermont Yankee. Therefore, the shape of the median Vermont Yankee ground spectrum was assumed to correspond to the median spectrum recommended for rock sites by NUREG/CR-0098 [Newmark and Hall, 1978]. Ten percent structure damping was considered to be a median value based on the recommendations of NUREG/CR-0098 for reinforced concrete structures at or near the yield point. Conservatism in the design basis floor spectra due to broadening and smoothing was also considered in the fragility analysis by inclusion of a median factor of 1.1 for subsystem spectral shape.

The slab fundamental vertical frequency was determined using a closed form solution. Accounting for potential cracking and continuity at the boundaries, a vertical frequency of about 25 Hz was estimated. Ten percent damping is considered to be a median value for the slab. Median slab shears due to vertical response were determined by factoring the dead load shears by the estimated median spectral acceleration of 0.14g. This value is increased by a factor of 1.15 above the SSE spectral acceleration to account for the difference between the median site specific ground spectrum at median structure damping and the SSE ground spectrum at five percent structure design damping for the structure fundamental vertical frequency of about 13 Hz. The increase factor reflects potential unconservatism of the design ground spectrum at the structure frequency relative to the median ground spectrum.

Seismic response of the pool water in the impulsive and convective modes causes transverse pressures to be exerted on the slab and walls under horizontal excitation. Even accounting for wall flexibility, response of the impulsive mode was determined to be essentially rigid. Fluid response was thus determined following the provisions of TID-7024 [USAEC, 1963]. Resulting seismic loads on the slab due to fluid response were found to be small and were therefore neglected.

The new, high density spent fuel storage racks are freestanding and not anchored to the structure. In this design, rack loads are transmitted to the slab only by the rack support pads. Seismic response of the racks was determined by dynamic, nonlinear analysis described in [Vermont Yankee, 1986]. This report contains maximum reactions imposed on the slab by individual support pads as well as maximum total reactions for the rack modules. Inspection of the individual support pad reaction time histories indicates that they are nearly harmonic with long impulse durations relative to the slab natural period. Based upon approximate methods for analysis of structure response to impulse loads described in [Biggs 1964], the rack loads acting on the slab have a dynamic amplification factor of unity. Maximum slab shears were therefore calculated using maximum total rack module reactions as static loads, with shears from separate modules combined by the square root of the sum of the squares (SRSS) since their phasing is random. Rack module reactions are estimated to have a median factor of safety of about 1.7, accounting for potential conservatism in the input ground motion and the use of bounding base coefficients of friction.

The highest applied slab shear load occurs at the interface with the drywell shield wall. Median slab shear strength at this location was determined from available test data for reinforced concrete beams. From Figure 7.13 of [Park and Pauly 1975], the ultimate concrete shear stress was estimated to be $2.6\ (f'_c)^{1/2}$, which represents an increase of about 25% above the ACI 349-80 Code value, not including the strength reduction factor. This shear strength implicitly accounts for moment-shear interaction. Reduction in shear strength due to axial tension imposed by wall reactions is relatively small at seismic levels corresponding to the lower tails of the fragility curves, which dominate the seismic risk and HCLPF capacity. A median ultimate shear strength of 120 kips per foot was calculated with the median concrete compressive strength of 7000 psi. This capacity was based upon one way action for the slab spanning in the short direction between the north and south supports. [ASCE 1985] recommends a very small increase in shear capacity for this slab accounting for two way action. However, due to the lack of shear reinforcement, shear failure will be nonductile. Because the applied loading is cyclic and the resulting failure mode is nonductile, any load redistribution will be unlikely and was therefore not included in this evaluation.

Following the methodology described above, the slab was found to have the following overall fragility parameters:

$$A_m = 1.4g$$
$$\beta_R = 0.26$$
$$\beta_U = 0.39$$

The median slab fragility curve with 5% and 95% confidence bounds are shown in Figure 3-6. Table 3.1 lists the median values and variabilities of the individual factors. Because seismic loads used to define the median strength factor were already modified to account for median response parameters, the median response factors are typically unity.

The HCLPF capacity for slab shear failure is calculated to be 0.5g. This acceleration is about 3.5 times the SSE pga and represents a significant margin of safety. This failure mode is considered to be brittle and it is probable that shear failure will lead to a loss of structural integrity with liner rupture and subsequent rapid loss of spent fuel pool water inventory. Additional redundancy provided by alternative remaining load paths, such as catenary action of the slab, may be possible. However, these load paths were not evaluated since the shear failure capacity is already well in excess of the SSE.

The HCLPF capacity determined for the Vermont Yankee spent fuel pool structure is consistent with NRC trial guidelines for seismic margin reviews. Following Table 2.1 of [Prassinos et al., 1985], the spent fuel pool would not require evaluation for a margin review earthquake with peak ground acceleration less than 0.3g, since the HCLPF capacity of shear wall structures is considered to be much greater than this input level. This is the case for the Vermont Yankee spent fuel pool structure which has a HCLPF capacity of 0.5g, even including higher loads from the new high density storage racks. The HCLPF capacity based upon the existing storage racks is estimated to be about 0.65g, which is well above the 0.3g pga at which shear wall structures are screened out.

In a generic study on seismic risk from spent fuel pool accidents, [Sailor et al., July 1987] assigned the greatest "weight" to the following structural fragility for the Oyster Creek reactor building developed by [Kennedy et al., 1980].

$$A_m = 0.75g$$
$$\beta_R = 0.37$$
$$\beta_U = 0.38$$

The HCLPF capacity from these fragility parameters is 0.22g, which is much less than the value for the Vermont Yankee spent fuel pool structure. There are two major reasons for this difference. First, there has been considerable evolution in techniques to quantify nuclear plant seismic fragilities since the Oyster Creek parameters were developed. These techniques generally result in greater seismic capacities than were previously calculated. Second, the Vermont Yankee spent fuel pool structure fragility has been derived from a plant specific analysis that considers the actual seismic capacities and loadings. This approach is preferable to the use of generic fragilities obtained for a structure whose configuration, resistance, and load paths may be markedly different.

3.2.3 Conclusions of the Structural Analysis

A detailed evaluation of the VYNPS spent fuel pool structure shows that there is high confidence of a low probability of failure due to an earthquake with an average peak ground acceleration of 0.5g. The HCLPF capacity is about 3.5 times the plant safe shutdown earthquake peak ground acceleration. Therefore, the Vermont Yankee spent fuel pool structure has significant safety margin above its design basis when more realistic evaluation criteria are employed.

3.3 H. B. Robinson, Unit 2 (HBR2) Spent Fuel Pool

3.3.1 HBR2 SFP Structure Description

The Robinson spent fuel pool structure is a seismic Category I, SSE=0.20g, reinforced concrete structure containing 35,167 cubic feet of water and is housed within the Fuel Handling Building (FHB). The spent fuel pool is 43 feet wide in the north-south direction and 53 feet 6 inches wide in the east-west direction measured from outside to outside face. It is normally filled with water to a depth of 37 feet above the bottom of the pool which is located at Elevation 236 ft 9 in.

The spent fuel pool structure is shown in Figures 3-7 and 3-8. It is built of reinforced concrete. The floor slab is 4'-6" thick with reinforcement of #11 bars at 6 in. spacing in the negative moment regions, and #10 bars at 12 in. spacing in the positive moment regions. A single steel column was installed below the pool slab during the plant modification for the spent fuel storage capacity expansion in 1982. The peripheral walls are all 6 ft thick with reinforcement of #9 bars at 12 in. spacing each way and each face. The interior of the spent fuel pool is lined with stainless steel plate anchored to the walls and slab.

3.3.2 HBR2 SFP Structure Evaluation

A detailed evaluation of the Robinson Unit 2 spent fuel pool structure was based on the maximum loading condition when the high density storage racks are filled to their total storage capacity. The following plant specific information formed the basis for this evaluation:

Structural drawings

Final Safety Analysis Report (Updated FSAR)

"Spent Fuel Pool Storage Extension New Column Under Fuel Pool Floor" Calculation No. HB-102 prepared by Ebasco Services Incorporated for Carolina Power & Lighting, March 1982.

A number of potential failure modes of the spent fuel pool structure were analyzed, including the following:

Out of plane bending failure of the East or South wall

Out of plane shear failure of the East or South wall

Out of plane shear failure of the pool floor slab

Out of plane bending failure of the pool floor slab

Punching shear failure of the pool floor slab at the added steel column

Failure of the added steel column underneath the spent fuel pool

Overall seismic stability of the spent fuel pool

Of these, the controlling failure mode with the lowest seismic capacity was determined to be out of plane bending failure of the East wall.

The East or South wall resists the lateral forces of the old fuel racks. It is modeled as a slab fixed on three sides and free at the top. The loads considered in the evaluation of the seismic capacity of this wall are:

Hydrostatic loads (normal water level El. 273.67')

Hydrodynamic loads induced by horizontal and vertical accelerations in earthquakes.

Wall inertia force

Reaction forces from the old fuel racks.

A realistic evaluation of the out-of-plane failure capacity of the wall was done by using the yield line analysis under a uniformly distributed load. The triangular hydrostatic pressure was converted into an equivalent uniform load.

Similarly, the pool slab was analyzed for static and dynamic loads. The static loads included dead weight of the pool water, dead weight of the slab, and dead weight of the fuel racks and cask. The dynamic loads included hydrodynamic loads due to vertical acceleration, slab inertia, vertical inertia of the fuel racks and cask, and reaction forces of the high density fuel storage racks due to horizontal ground motion. Since the factors of safety of the pool slab based on the elastic analysis were found to be much higher than those of the east wall, no further analysis such as the yield line analysis was performed for the pool slab.

The various factors needed in the estimation of the ground acceleration capacity of the pool were evaluated as follows:

Strength Factor

The spent fuel pool concrete was specified to have a minimum compressive strength of 3,000 psi at 28 days. Since no cylinder test results were available, the median compressive strength (taking into account aging effects) was estimated by using the previous PRA results as 4,900 psi and the logarithmic standard deviation of 0.17 was also estimated.

Reinforcement for the spent fuel pool was specified to be Grade 40. Rebar strength test data was not available. A median strength of 48,000 psi and a logarithmic standard deviation of 0.10 were estimated based upon past nuclear plant fragility evaluations.

The median strength factor was estimated to be 7.7 for the critical failure mode of flexural failure of the pool wall based on the yield line analysis. The uncertainty in this factor comes from the material strength uncertainty (i.e., steel yield strength (β_U = 0.10)), uncertainty in the moment capacity equation (estimated to be (β_U = 0.15)) and other uncertainties in the yield line analysis and torsional effect (β_U = 0.15). Therefore, the total uncertainty in the strength factor is estimated to be 0.23.

Inelastic Energy Absorption Factor

Based on the recommendations in Appendix C of ACI 349, a ductility factor of 10 was estimated for the east wall. The elastic natural frequency of this wall, which is a subsystem of the spent fuel pool, was estimated to be about 50 Hz which is in the rigid range. Hence, the inelastic energy absorption capacity factor was estimated to be equal to (10 x 0.13 = 1.3). The logarithmic standard deviations in this factor were estimated to be β_R = 0.06 and β_U = 0.04.

Spectral Shape Factor

For the fragility evaluation, design seismic input to the spent fuel pool were factored to reflect input that would result from the use of median centered seismic response parameters. Median site specific ground spectra are not currently available for Robinson. Therefore, the shape of the median Robinson ground spectrum was assumed to correspond to the median spectrum recommended by NUREG/CR-0098 [Newmark and Hall, 1978]. The median fundamental natural frequency of the spent fuel pool including the soil and the piles that the structure is founded on is estimated to be 3.8 Hz based on the information provided in the Updated FSAR. Ten percent damping is estimated to be the median value for the system in consideration of the interaction between the reinforced concrete structure and the foundation soil and piles. Since the dynamic response of the spent fuel pool was estimated by using the NUREG/CR-0098 10% median ground response spectrum, the median spectral shape factor is 1.0. The logarithmic standard deviations of this factor taking into account the peak-to-peak variability and earthquake directional variability are estimated as β_R = 0.25 and β_U = 0.10.

Damping Factor

The response of the pool was calculated using 10 % damping which is considered to be a median damping value. Therefore, the median damping factor is 1.0. The system frequency is estimated to be 3.8 Hz, considering the foundation media of the spent fuel pool. This frequency falls within the amplified acceleration region of the NUREG/CR-0098 spectrum. The variabilities in damping factor were estimated by taking 7% as a 16 percentile value. The

estimated values of β_R and β_U for damping factor are 0.03 and 0.14 respectively.

Modeling Factor

The median modeling factor was assumed to be 1.0 with the value of β_U estimated to be 0.15.

Soil Structure Interaction Factor

Robinson Fuel Handling Building is founded on piles. The median soil-structure interaction factor is estimated to be 1.0 with logarithmic standard deviations $\beta_R = 0.05$ and $\beta_U = 0.20$. Note that a higher value of β_U is assigned for this factor compared to the Vermont Yankee evaluation because the Robinson spent fuel pool is supported on piles.

Subsystem Analysis Factors

The subsystem analysis of the pool is considered to be median centered; since the load estimation on the wall is relatively straight forward compared to the estimation of loads acting from the high density fuel racks on the pool slab (as in Vermont Yankee), the uncertainty in the modeling of the subsystem was estimated to be lower and equal to $\beta_U = 0.10$. The median factor for conservatism or unconservatism arising out of the modal combination method used is estimated to be 1.0 with a nominal value of $\beta_R = 0.05$. With the natural frequency of the East wall falling in the rigid region, the uncertainty in the spectral shape and damping factors was estimated to be zero.

Earthquake Component Combination Factor

The median response analysis was done by combining the seismic responses from different directions by the 100%, 40% and 40% rule proposed by Newmark [Newmark and Hall, 1978]. If we assume that the maximum vertical earthquake component occurring simultaneously with the horizontal component as the 3 logarithmic standard deviation case, the value of β_R is estimated as 0.06.

Following the methodology described above, the overall fragility parameters for the spent fuel pool wall were estimates as:

$$A_m = 2.0g$$
$$\beta_R = 0.28$$
$$\beta_U = 0.40$$

The median slab fragility curve along with the 5% and 95% confidence bounds are shown in Figure 3-9. Table 3.2 lists the median values and variabilities of the individual factors. Because seismic loads used to define the median strength factor were already modified to account for median response parameters, the median response factors are typically unity.

The HCLPF capacity for pool wall flexure failure is calculated to be 0.65g. This acceleration is about 3.3 times the SSE pga and represents a significant margin of safety.

3.3.3 Conclusions of the Structural Analysis

A detailed evaluation of the Robinson Unit 2 spent fuel pool structure shows that there is high confidence of a low probability of failure due to an earthquake with an average peak ground acceleration of 0.65g. The HCLPF capacity is about 3.3 times the plant safe shutdown earthquake peak ground acceleration. Therefore, the Robinson Unit 2 spent fuel pool structure has significant safety margin above its design basis when more realistic evaluation criteria are employed.

Table 3.1

Median Factors of Safety and Variabilities
of Spent Fuel Pool Structure at Vermont Yankee

Factor	Median	β_R	β_U
Strength	8.8	0.	0.30
Inelastic Energy Absorption	1.0	0.	0.
Spectral Shape	1.0	0.24	0.10
Damping (Structure)	1.0	0.02	0.08
Modeling (Structure)	1.0	0.	0.13
Soil-Structure Interaction	1.0	0.01	0.05
Spectral Shape (Subsystem)	1.1	0.	0.05
Damping (Subsystem)	1.0	0.	0.05
Modeling (Subsystem)	1.0	0.	0.15
Modal Combination	1.0	0.02	0.
Comb. of EQ Components	1.0	0.10	0.
TOTAL	9.7	0.26	0.39

Median pga capacity = 9.7 (0.14g) = 1.4g

HCLPF capacity = 1.4 exp [-1.64(0.26+0.39)] = 0.50g

Table 3.2

Median Factors of Safety and Variabilities of
Spent Fuel Pool Structure at H.B. Robinson 2

FACTOR	Median	β_R	β_U
Strength	7.7	0.	0.23
Inelastic Energy Absorption	1.3	0.06	0.04
Spectral Shape	1.0	0.25	0.10
Damping (Structure)	1.0	0.03	0.14
Modeling (Structure)	1.0	0.	0.15
Soil-Structure Interaction	1.0	0.05	0.20
Spectral Shape (Subsystem)	1.0	0.	0.
Damping (Subsystem)	1.0	0.	0.
Modeling (Subsystem)	1.0	0.	0.10
Modal Combination	1.0	0.05	0.
Comb. of EQ Components	1.0	0.06	0.
TOTAL	10.0	0.28	0.40

Median pga capacity = 10 (0.20g) = 2.0g

HCLPF Capacity = 2.0 exp (- 1.64 (0.28 + 0.40)) = 0.65 g

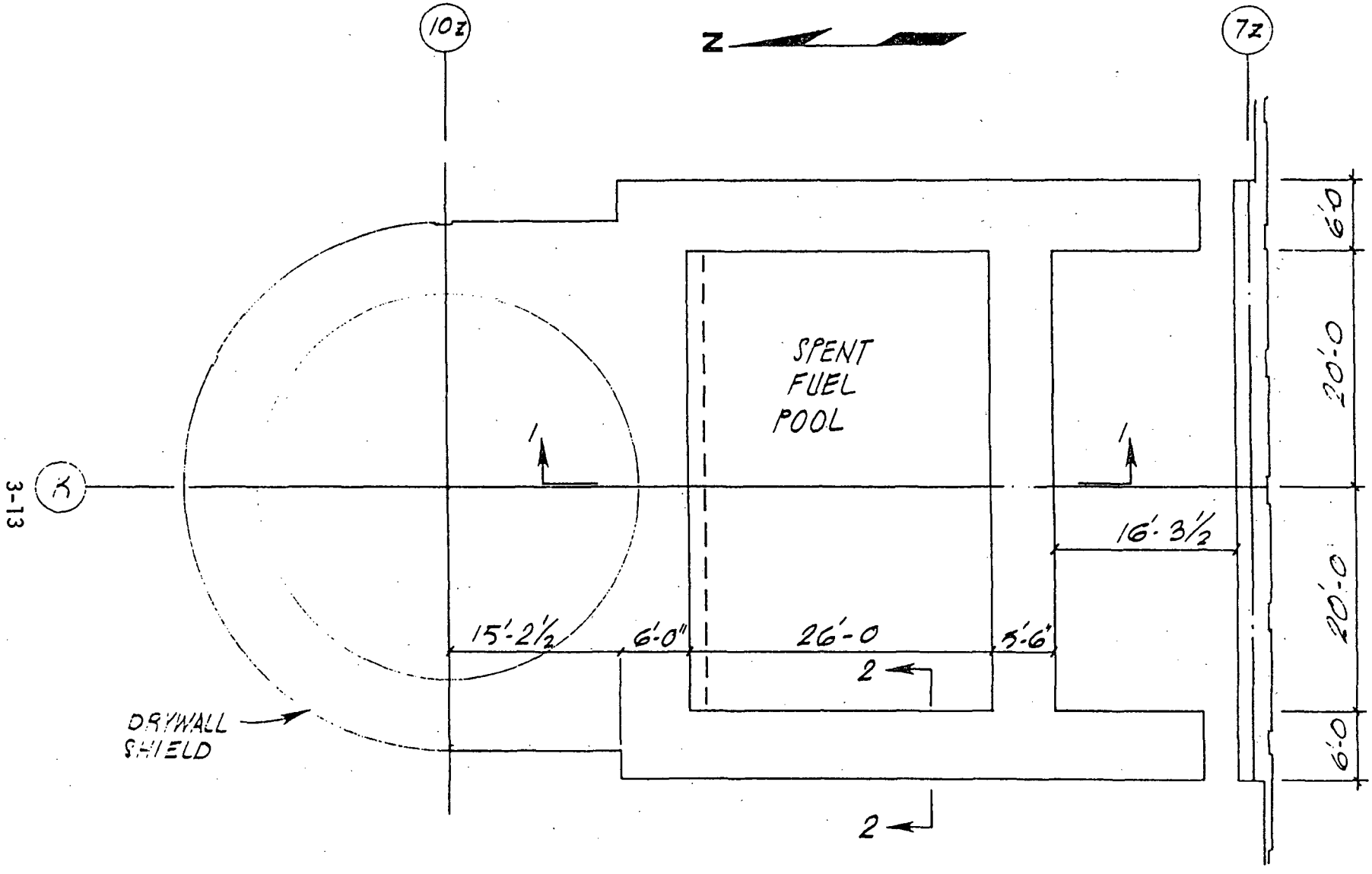

Figure 3-1: Reactor Building Plan at Elevation 303'-0"

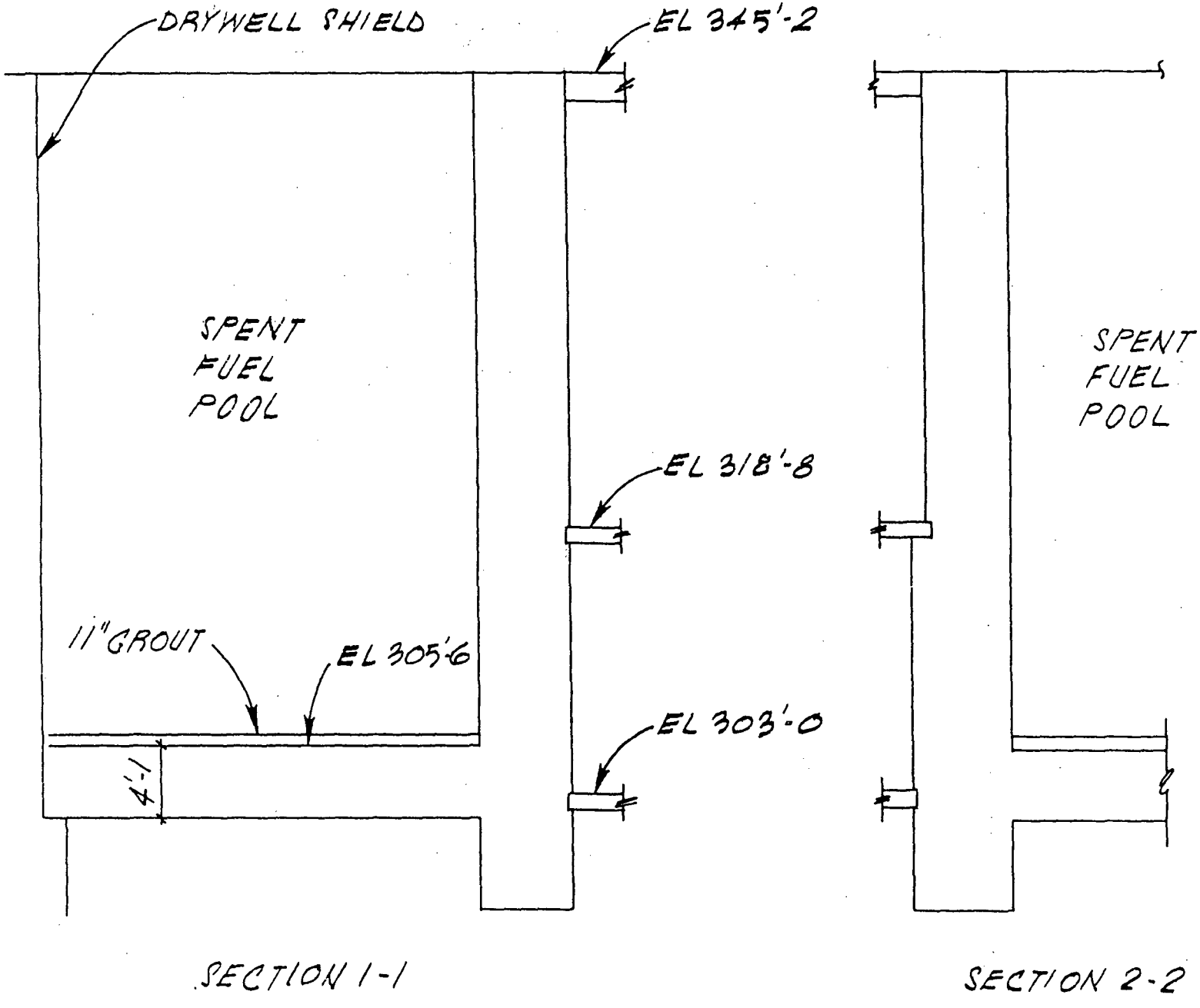

Figure 3-2: Cross-Sections of the Spent Fuel Pool

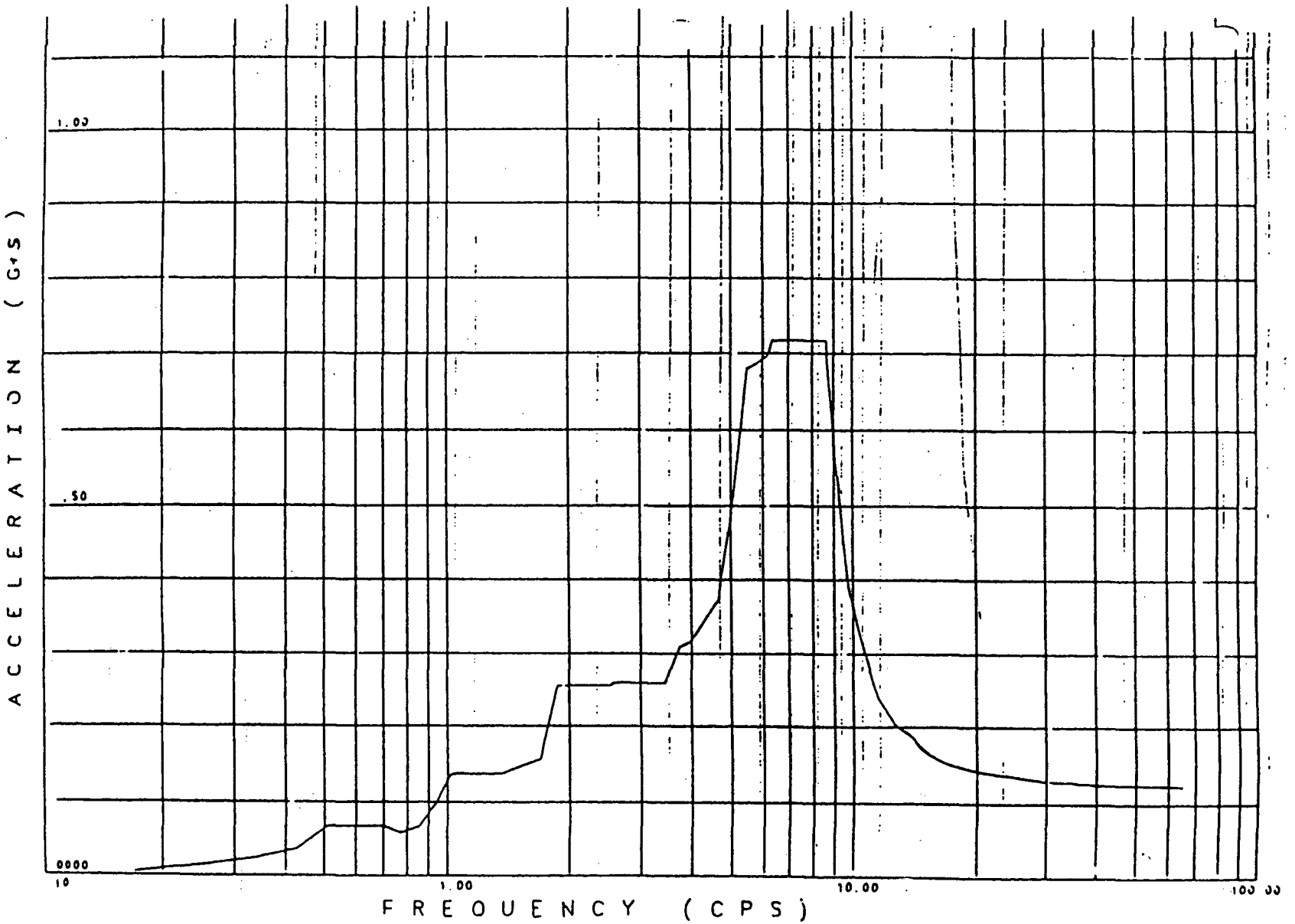

Figure 3-3: Reactor Building OBE Floor Spectrum, Elevation 303'-0", N-S Direction, 5% Damping

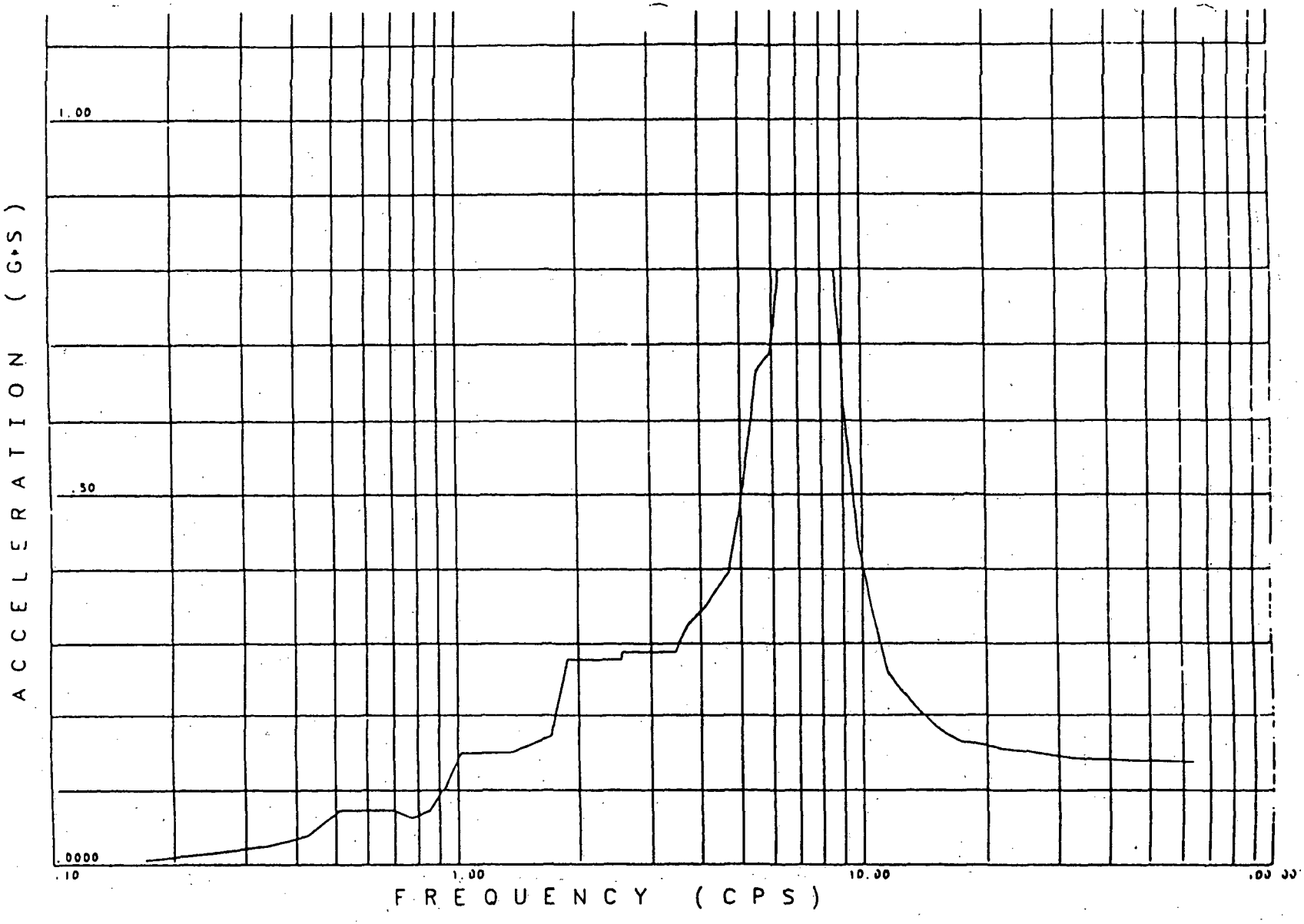

Figure 3-4: Reactor Building OBE Floor Spectrum, Elevation 303'-0", E-W Direction, 5% Damping

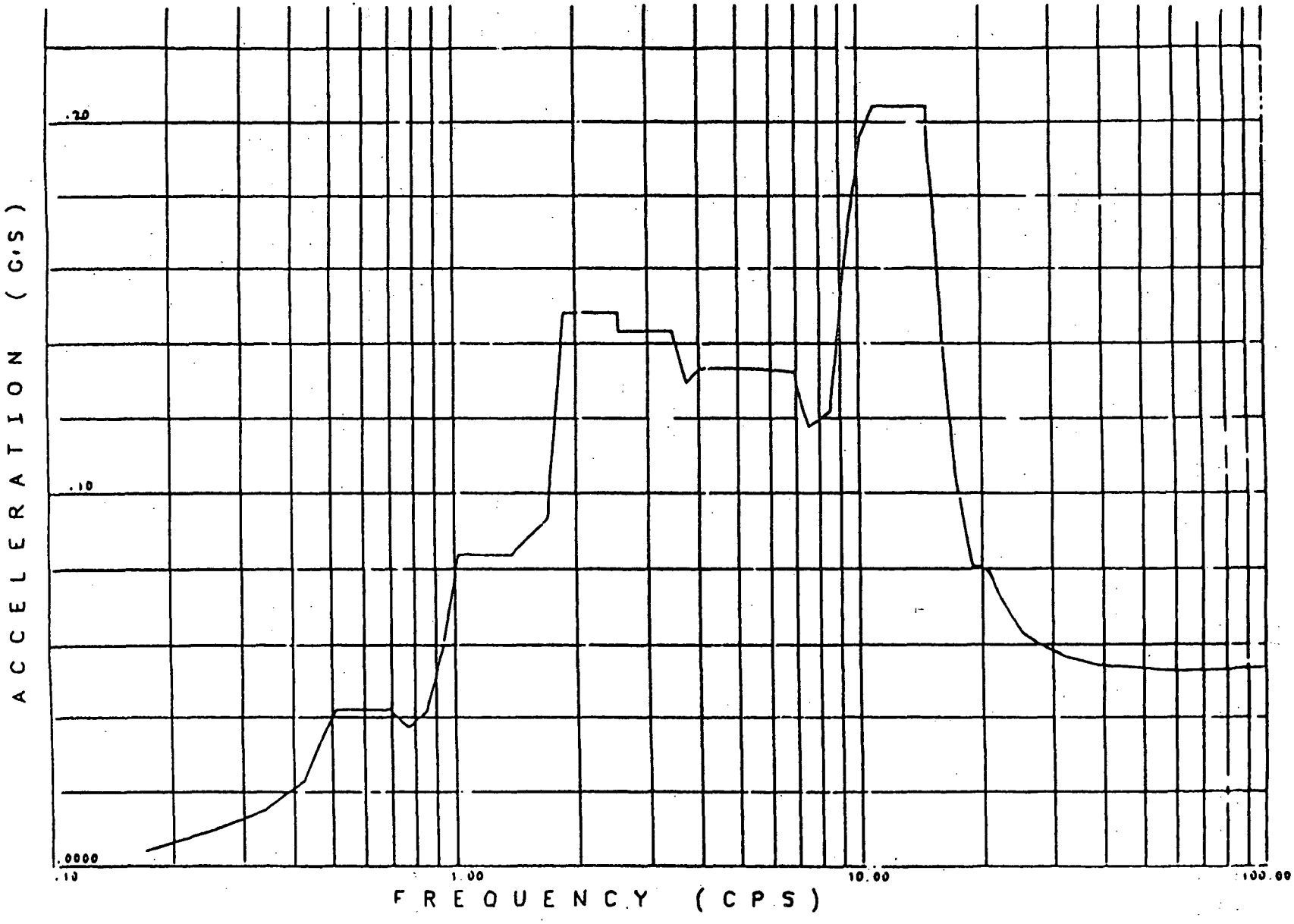

Figure 3-5: Reactor Building OBE Floor Spectrum, Elevation 303'-0", Vertical Direction, 5% Damping,

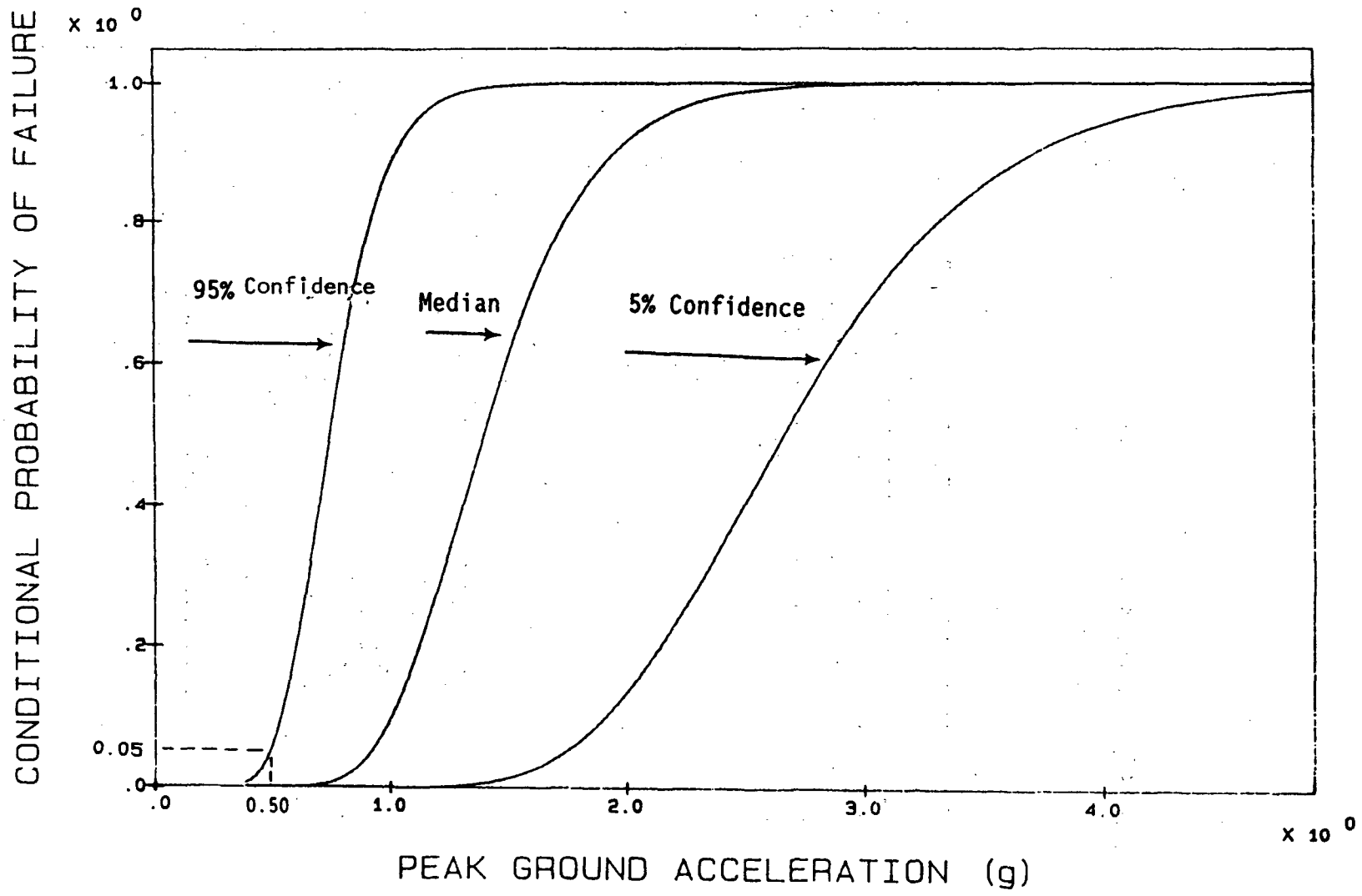

Figure 3-6: Spent Fuel Pool Structure Fragility

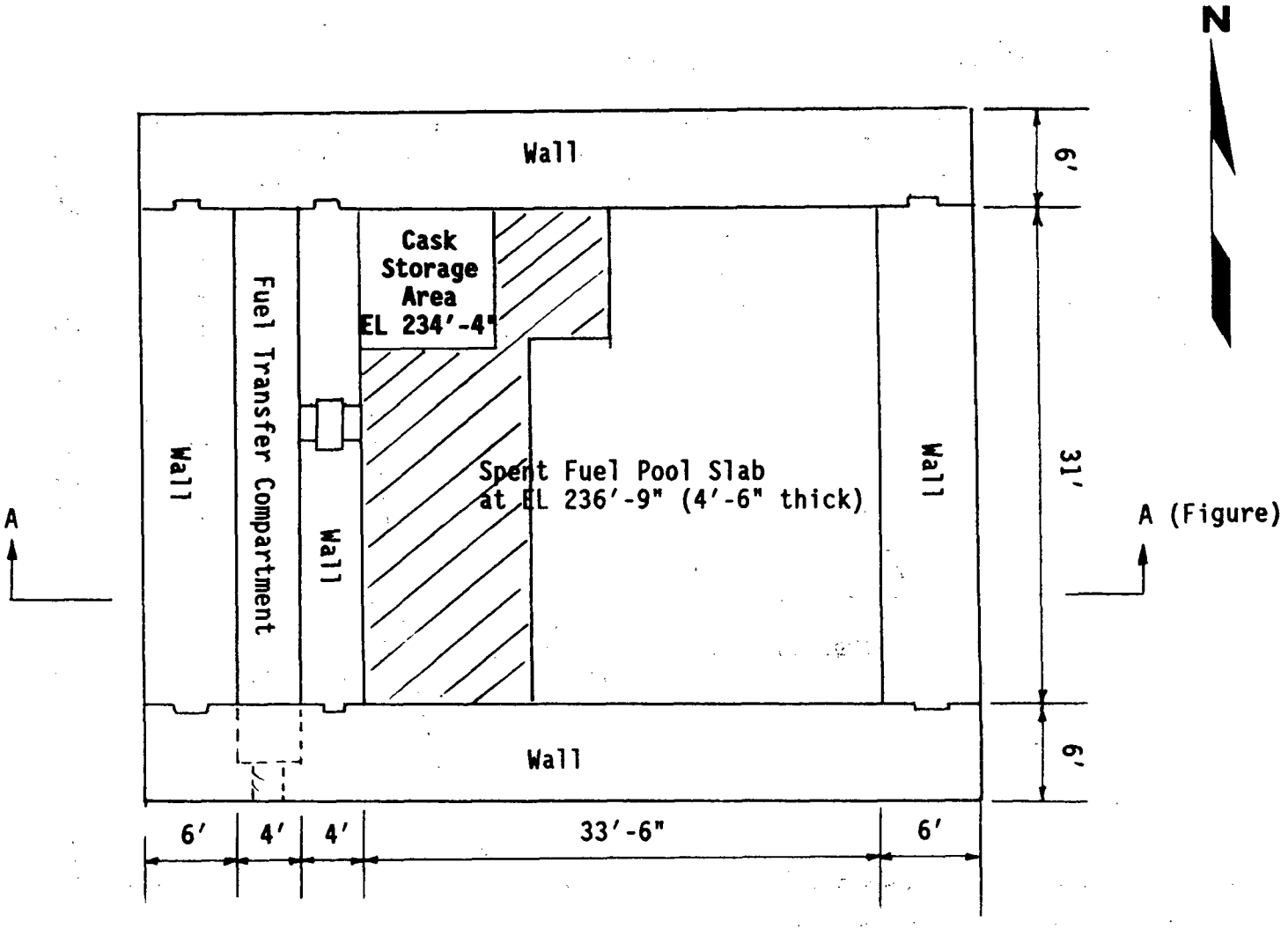

Note: Crosshatched Area Indicates High Density Fuel Storage Racks

Figure 3-7: HBR2 Spent Fuel Pool Slab at EL 236'-9" (Top of Slab)

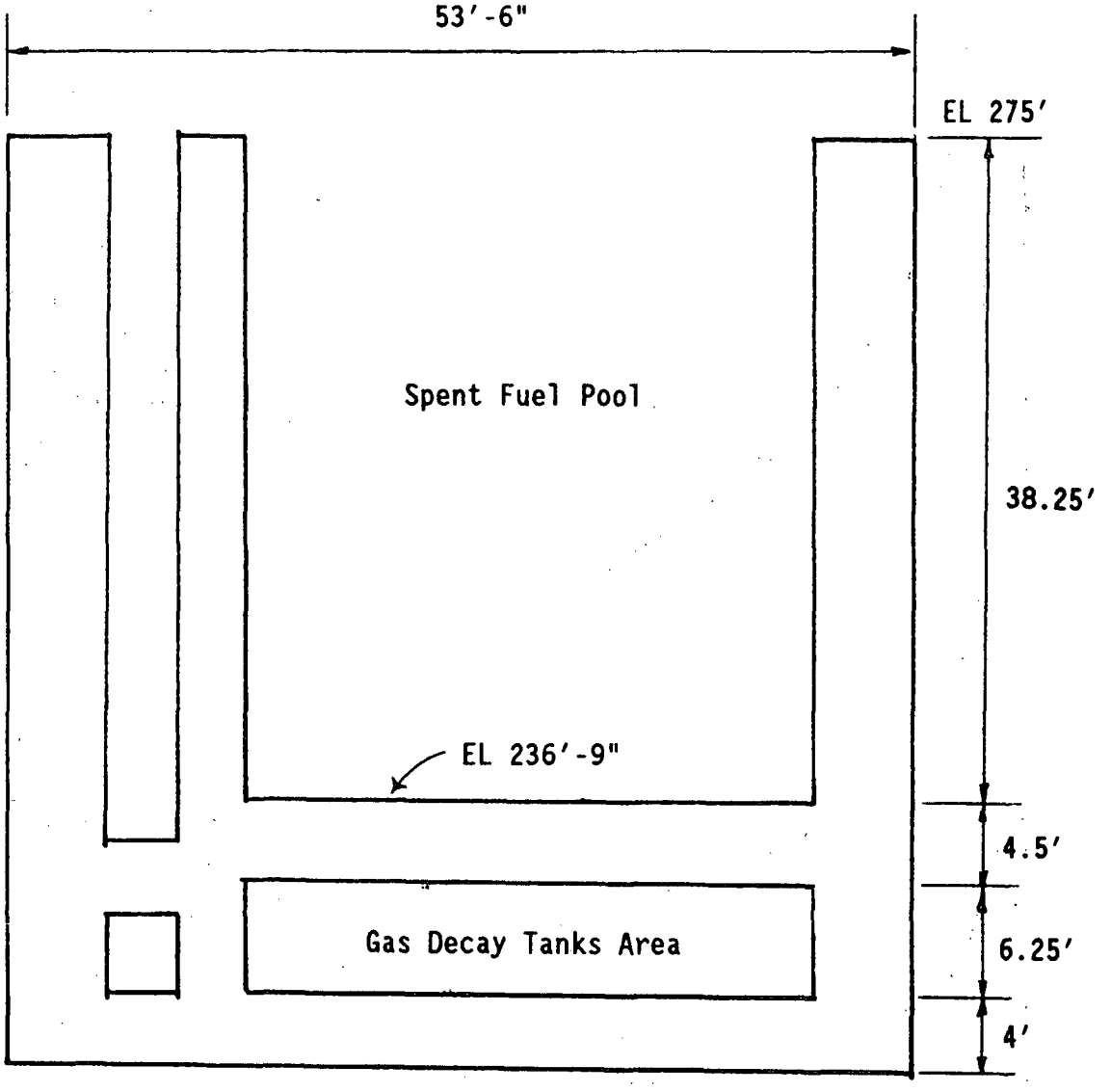

Section A-A

Figure 3-8: Cross Section of HBR2 Spent Fuel Pool

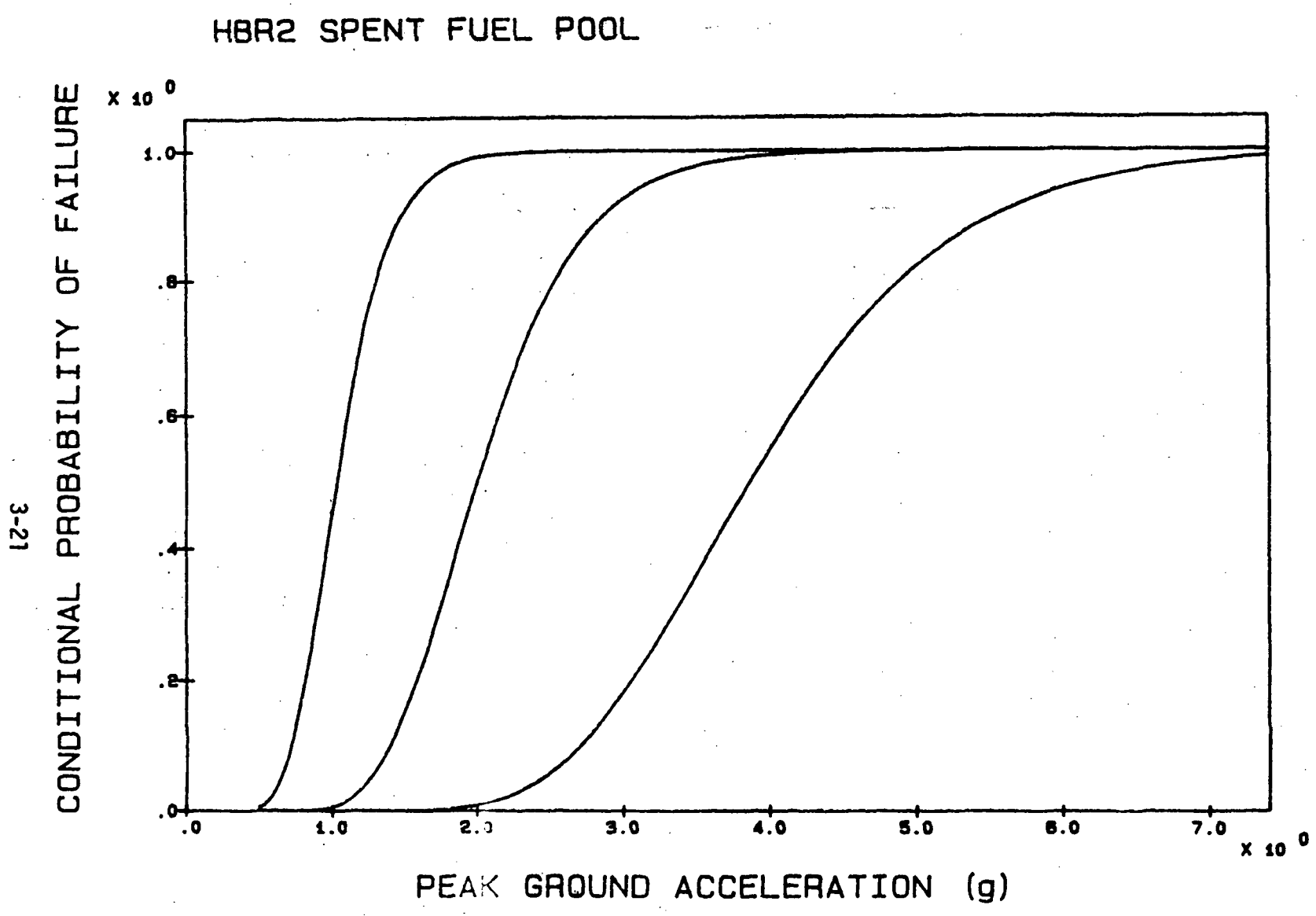

Figure 3-9: HBR2 Spent Fuel Pool Structure Seismic Fragility Curves

4. SPENT FUEL POOL SYSTEMS ANALYSIS

The spent fuel pool systems analyses was performed to gain an understanding of the seismic response and capacity of pool cooling and makeup water systems at selected nuclear power plants: Vermont Yankee Nuclear Power Station and H.B. Robinson, Unit 2, Nuclear Power Plant. The analyses follows a seismic margins approach utilizing the event tree, fault tree, and screening techniques discussed in Chapter 2.

The initiating event considered for this analysis is the occurrence of an earthquake at the plant site. As a result, loss of offsite power is assumed to occur due to the low seismic capacity of ceramic insulators in power plant switchyards. Emergency electrical power sources were assumed available for the analysis.

For the systems analysis, spent fuel pool failure is defined as loss of water inventory leading to spent fuel rupture or degradation and possible radioactive material release. Loss of pool inventory occurs due to water boil-off following the failures of the pool cooling system and the systems that provide water makeup. Loss of pool inventory can also occur due to leakage from the pool concurrent with failure of the makeup systems.

The scope of the systems analysis included only those front-line systems that perform the primary functions of pool cooling and inventory makeup, and the immediate systems or components that support these systems. The scope of this effort did not allow a complete analysis of all the support systems within the plant.

For the electrical support systems, only the cabinets, transformers, and motor control centers that contain the primary power sources for the front-line and support system components were included. The analysis of emergency electrical power sources was not relevant to this effort and was not performed.

For secondary cooling of spent fuel heat exchangers, only those components needed to perform secondary cooling were included. The complete analysis of the closed loop component cooling systems that perform fuel pool secondary cooling was not performed. In addition, the systems that provide cooling for these closed-loop component cooling systems, like service water systems, were not analyzed as part of this effort. An evaluation of these systems was performed for VYNPS and found to be not significant.

The remainder of this chapter describes the spent fuel pool systems analyses performed for this study. The analysis of the Vermont Yankee Nuclear Power Station is presented in Section 4.1 followed by the analysis of the H. B. Robinson Unit 2 Nuclear Power Plant (Section 4.2).

4.1 Analysis of the VYNPS SFP Systems

The Vermont Yankee Nuclear Power Station is a General Electric (GE) boiling water reactor (BWR) located outside of Vernon, Vermont. The Vermont Yankee plant commenced operation in 1972 with a rated output of 514 MWe.

The spent fuel pool (SFP) at Vermont Yankee is elevated above grade and forms part of the operating deck. The SFP concrete structure, metal liner and fuel storage racks are seismic category Class I. A description of the structure is given in Chapter 3. The plant is currently licensed to store a maximum of 2000 spent fuel assemblies using both low and high density fuel storage racks.

4.1.1 VYNPS SFP Systems Description

The fuel pool cooling and demineralizer system is shown in Figure 4-1 [VYNPS October 1985]. The cooling system transfers the spent fuel decay heat through heat exchangers to the reactor building closed cooling water system (RBCCWS) [VYNPS September 1985]. Water purity and clarity in the pool is maintained by circulation through a filter-demineralizer system shown in Figure 4-2 (VYNPS, FSAR).

The SFP cooling and demineralizer system consists of two circulating pumps connected in parallel, two heat exchangers, two filter-demineralizers, and the required piping, valves and instrumentation. Each pump has a rated capacity equal to the system design flow rate and is capable of simultaneous operation with the other pump. Two filter-demineralizers are provided, each with a design capacity equal to the design flow rate. The pumps circulate the pool water in a closed loop, taking suction from the pool, circulating the water through the heat exchangers and filters, and discharging through diffusers at the bottom of the pool. Water suction lines from the pool are equipped with anti-siphon valves or a series of holes located below the water surface to limit inadvertent pool drainage. Water discharge lines to the pool are equipped with check valves.

The SFP cooling system is designed to maintain the pool water temperature below 125 deg. F. during normal refueling operations. If the complete reactor core is discharged to the pool, the water temperature may increase to greater than the 125 deg. F. If this occurs, the RHR system using the train A heat exchanger can be used to supplement the SFP cooling system to maintain the pool temperature below 150 deg. F.

The RBCCW system provides cooling to the secondary side of the SFP heat exchangers [VYNPS September 1985, VYNPS, FSAR]. Figures 4-3 and 4-4 show the pertinent portions of the RBCCW system that provide this secondary cooling. The RBCCWS is a closed loop cooling system consisting of two 100% capacity pumps and two 100% capacity heat exchangers. A RBCCW surge tank is provided to accommodate differential expansion of the water and is located on the

suction side of the pumps. The system consists of four parallel cooling loops with the ability to isolate portions of the system to maintain essential cooling water services. Service water is used to cool the secondary side of the RBCCW heat exchangers.

Normal makeup to the pool is supplied from the condensate transfer system shown in Figure 4-5. Water removal from the pool via the pumps is through filter-demineralizer units to the condensate storage tank. Water makeup to the pool, however, can be provided by any of the following means (VYNPS ON3157):

- o normal pool fill line through valve DW-111 on the refueling floor, if radiation levels permit (from the demineralized water/storage tank (DWST), Figure 4-6).
- o 8-inch condensate transfer fill line through valve FPC-29.
- o charge any accessible fire hose and direct stream toward the pool.
- o if the reactor building is unaccessible, through valves CST-14A, FPC-SP25A and FPC-FCV-16A or CST-14B, FCP-SP25B and FPC-FCV-16B (from the condensate storage tank).
- o rotate the spectacle flange at FPC-50 and initiate service water makeup through RHR-183 and RHR-184, bypassing the pool demineralizers (from service water system).

The SFP instrumentation is provided for both automatic and remote manual operation to detect, record and control pump operation, pool temperature and level, and system flow. A pool leak detection system is provided to monitor pool leakage that consists of interconnected drainage paths behind the liner welds that lead to an instrumented collection system.

4.1.2 VYNPS SFP Systems Analysis

The analysis methodology is described in Chapter 2. An event tree was used to identify possible accident sequences that could lead to loss of water inventory. Fault trees were used to analyze the failure of the systems given in the accident sequences. The results of the systems analysis is a Boolean expression indicating the component failures that will lead to pool failure and possible radioactive material release.

4.1.2.1 VYNPS SFP Event Tree Analysis

The initiating event is the occurrence of an earthquake at the plant site. The event tree is then drawn for this initiating event. The VYNPS spent fuel pool event tree is shown in Figure 4-7. This event tree depicts the success or failure of gross pool structural integrity, water tight integrity (leakage), pool cooling and water makeup. These events are displayed across the top of the figure and given an alphabetic designation, A through E. Pool

water makeup was divided into two events on the event tree, primary water makeup and backup water makeup. The alphabetic designations are given below:

A = Gross pool structural integrity

B = Pool water tight integrity (leakage)

C = Primary pool water makeup

D = Pool cooling

E = Pool backup water makeup.

At each event in the tree, failure is represented by an upward branch and success by a downward branch. Each path through the event tree represents an accident sequence. Those sequences that end with a status of success indicate successful operation of the pool systems and adequate water inventory in pool following the initiating event. Those sequences with a status of failure indicate possible loss of pool water inventory and spent fuel uncover as a result of the earthquake. Total pool failure is the logical summation of the failure accident sequence.

Each event in the failure accident sequences is analyzed to determine its failure. Events that consist of systems failures are analyzed using fault trees. The result of the systems analysis is minimum cut sets and a Boolean expression for pool failure.

Inspection of the VYNPS event tree indicates that there are four accident sequences that lead to possible pool failure. These failure accident sequences are given below. Failure is indicated by the alpha designator (i.e. A), success is indicated by `not` preceding the alpha designator (notA).

S1 = A

S2 = notA B C E

S3 = notA B notC D E

S4 = notA notB C D E

The first failure sequence is S1, gross structural failure of the pool leading to complete loss of water inventory. This event is analyzed in Chapter 3.

The next accident sequence is S2. This sequence occurs following success of the gross pool structure integrity but loss of pool water tight integrity and complete failure to provide makeup water to the pool. Loss of water tight integrity of the pool is defined as pool leakage resulting from partial pool structural failure or the failure of the piping connected to the pool requiring both primary and backup water makeup to keep the spent fuel

covered. Notice in this accident sequence, pool cooling is not considered since this function will not replace the water leaking from the pool.

The next accident sequence, S3, occurs following success of gross pool structural integrity and primary water makeup but failure in pool water tight integrity. Pool failure occur due to failure of both pool cooling and backup water makeup. If loss of fuel pool water tight integrity is defined as above, pool cooling should not make a difference, since cooling will not supply water to the pool.

This situation was considered in more detail by performing a conservative thermal analysis of the pool to estimate the timing involved for water boil-off due to loss of pool cooling. Two failure states were considered that correspond to the cooling requirements of the pool:

Pool State 1 (PS1): Maximum number of fuel subassemblies in the fuel pool as presently licensed (2000), approximately 1/3 of a reactor core recently discharged to the pool, reactor operational and at power, recently discharged fuel has undergone maximum fuel burn-up.

Pool State 2 (PS2): Maximum number of fuel subassemblies in the fuel pool as presently licensed (2000), full core discharge to the pool 10 days after reactor shutdown, fuel has undergone at least 30 days burn-up at full power, reactor is down for inspection or maintenance.

Both analyses assumed all decay heat went into heating and boiling the pool water. No heat transfer was considered to the pool walls or out of the pool surface. The thermal analysis is given in Appendix A.

The results of the thermal analyses indicate that for PS1, it would take about seven days for the pool water to heat up and boil-off such that the pool level would decrease to the top of the spent fuel bundles following the loss of pool cooling. For PS2, the time for the level to decrease to the top of the spent fuel bundles was estimated to be about three days following the loss of pool cooling.

In light of the long lead times, it was considered that for accident sequences with coolant makeup from the primary makeup water source and successful operation of the pool cooling system, there would be sufficient time to obtain additional pool makeup water. Therefore, these accident sequence were considered as successes and not analyzed further.

The last accident sequence, S4, occurs following the success of both gross pool structural and water tight integrity. The failure sequence results from complete loss of water makeup and pool cooling.

4.1.2.2 VYNPS Fault Tree Analysis

For the pool failure accident sequences, fault tress were developed for each of the front-line system failures. Fault trees were also developed for the

support systems to the front-line systems. The individual fault trees were then combined with respect to the accident sequence to analyze pool failure. The individual fault trees were also analyzed separately.

The fault tree analysis was carried out using the FTAP computer code [R. R. Wylie Computer Aided Fault Tree Analysis, Operation Research Center, Universidy of California, August 1978] which gives the combination of single (first order), double (second order), etc., component failures that lead to the top event. The analysis of the fault trees was limited to the consideration of cut sets up to fourth order (consisting of, at most, four component failures). Cut sets greater than fourth order were not considered.

The overall pool failure cut sets were then inspected for components with HCLPF capacity greater than 0.3g. If a cut set was found to contain a high capacity component, it was eliminated from further consideration. The remaining cuts sets were then combined into the Boolean expression for overall pool failure.

Front-line system fault trees were developed for;

- o loss of water tight integrity
- o loss of primary water makeup
- o loss of pool cooling from SFP cooling system
- o loss of pool cooling from RHR system
- o loss of backup makeup

Support system fault trees were developed for;

- o loss of secondary cooling to the SFP heat exchanger (failure of the RBCCW system to support the secondary cooling)
- o loss of the secondary cooling to RHR heat exchanger A (failure of the RHR service water system to support secondary cooling)

The fault trees for these systems are given in Appendix B. The scope of the fault trees include only those immediate components that support the operation of the front-line and support systems. The components used in the construction of the fault trees are listed on Table 4.1.

The fault tree for loss in pool water tight integrity considered failures consisting of pipe breaks, failures of anchorages on heat exchangers, pumps, and the demineralizer tanks leading to piping breaks and failures of check valves and anti-siphon valves from stopping or limiting pool drainage. The

analysis of this fault tree indicated that there were nine second order cut sets consisting of either pipe breaks or equipment anchorage failures coupled with failures of either check valves or anti-siphon valves. There were thirteen third order cut sets.

The fault tree for loss of primary water makeup consists of failures in makeup from the demineralized water systems (DWS) and the condensate storage system (CSS) along with a failure of the pool level instrument to indicate makeup is needed. The DWS component failures consist of demineralized water storage tank failure, the transfer pumps and human errors in not manually aligning the DWS for SFP makeup. The CSS component failures consist of similar events. Transfer pump failures consist of associated anchorage failure or motor control center failure.

The analysis of the primary water makeup fault tree indicated that there is one single order cut set and six second order cut sets along with several high order cut sets. The single order cut set consisted of failure of the pool level alarm system to indicate loss of water inventory. The second order cut sets consist of combinations of opposite system (DWS and CSS) failures in tanks, electrical power and human errors in aligning manual makeup water valves.

The spent fuel pool cooling system fault tree considers failures in pool suction from alternate paths, failures in the parallel pump/heat exchanger arrangement and failures in the two parallel demineralizer-filters. The demineralizer-filters also have a bypass line that was included in the model. The component failures consist of a clogged strainer, inadequate anchorage, human error, loss of electrical power and failure of secondary cooling to the SFP heat exchangers.

The loss of secondary cooling to the SFP cooling system heat exchangers was determined by developing a fault tree for the RBCCWS which provides this function. This fault tree considers failures in the two parallel RBCCW pumps, the two parallel heat exchangers, and failure of the RBCCW surge tank. The component failure consist of inadequate anchorage, loss of electrical power and failure of secondary cooling to the RBCCW heat exchangers which is provided by the service water system (SWS). The loss of secondary cooling to the RBCCW heat exchangers (failure of the SWS) was not developed further.

The analysis of the SFP cooling fault tree after combining it with the RBCCWS fault tree indicated that there is one single order cut set, sixteen double order cut sets, twelve third order cut sets, and one fourth order cut. The singleton failure was the RBCCW surge tank. The doubleton failures consisted of combinations of opposite SFP pump train failures in pump and heat exchanger anchorage and electrical power.

Spent fuel pool cooling provided by the RHR system was analyzed by developing a RHR fault tree. This fault tree considers human error in properly aligning the RHR system for pool cooling, failures of the two RHR pump trains with associated motor operated valves (MOV) and failure of the RHR A heat exchanger

to provide pool cooling. The component failures consist of anchorage failure and loss of electrical power to the pumps and MOVs.

Loss of secondary cooling to the RHR A heat exchanger was analyzed by developing a fault tree of a portion of the dedicated RHR service water system which provides this function. This fault tree considers failure to properly align the RHR A secondary cooling MOV, which automatically closes on loss of electrical power and requires manual opening, failure of the two pumps within this system to provide cooling flow and failure of the normal service water system which can provide this function. The normal SWS was not analyzed. The component failures consist of anchorage failure and loss of electrical power.

The analysis of the RHR pool cooling fault tree after combination with the RHR SWS tree indicated there are five single order cut sets, twenty second order cut sets, eight third order cut sets and one fourth order cut set. The single order cut sets consisted of human error in aligning the RHR system for pool cooling, MCC 9B failure and RHR A heat exchanger anchorage failure.

The fault tree for the loss of backup water makeup to the SFP considers makeup from the fire water system, the SWS and an alternate path from the CST (through valves SP-25A(B) and CST-14A(B)). Due to the long recovery time, failure of the fire water system and SWS to provide makeup to SFP was not analyzed. Therefore, this fault tree only consisted of human errors in properly aligning an alternate makeup water path from the CSS. The analysis of this fault tree indicated that there is one first order cut set and ten second order cut sets. The singleton is failure of the CST. The doubletons consist of combinations of electrical power and anchorage failures from the two trains of the CSS system.

4.1.2.3 VYNPS Accident Analysis

The development of a Boolean expression for the SFP involves combining the individual fault trees as indicated by the failure accident sequences and logically summing over all the sequences. This logical summation is accomplished by developing a high level fault tree for pool failure consisting of the four failure accident sequences given in Section 4.1.2.1.

Two overall high level pool fault trees were developed. One for each of the Pool States discussed in Section 4.1.2.1 because of the different pool cooling requirements. For PS1, pool cooling is accomplished by the SFP cooling system. The high level fault tree for PS1 is shown in Figure 4-7.

For PS2, the SFP cooling system is not adequate and the RHR system is required to cool the pool. The high level fault tree for PS2 is shown in Figure 4-8.

The high level fault trees were analyzed to obtain the cut sets for pool failure. The analysis considered cut sets only up to fourth order. The results of the analysis indicated that for PS1 case, there was 1 first order cut set, 135 fourth order cut sets and over 20,000 higher order cut sets. For the spent pool with fuel loading described by the assumption of PS1, pool

failure result from gross structural failure or many combinations of component failures, one from each the four system that support the pool: primary water makeup, pool cooling from the SFP cooling system, pool cooling from the RHR system and backup water makeup.

For the PS2 case, there was 1 first order cut set, 35 third order cut sets, 365 fourth order cut sets and over 20,000 higher order cut sets. Spent fuel pool failure with a fuel loading as assumed by PS2 results from gross structural failure, or many combinations of component failures, one from each of the three system that support the pool: primary water makeup, pool cooling from the RHR system and backup water makeup. Pool cooling from the SFP cooling system was not sufficient under the condition of PS2.

Each third and fourth order cut set was examined and those cut sets containing high capacity component were eliminated. The remaining cut sets were combine into the Boolean expressions for each pool state given below:

PS1 = 12 + (7 + 11 + 1 * 2) * (5 * { 4 + 9 + 8 + 10)

+ 4 * { 3 + 6 })

PS2 = 12 + (7 + 11 + 1 * 2) * (4 + 9 + 10)

where the number represent the component seismic fragilities and random failure rates given in Table 4.2. It may be noted that components 1, 2, 7, and 11 are all in the non-safety electrical systems of the plant.

4.2 Analysis of the H. B. Robinson Unit 2 (HBR2) Spent Fuel Pool Systems

The H. B. Robinson Steam Electric Plant, Unit 2 is a Westinghouse pressurized water reactor (PWR) located near Hartsville, South Carolina. The H. B. Robinson plant commenced commercial operation in 1971 with a rated output of 665 MWe.

The spent fuel pool at HBR2 is elevated and forms a separate structure from the containment and auxiliary building. The SFP structure is seismic category Class I with a stainless steel liner of all welded construction. A description of the SFP structure is given in Chapter 3.

Fuel subassemblies are transferred to and from the pool via a fuel transfer tube that connects the SFP structure with the containment building. The pool is licensed to store 544 spent fuel subassemblies using both low and high density storage racks.

4.2.1 HBR2 SFP Systems Description

The Spent Fuel Pool Cooling and Purification System consists of the pool structure and piping loops through which borated water is circulated to remove

decay heat dissipated from the spent fuel subassemblies and through filter/demineralizers as a means to purify and maintain water clarity [HBR2 November 1986]. The SFP Cooling and Purification System is shown in Figure 4-9.

The SFP cooling system consists of two 100 percent capacity pumps, one heat exchanger, filter, demineralizer, associated valves and piping, and instrumentation. The two SFP cooling pumps, one operating and the other as backup, draw water from the pool to circulate through the heat exchanger and return to the pool. The demineralizer is sized to pass 5 percent of the loop flow and the purification loop can be used to circulate water from the refueling water storage tank (RWST) in a loop back to the RWST using the refueling water purification pump.

The SFP pumps are manually controlled locally or from the SFP operating deck. Two emergency connection are provided across the SFP pumps. One at the suction of pump "B" and the other downstream of the pumps to allow the use of another "portable" pump for cooling under abnormal condition.

The pool has two suction lines to the pumps. The upper suction line penetrates the pool wall four feet below the normal water level and about nine feet above the top of the spent fuel assemblies. The other suction line is located at the bottom of the pool and provides for complete pool drainage. This line is equipped with a closed and locked valve inside the pool to prevent drainage if an external severance of this line should occur. The bottom line is also equipped with an external closed and locked valve.

The return piping to the pool, from the pumps, discharges at six feet above the fuel assemblies and is equipped with a 1/2 inch hole, six inches below the normal water level to serve as a vacuum breaker to prevent siphoning.

The SFP cooling system is designed to maintain the pool water temperature below 120 deg. F. during normal refueling operations when 1/3 of a core is discharged to the pool. During the discharge of a complete reactor core into the pool, the water temperature is maintained at or below 150 deg. F. (HBR2 FSAR). Should the pool water temperature exceed 150 deg. F., fuel assemblies are transferred back to the reactor cavity until the temperature falls to 150 deg. F. or less.

During normal operations the SFP pool water level is maintained at 22 ft. 5 in. above the fuel assemblies. The pool water level is monitored continuously with alarm set points at 2 inches above and 7 inches below the normal water level.

The component cooling system provides cooling to the secondary side of the SFP heat exchanger. The component cooling water (CCW) system is a closed loop cooling system consisting of three pumps, two heat exchangers, a surge tank, and the associated piping, valves and instrumentation [HBR2 June 1987].

During normal full power operation, one CCW pump and one heat exchanger accommodates the heat removal loads. All three pumps and two heat exchangers are needed to remove sensible and residual heat during plant shutdown.

Component cooling water is supplied to the SFP heat exchanger to maintain pool temperature within specified limits. Temperature is control by throttling a manual valve on the outlet of the heat exchanger. Emergency cooling connections are provided across the secondary side of the SFP heat exchanger so an external cooling system (i.e. fire system) can be used if the CCW has to be isolated.

The service water system (SWS) supplies secondary cooling to the CCW heat exchangers. The SWS was not modelled as part of the systems analysis of the HBR2 spent fuel pool.

Normal water makeup to the pool [HBR2 April 1985] is supplied from the refueling water storage tank (RWST) via the refueling water purification (RWP) pump. The reactor coolant drains pump can also deliver water to the RWP pump from the reactor coolant drains tank. Makeup water can also be provided to the pool from the condensate storage tank (CST) via the demineralized water pump (DW) delivered directly to the SFP purification loop or to a service connection (faucet) at the operating deck the fuel handling building.

The SFP instrumentation is provided for remote manual operation to detect, record and control pump operation, pool temperature and level, and system flow. A pool leak detection system is provided to monitor pool leakage that consists of 10 one-inch diameter pipes embedded in the concrete along the bottom of the pool where the walls join the floor behind the liner. These pipes are interconnected and lead into a valved end. The leak detection system is checked daily during shift change to monitor pool leakage.

4.2.2 HBR2 Systems Analysis

The HBR2 systems analysis follows the same general process that was used in the VYNPS analysis. The systems analysis of the HBR2 spent fuel pool utilized a seismic margins screening approach as described in Chapter 2. An event tree was developed to identify possible accident sequences that could lead to loss of pool water inventory. Fault trees were used to analyze the failure of the systems given in the accident sequences.

4.2.2.1 HBR2 Event Tree Analysis

The HBR2 spent fuel pool event tree is shown in Figure 4-10. This event tree was developed with consideration of an earthquake at the plant site as the initiating event and depicts the success or failure of gross pool structural integrity, water tight integrity (leakage), pool cooling and makeup water. These events are displayed across the top of the event tree and given alphanumeric designators as shown.

Inspection of the HBR2 event tree indicates that there are three accident

sequences that lead to possible complete loss of water inventory. These three accident sequences are given below. Failure is indicated by the alphanumeric designator (i.e. W), success is indicated by 'not' preceding the alphanumeric designator (notW).

AS1 = W

AS2 = notW X Z

AS3 = notW notX Y Z

The first accident sequence is AS1, gross failure of the spent fuel pool structure which results in the complete loss of pool water inventory. This event is analyzed in Chapter 3.

The next accident sequence is AS2. This accident sequence occurs following an earthquake where the spent fuel pool has survived a gross failure but the water tight integrity of the pool has not been maintained. Pool leakage occurs through possible pipe breaks or severe leakage from the pool liner. Pool leakage occurs over a relatively long time, however, pool make-up is required to prevent fuel uncover, damage and possible radioactivity release. SPF failure occurs from seismic failure of the water make-up systems.

The third accident sequences is AS3, which occurs following an earthquake where pool water tight integrity has been maintained. Fuel uncover, damage and possible radioactivity release occurs from failure to cool the water in the pool resulting in water boil-off and failure to provide make-up water in the event cooling fails. If pool cooling is successful or the pool makeup systems are available, then SFP success is maintained.

A thermal analysis of the HBR2 SFP was reviewed in [USNRC 1982]. This review indicated that with the maximum heat load in the pool (full core discharge), the time it would take for water temperature to rise from its allowable maximum temperature of 150 deg. F. to boiling would be 6.83 hours and that the boil-off rate would be 41.23 gpm (5.51 cu.ft./min.). Using this boil-off rate and the water heat time, it takes about 3.2 days for the pool inventory (23352.7 cu. ft.) to decrease to the top of the fuel assemblies (22.41 ft.) after a full core discharge to the pool following loss of pool cooling and water make-up.

4.2.2.2 HBR2 Fault Tree Analysis

Fault trees were developed for those front-line and support systems failures that were indicated in the accident sequences derived from the event trees. Front-line system fault trees were developed for:

- loss of SFP cooling, and
- loss of water make-up to the pool.

A support system fault tree was developed for failure to supply secondary cooling to the SFP heat exchanger. The HBR2 fault trees are given in Appendix C. The component that were used to develop these fault trees are given in Table 4.3.

The fault tree analysis considered only those component and systems that support the operation of the front line systems. The service water system that provides secondary cooling to the CCW system was not analyzed.

The loss of water tight integrity event was not modeled. Pipe breaks and tank failures were considered in the other two fault trees for the SFP systems that are connected to the pool water.

The SPF cooling fault tree considers failure of the SFP heat exchanger to provide cooling and failure of the SFP pumps to circulate the cooling flow. The component failures consist of inadequate anchorages on the heat exchanger and the pumps, loss of electrical power, failure of the pool temperature instruments to indicate temperature increase, human error in properly aligning the alternate pump and cooling loop pipe failure.

The loss of secondary cooling to the SFP heat exchanger was determined by developing a fault tree of the component cooling system that provides this function. The CCW fault tree considers failure of the CCW pump to provide cooling flow, failure of the CCW surge tank, and failure of the CCW heat exchangers. The component failures consist of inadequate anchorage of the CCW pumps and heat exchangers, loss of electrical power, human error in properly aligning the alternate pumps and heat exchangers and failure to utilize the fire water system for alternate cooling of the SFP heat exchanger secondary. The fire water system was assumed available and not analyzed.

The analysis of the SFP cooling fault tree indicated that there were four first order cut sets, 2 second order cut sets and 26 third order cut sets. The first order cut sets were pipe breaks, failure of the CCW surge tank and failure of the SFP heat exchanger. The second order cut sets consisted of a combination of the temperature instrument failure and pump failures. One pump fails because of inadequate anchorage and the other due to failure in electrical power. Failure in the temperature instrument results in no indication of pool heat up and thus no alignment of an alternate cooling path for the pool.

The loss in water make up fault tree considered failure of pool make up through the purification loop utilizing the refueling water purification pump and failure to provide make up flow from the faucet located on the SFP operating floor. Component failures consist of inadequate anchorage on the RWP pump and the demineralizer. Water pump, failure of the condensate storage, refueling water storage and demineralizer tanks, loss of electrical power, failure in pool level and area radiation instruments and human error in properly aligning the primary and alternate make up water paths.

The analysis of the pool water inventory make up fault tree indicates that there are 21 second order cut sets. These cut sets consist of combinations of failures in the systems that monitor and supply make up water to the pool. Double component failures of the CST, RWST, demineralizer tank, electrical power cabinets, pump anchorage, level sensor and area radiation monitor, and human error in properly aligning the make up supply.

4.2.2.3 HBR2 Accident Analysis

The development of the Boolean expression for the SFP involves combining the individual fault trees as indicated by the accident sequences and logically summing over all the sequences. For the HBR2 analysis, the summation was accomplished by a logical union of the three accident sequence equations.

The analysis resulted in one first order cut set, 29 second order cut sets, 84 third order cut sets and 92 fourth order cut sets. The first order cut set was gross failure of the pool structure leading to complete loss of pool inventory. Each cut set was examined, and those containing high capacity component were eliminated. The remaining cut sets were combined into the Boolean expression for pool failure given below:

HBR2 pool failure = 1 + (4 + 5 + 7 + 9) * (6 + 8 + 12)

where the numbers represent component seismic fragilities and random failure rates given in Table 4.4.

Table 4.1

Components of VYNPS Spent Fuel Pool Systems

Description
MCC 7b fails (SS Transformer 7)
MCC 7C fails (SS Transformer 7)
MCC 8b fails (SST 8)
MCC 9b fails (SST 9)
SWGR 8 fails (SST 8)
SWGR 9 fails (SST 9)
4160 SWGR bus fails (SST 3)
4160 SWGR bus 4 fails (SST 4)
no SFP low level alarm
condensate storage tank fails
demineralized water storage tank fails
ops fails to open manual valve DW-111
ops fails to open manual valve CST-14a
ops fails to open manual valve CST-14b
ops fails to open manual valve SP-25a
ops fails to open manual valve SP-25b
ops fails to open manual valve FPC-28
ops fails to open manual valve FPC-29
ops fails to open manual valve DW-35c
ops fails to open manual valve V-53
condensate transfer pump P-4-1a fails
condensate transfer pump P-4-1b fails
demin transfer pump P-63-1a fails
demin transfer pump P-63-1b fails
rbccw pump P-59-1a fails
rbccw pump P-59-1b fails
rbccw heat exchanger E-8-1a fails
rbccw heat exchanger E-8-1b fails
rbccw surge tank TK-7-1a fails
RHR heat exchanger E-14-1a fails
ops fails to open MOV V-13a
ops fails to open MOV V-13c
ops fails to open MOV V-15a
ops fails to open MOV V-15c
ops fails to open MOV V-89a
ops fails to open manual valve V-25
ops fails to open manual valve V-50

Table 4.1
(Continued)

Components of VYNPS Spent Fuel Pool Systems

Description
RHR pump P-10-1a fails
RHR pump P-10-1c fails
SWS RHR pump P-8 1a fails
SWS RHR pump P-8-1e fails
SFP demineralizer/filter DM-2-1a fails
SFP demineralizer/filter DM-2-1b fails
SFP heat exchanger E-9-1a fails
SFP heat exchanger E-9-1b fails
ops fails to open manual valve V-39
ops fails to open manual valve V-46
ops fails to open manual valve SF-77
SFP cooling pump P-9-1a fails
SFP cooling pump P-9-1b fails
fuel pool outlet strainer fails (clogged)
dmin/filter DM-2-1a strainer S-12-1a fails
dmin/filter DM-2-1b strainer S-12-1b fails
dmin/filter DM-2-1a fails causing pipe break
dmin/filter DM-2-1b fails causing pipe break
HTX E-9-1a fails causing pipe break
HTX E-9-1b fails causing pipe break
pump P-9-1a fails causing pipe break
pump P-9-1b fails causing pipe break
pipe break in segment fpc-19 below RHR connection
anti-siphon valve SF-11 fails
check valve V-18 fails
check valve V-21a fails
check valve V-21b fails
undeveloped event-failure of fire water system to provide make-up
station service transportation

Table 4.2

VYNPS SFP Component Failures

Number	Component Failure
1	Seismic failure of MCC 7B
2	Seismic failure of MCC 7C
3	Seismic failure of MCC 8B
4	Seismic failure of MCC 9B
5	Seismic failure of RBCCW Surge Tank (TK-7-1A)
6	Seismic failure of the SFP Heat Exchanger (E-9-1A)
7	Seismic failure of the Station Service Transformer (SST 7)
8	Operator fails to open motor operated valve (MOV V-89A)
9	Operator fails to open manual valve (V-25)
10	Operator fails to open manual valve (V-50)
11	Seismic failure of Switchgear (4160V SWGR Bus 4)
12	Gross seismic failure of the SFP Structure

Table 4.3

H. B. Robinson 2 Nuclear Power Plant
Component List

SPENT FUEL POOL COOLING (SFPC) SYSTEM

Valves

type	designation	position*
MV	SFPC-796	NO
MV	SFPC-836A	NO
MV	SFPC-793	LC
MV	SFPC-797	NC
MV	SFPC-837	NO
MV	SFPC-836	NO
MV	SFPC-819	NO
CV	SFPC-820	--

Pumps

SFPC Pump A - 480v Bus No.3
SFPC Pump B - 480v Bus No.1

SFPC Heat Exchanger

Instruments

Pool Level - LA-651
Pool Temperature - TIC-651
SFPC HTX Temp. - TI-653

PURIFICATION LOOP OF SFPC SYSTEM

Valves

type	designation	position
MV	SFPC-798A	NO
MV	SFPC-800A	NC
MV	SFPC-799B	NC
MV	SFPC-799C	NC
MV	SFPC-801	NO
MV	SFPC-811	NO
MV	SFPC-812	NO
MV	SFPC-813	NO
MV	SFPC-800B	NC
MV	SFPC-798B	NO

*See legend at end of table.

Tanks
SFP Pit Demineralizer

Filter
SFP Filter

Instruments
Pressure - PI-670
PI-655A
PI-656A
PI-656B
Flow - FI-654
FE-654

SFPC MAKE-UP WATER

From the Condensate Storage Tank (CST)
(SFPMU-CST)

Valves

type	designation	position
MV	SFPC-808	LC
MV	DW-255	NO
MV	DW-252	NO
CV	DW-293	--
CV	DW-290	--

Tanks
Condensate Storage Tank (CST)

Pumps
Demineralized Water Pump - 120v/208v MCC No.8

From the faucet in the SFP Pit
(SFPMU-FA)

Valves

type	designation	position
MV	DW-269	NC
MV	DW-267	NO
MV	DW-257	NO

Hose stored in SFP Pit area

Instruments
Flow - FI-6420

From the Liquid Disposal System
(SFPMU-LDS)

Valves

type	designation	position	failure mode
AOV	LCV-1003A	NC	fails closed
AOV	LCV-1003B	NC	fails closed
AOV	FCV-1018A	NO	fails closed
AOV	WD-1721	NO	fails closed
AOV	FCV-1018B	NO	fails closed
AOV	WD-1722	NO	fails closed
CV	WD-1724	--	---
CV	WD-1725	--	---

Tanks
Reactor Coolant Drain Tank (RCDT)

Pumps
Reactor Coolant Drain Pump A - 480v MCC No.2
Reactor Coolant Drain Pump B - 480v MCC No.1

Instruments
Pressure - PI-1018A
PI-1018B

Temperature- TE-1058

From the incoming header IVSW between FCV 1018A & 1018B
(SFCMU-IVSW)

Valves

type	designation	position
MV	SFPC-804	NC
MV	SFPC-802A	NO
CV	SFPC-803	--

Pump
Refueling Water Purification (RWP) Pump - 480v MCC No.1

From the RWST
(SFPMU-RWST)

Valves

type	designation	position
MV	SFPC-805A	NO
MV	SFPC-805B	NO

Tanks
Refueling Water Storage Tank (RWST)

SECONDARY SIDE TO THE SFP HEAT EXCHANGER
(SFP-HTX-CCS)

Component Cooling System (CCS) Components

Valves

type	designation	position
MV	CC-701A	NO
MV	CC-701B	NO
MV	CC-701C	NO
MV	CC-703A	NO
MV	CC-703B	NO
MV	CC-703C	NO
MV	CC-710	LO
MV	CC-713A	CO
MV	CC-713B	CO
MV	CC-712A	CO
MV	CC-712B	CO
MV	CC-772	NO
MV	CC-776	CO
MV	CC-775	NO

Pumps
Component Cooling
Pump A - 480v Dedicated Shutdown Bus
Pump B - 480v Bus No.E1
Pump C - 480v Bus No.E2

Component Cooling Heat Exchangers
CC HTX A
CC HTX B

Tank
Component Cooling Water Surge Tank

Instruments
flow element - FE-622

Temperature - TI-621

Service Water Cooling to Secondary Side of Component Cooling Water System

Valves

type	designation	position	failure mode
MOV	V6-12B	NO	fails as is - 480v MCC No.5
MOV	V6-12C	NO	fails as is - 480v MCC No.6
MOV	V6-12A	NO	fails as is - 480v MCC No.5
MOV	V6-12D	NO	fails as is - 480v MCC No.6 (alternate - 480v MCC No.5)
MV	SW-20	NO	---
MV	SW-21	NO	---
MV	SW-739	NO	---
MV	SW-740	NO	---
MV	SW-5	LO	---
MV	SW-6	LO	---
MV	SW-7	LO	---
MV	SW-8	LO	---
CV	SW-374	--	---
CV	SW-375	--	---
CV	SW-376	--	---
CV	SW-377	--	---

Pumps
Service Water Pumps
SW Pump A - 480v Bus No.E1
SW Pump B - 480v Bus No.E1
SW Pump C - 480v Bus No.E2
SW Pump D - 480v Bus No.E2
(alternate - 480v Dedicated Shutdown Bus)

Strainers
SW S6-1A
SW S6-1B

Instruments
Pressure - Px-1615A
Px-1615B

Temperature - Tx-1682A
Tx-1682B
Tx-1683A
Tx-1683B
TI-1655
TI-1656

LEGEND

MV - manual valve
MOV - motor operated valve
AOV - air operated valve
CV - check valve
NO - normally open
LO - locked open
NC - normally closed
LC - locked closed
CO - chained open

Table 4.4

HBR2 SFP Component Failures

Number	Component Failure
1	Gross seismic failure of the SFP Structure
4	Seismic failure of the Demineralizer tank
5	Seismic failure of the RWST
6	Operator fails to align CST for make up
7	Seismic failure of 480v MCC No.1
8	Seismic failure of 480v MCC No.8
9	Operator fails to align RWST for make up
12	Seismic failure of the CST

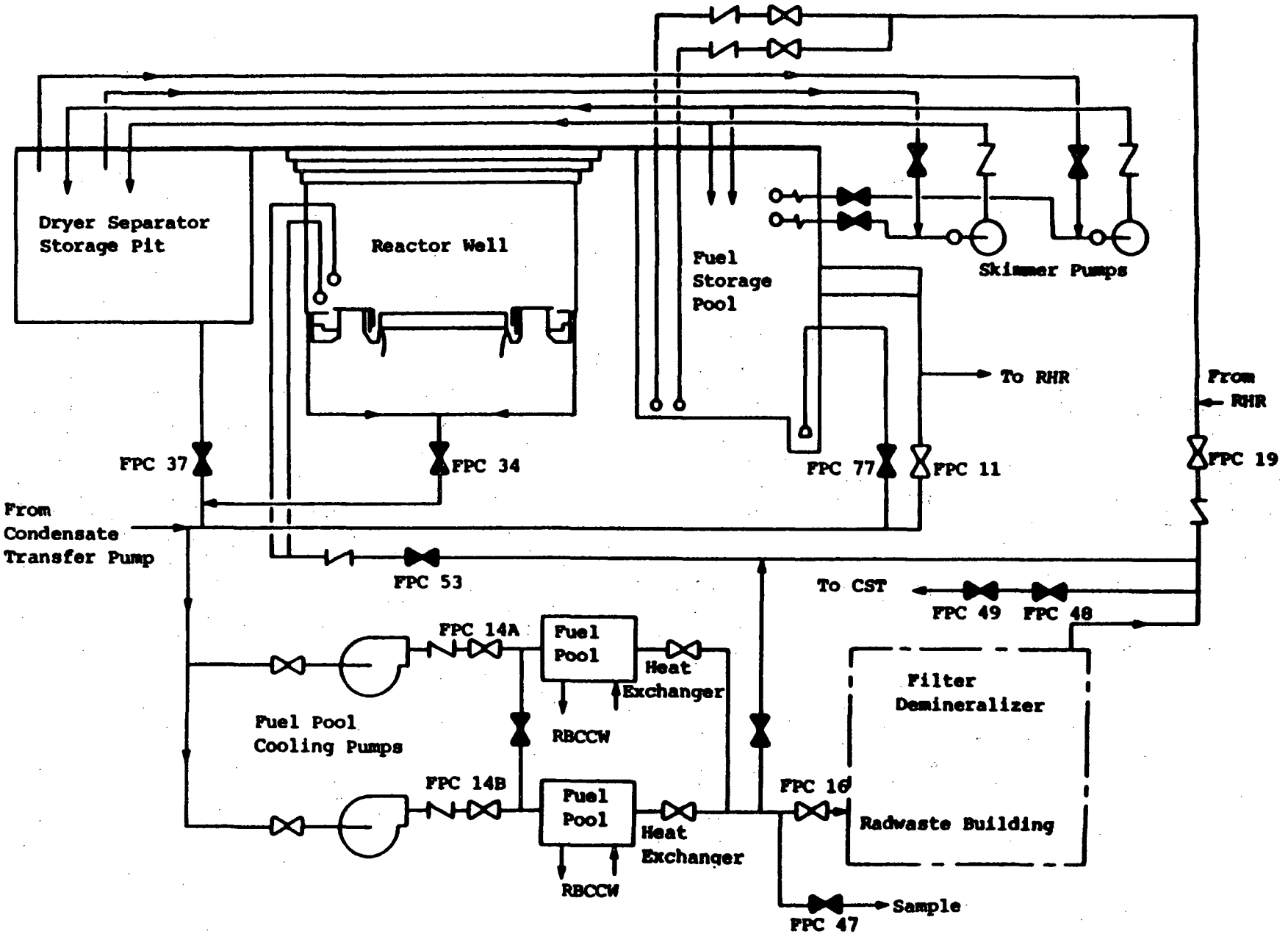

Figure 4-1: Fuel Pool Cooling System

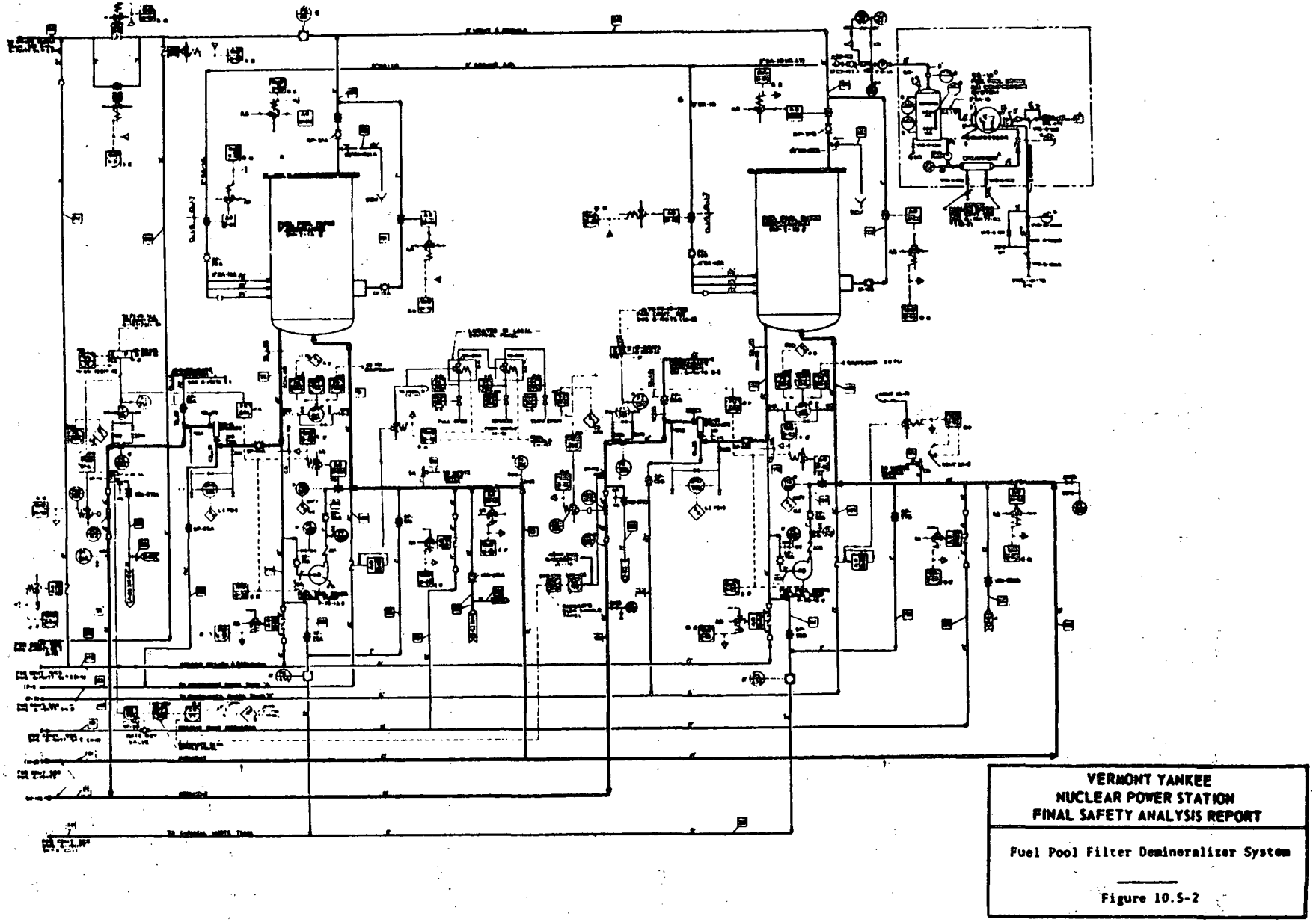

Figure 4-2: Fuel Pool Filter Demineralizer System

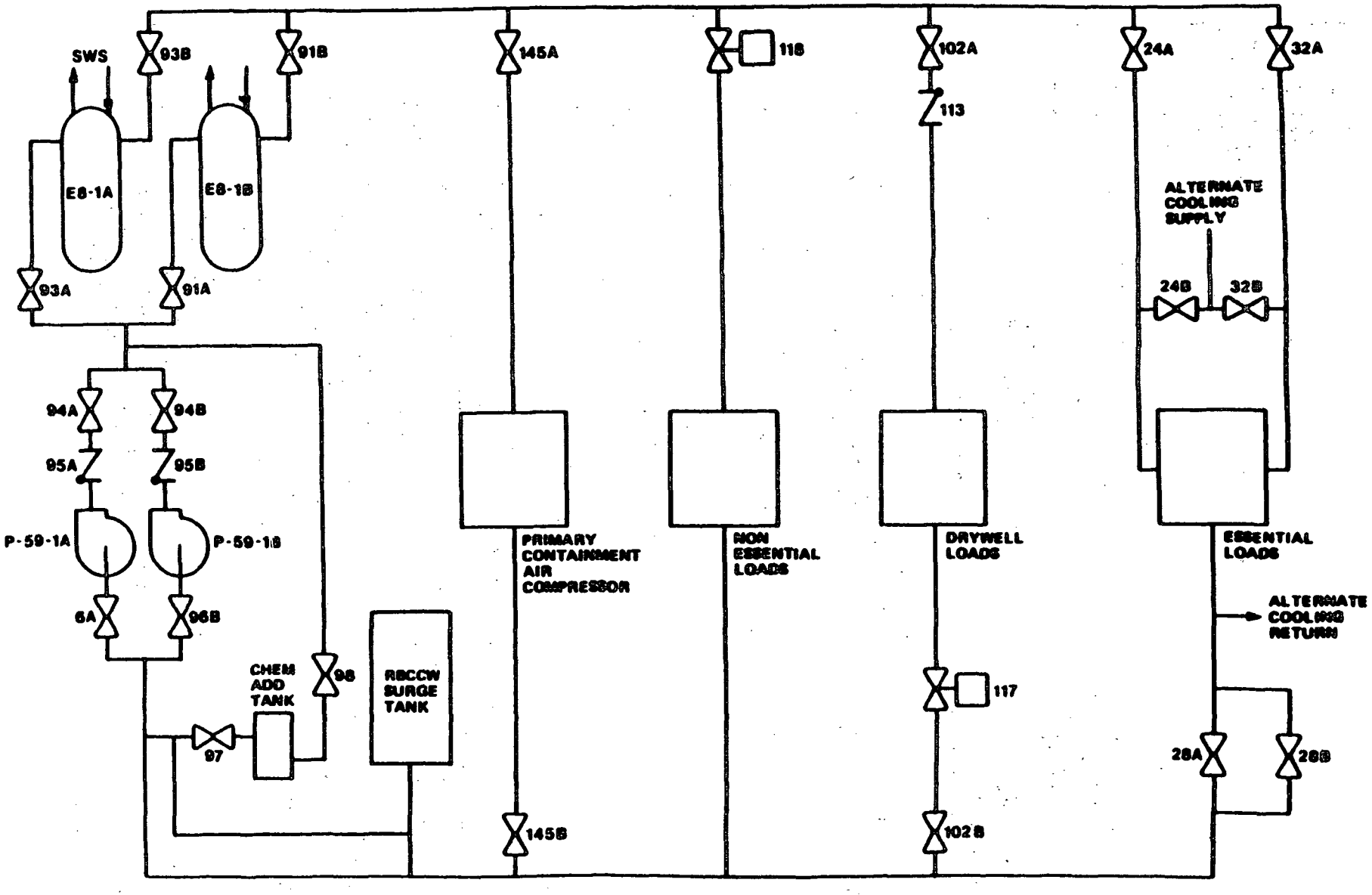

Figure 4-3: VY Simplified Reactor Building Closed Cooling Water System

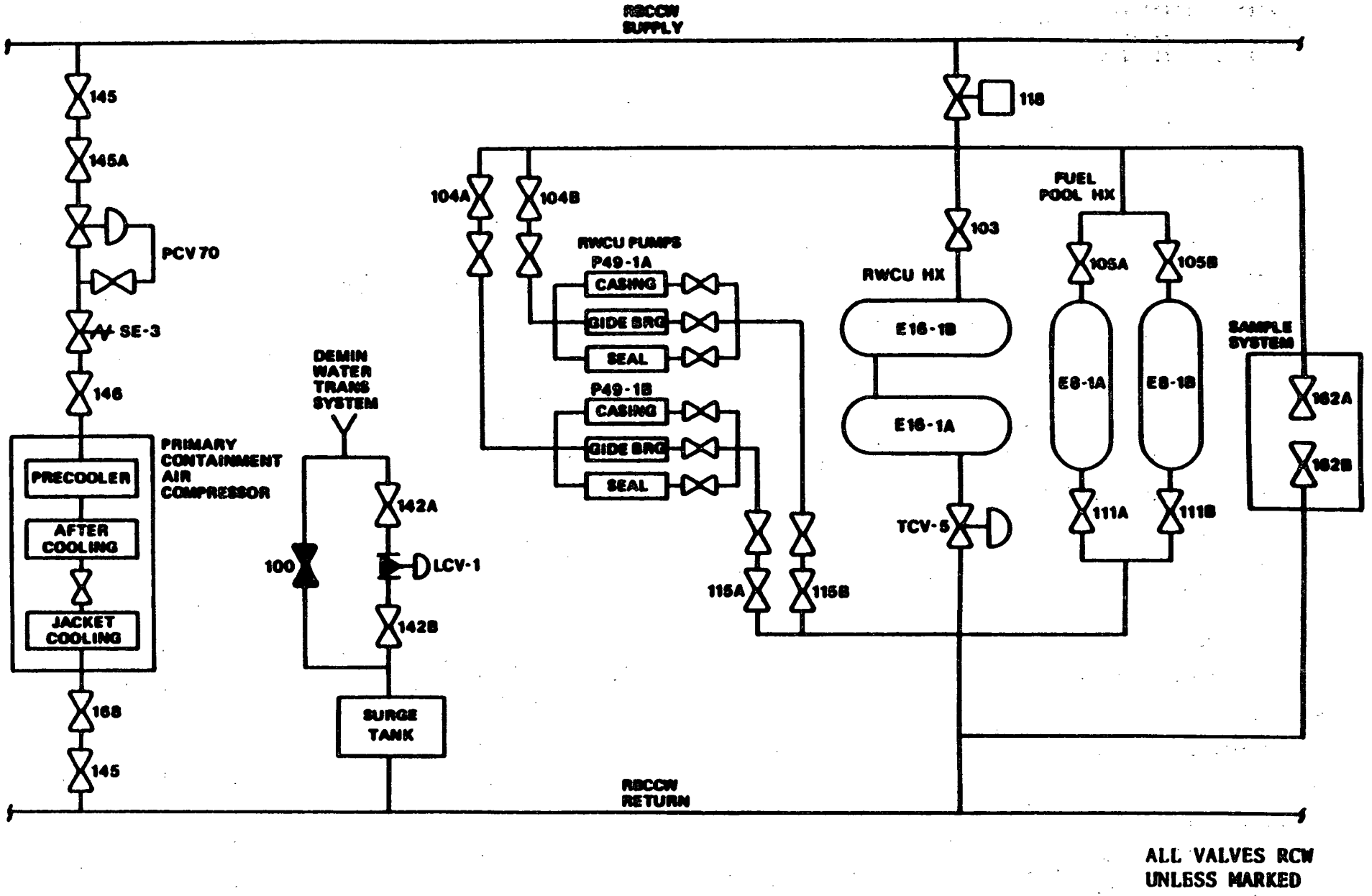

Figure 4-4: VY Simplified Reactor Building Closed Cooling Water System Loops 1 & 2

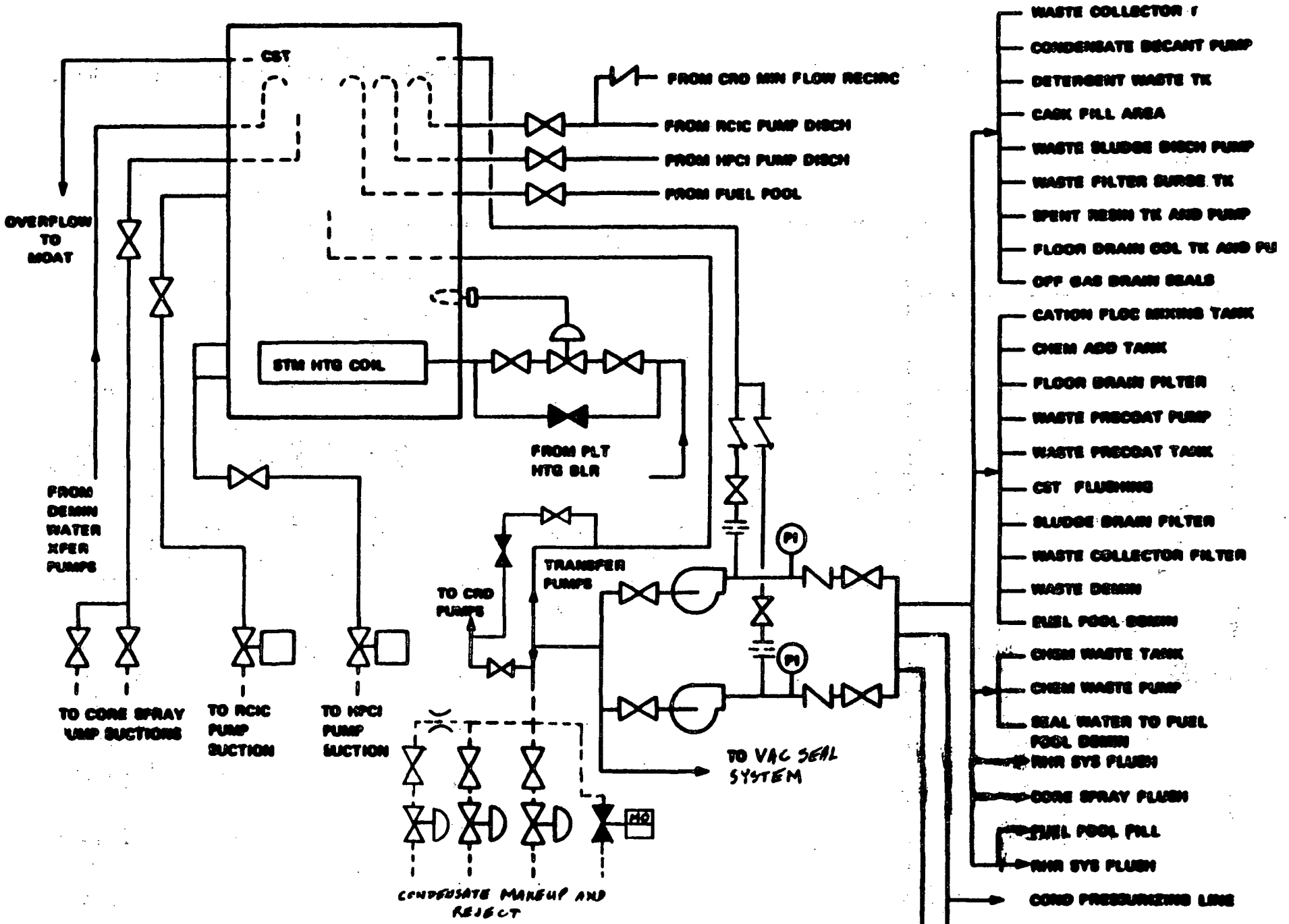

Figure 4-5: VY Condensate Transfer System

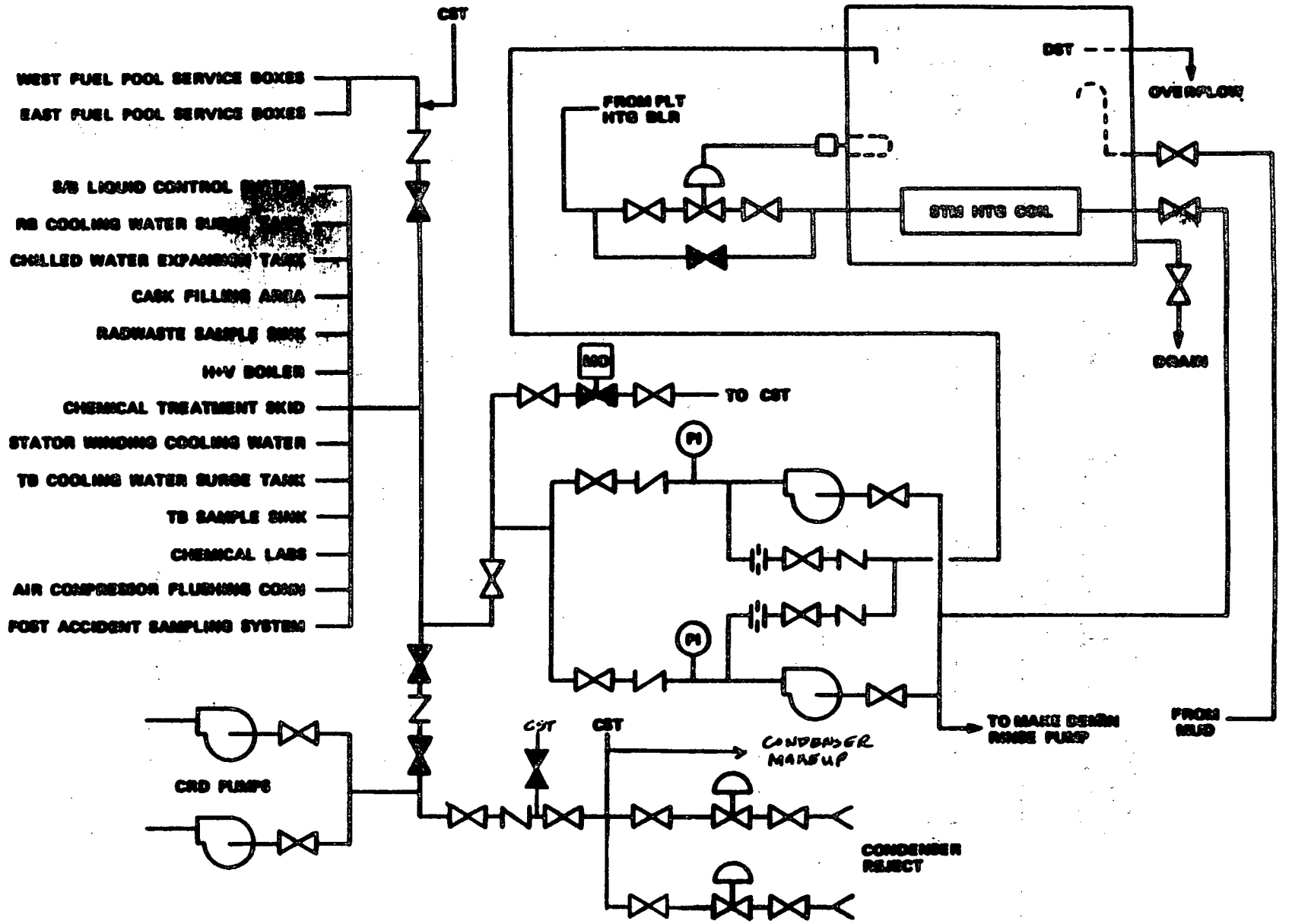

Figure 4-6: VY Demineralized Water Transfer System

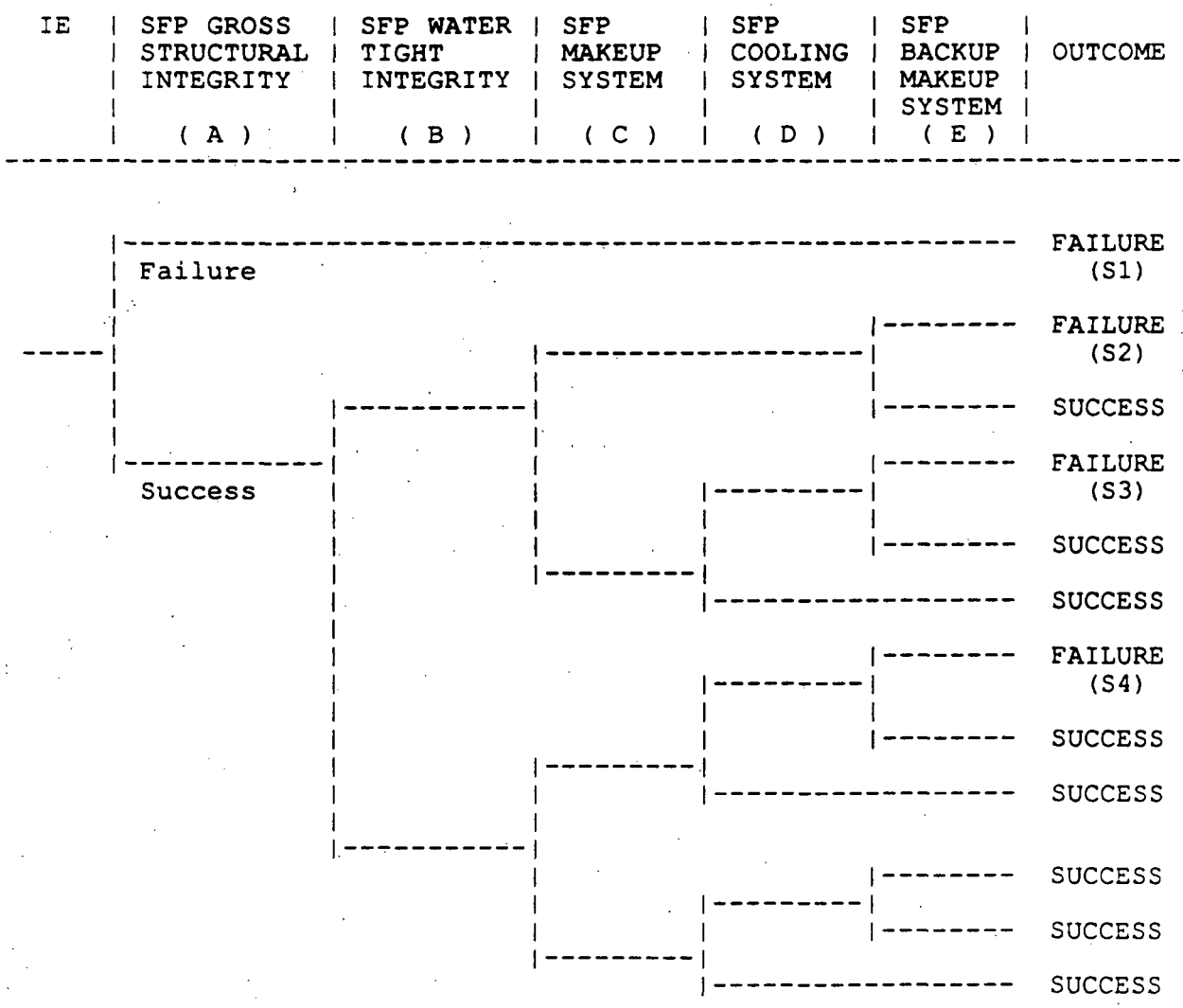

Figure 4-7: VYNPS Event Tree

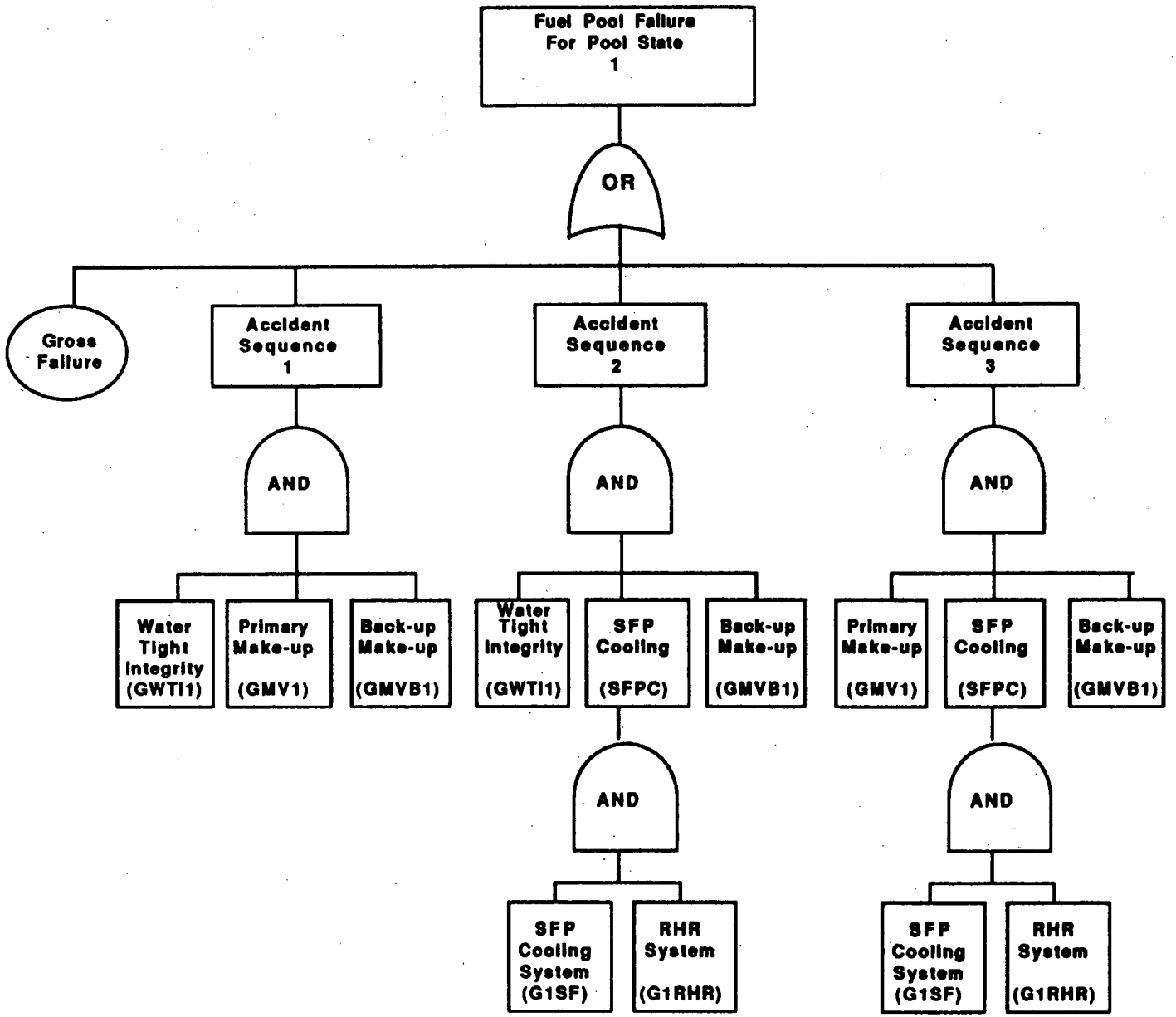

Figure 4-8: VYNPS Fault Tree for Pool State 1

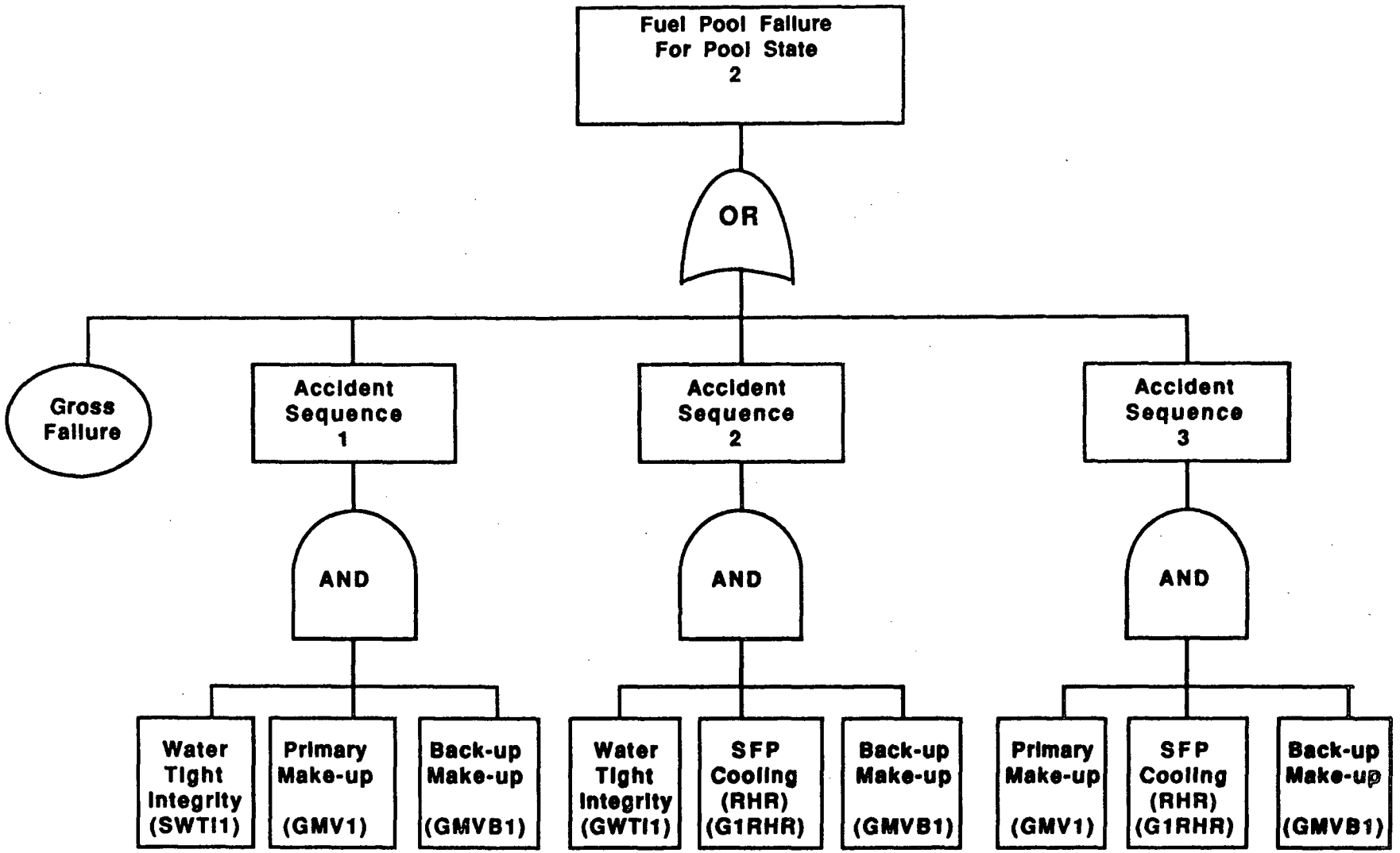

Figure 4-9: VYNPS Fault Tree for Pool State 2

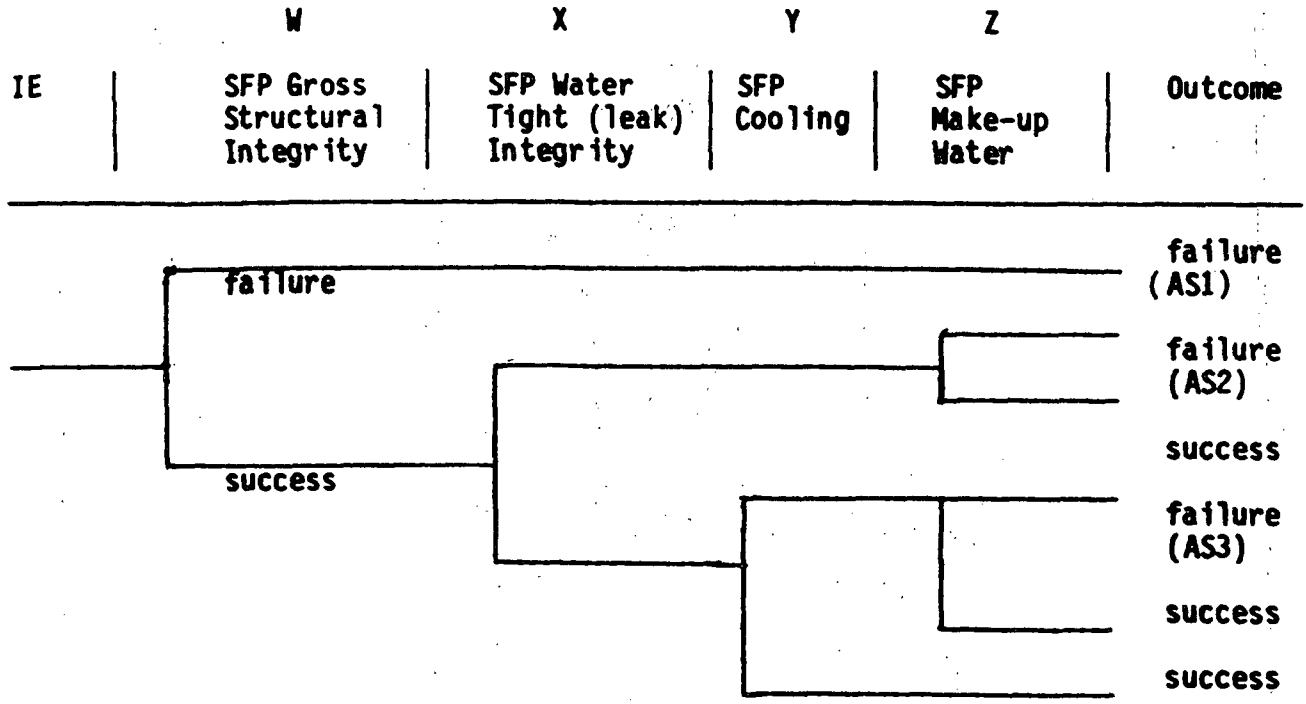

Figure 4-10: H. B. Robinson Spent Fuel Pool Event Tree

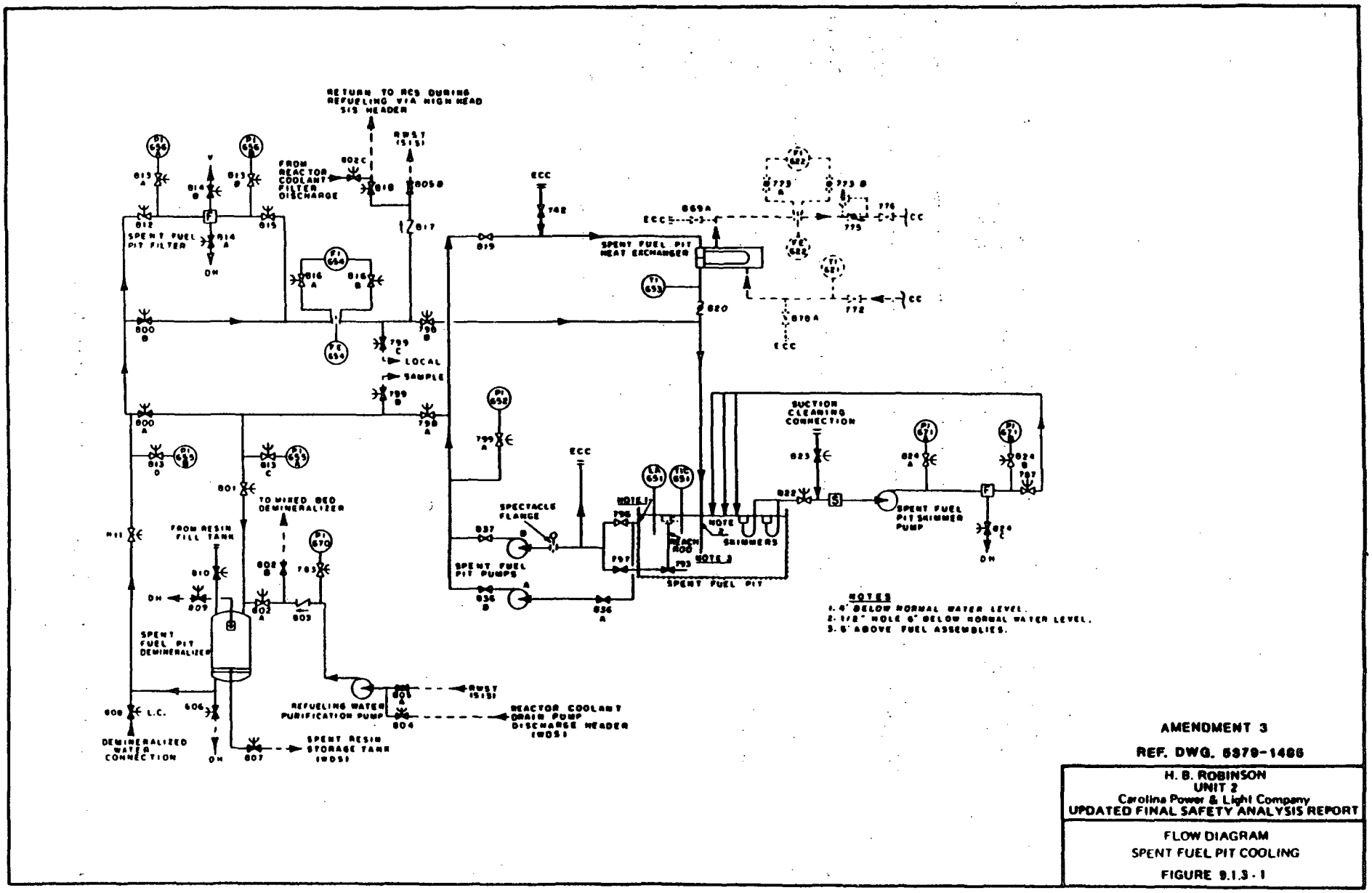

Figure 4-11: Spent Fuel Pit Cooling

5. EQUIPMENT FRAGILITIES

In this chapter, seismic fragilities of equipment that comprise cooling and makeup systems for the spent fuel pool are discussed. The seismic capacity of the fuel racks is also evaluated.

5.1 Vermont Yankee Nuclear Power Station (VYNPS) Equipment

5.1.1 VYNPS Fuel Racks

The seismic capacity of the fuel rack assembly was derived using the design information and results of analysis performed for the proposed replacement racks [Vermont Yankee, 1986]. The racks are freestanding with no connections to the spent fuel pool walls. The design of the racks has been performed to the requirements of the Standard Review Plan Section 3.8.4. Racks are of cold formed stainless steel honeycomb construction. There is a clearance of 2 3/8 in between the racks and the pool walls; the clearance between the racks is 2 3/4 in. The above reference [Vermont Yankee, 1986] has shown that the maximum displacement during an SSE is 0.62 in which includes sliding, tilting, flexure and rotation; sliding of the racks alone is 0.31 in.

Rack behavior under seismic loading is nonlinear and extrapolation of linear analysis results is not very accurate. But, for purposes of a rough comparison to other fragilities reported herein, such an extrapolation is made. It is assumed that impact would occur when the sliding of the racks exceeds about 2 in. Hence, there is a factor of 2/0.31 = 6.5 over the SSE acceleration for this to occur. Such extrapolation for other failure modes (tilting, flexure, and rotation) is judged not appropriate. The median acceleration capacity of the racks for incipient impact is estimated to be 1.0g. Failure of the racks would require more than impact; perhaps, 1.5 to 2 times the acceleration is required to cause impact and damage. Therefore, the earthquake peak ground acceleration should exceed a value of 1.5 to 2.0g before failure occurs. Even then, the fuel rack design is such that the assembly cannot be compressed into a critical mass. According to the analysis reported in Chapter 4, no serious effects can result (i.e., criticality and melt) as long as the fuel is covered. Thus margins above SSE for impact and stress allowables are not particularly meaningful. Therefore, it is concluded that crushing of fuel and assemblies is a not a credible failure mode of the spent fuel pool system.

The cited reference also indicates that the maximum rack stress under SSE as 14.2 ksi where the allowable stress, S_y, is 25 ksi. The report does not state the type of stress or the location. For a free standing rack, the stresses are expected to be flexural. Since the rack slides, the flexural stresses are limited and will not increase with the increasing peak ground acceleration. Therefore, failure of the rack by exceeding the flexural capacity is not a credible failure mode.

The seismic failure of fuel pool racks and fuel assemblies is therefore not modeled further in this risk analysis.

5.1.2 VYNPS Cooling and Makeup Systems

A preliminary list of components comprising these systems is provided in Table 4.2. The generic categories of components in this list include motor control centers, switchgear, pumps, tanks, valves, heat exchangers, filters and strainers.

During a visit to Vermont Yankee Station, the focus was only on the spent fuel pool structure and a detailed examination of the cooling and makeup systems was not performed. However, a brief walkdown of these systems was conducted; some photographs were taken and notes on the existing conditions of the equipment were made. Detailed equipment drawings showing anchorage and support details were not reviewed for this evaluation.

The equipment fragilities were estimated using generic information and based on the applicable design codes. A brief description of the procedures used in this fragility evaluation is given. First, the deterministic capacity called the High Confidence Low Probability of Failure (HCLPF) capacity is estimated. Assuming the values of β_R and β_U to be 0.3 and 0.4 respectively, the median acceleration capacity, A_m, of the component is calculated.

Motor Control Centers

It was assumed that the motor control centers were all located at Elevation 303'. The peak spectral acceleration was compared to the Generic Equipment Ruggedness Spectrum GERS, [EPRI 1987] at 5% damping using a reduction factor of 1.3 as recommended in the EPRI Seismic Margins Methodology [NTS, 1987]. The HCLPF capacity corresponding to a non-recoverable failure mode was estimated to be 0.27g. The inspection of the anchorage photos indicated that there are 10 cabinets in a row. Assuming 2 bolts per cabinet of 1/2" diameter non-shell type, the spectral acceleration capacity of the cabinet against anchorage failure was estimated from [EPRI, 1987] to be 1.7g. The corresponding HCLPF capacity of the cabinet was derived as 0.16g. The median capacity of the cabinet was estimated as 0.50g. Anchorage failure is the lower of the two failure modes i.e., cabinet/device failure and anchorage failure. In the above calculation, only two bolts were assumed to be installed per cabinet; however, if 4 bolts of 3/8" nonshell type were installed instead, the median capacity would be about 0.72g with a HCLPF of 0.23g which is much closer to the generic capacity of the MCC units as defined by GERS.

Station Service Transformer # 8

There are 4 1/2" diameter expansion anchors on this transformer. The bolts are subjected to bending due to the presence of shims below the transformer. The weight of the transformer was estimated to be 6.3 kips. The HCLPF capacity of the anchorage was evaluated using the interaction formula for bending and shear. The HCLPF capacity obtained was 0.16g and the median ground acceleration capacity was 0.51g.

Station Service Transformer # 9

A review of the photographs of the item indicated that one anchor bolt was missing but unlike SST #8, the flange of the transformer is bolted directly to the floor without any spacer being provided. The HCLPF capacity of this transformer is considered to be higher than #8 and is 0.28g with a median capacity of 0.89g.

4 kV Switchgear/Bus

The photograph shows that angles have been added to the inside of the cabinet which were fastened to the floor with 3/8" expansion anchors. The cabinet is 2' x 5' and is 7' tall. The anchorage in the back was not observed. Assuming non-shell anchors, the spectral acceleration capacity was estimated to be 1.6g. The HCLPF capacity and the median capacity were estimated to be 0.14g and 0.44g respectively.

RBCW Surge Tank

The photograph shows that the tank is mounted on 4 legs resting on concrete pads. There is lateral bracing but no longitudinal bracing is present. The tank is about 3.5 ft in diameter and 5.5 ft long. The total weight of the tank with water and framing is estimated to be 2.5 kips. The tank support is fairly flexible but the strength of the anchorage could not be ascertained from the photograph. The diagonal bracing looked minimal. Two failure modes were investigated: failure of the diagonal bracing and overturning. The overturning failure mode was found to govern the capacity. The HCLPF capacity was estimated to be 0.09g; the median capacity was calculated as 0.29g.

RB CCW Heat Exchanger

This is a large horizontal tank. The photograph showed that it is supported on saddles which are adequately reinforced in the longitudinal direction. On the fixed end, there are 4 bolts of probably 1/2" diameter. Assuming the HCLPF capacity corresponds to the earthquake level when the shear stress exceeds the allowable value of 0.6 S_y, it is estimated to be 0.46g and the median capacity as 1.46g.

Spent Fuel Pool Heat Exchanger

This heat exchanger has an over and under horizontal cylinder arrangement. The photographs did not show details of the anchorage. There does not appear to be any top brace on the assembly. Lateral overturning appears to be the critical failure mode. Field notes indicated that there is one 3/4" bolt in each support leg. Assuming that the bolts are cast in place, the HCLPF capacity is estimated to be 0.23g and the median capacity as 0.73g.

RHR Heat Exchanger

Based on a comparison of this component with the heat exchangers reviewed in a number of seismic PRAs, the HCLPF capacity is estimated to be larger than 0.5g with the median capacity in excess of 2.0g.

RHR Pumps

The HCLPF capacity of this component is estimated larger than 0.5g based on a comparison to similar pumps in the seismic PRA database.

Fuel Pool Demineralizer Tank

The demineralizer tank is located low in the radioactive waste building. It has four legs of 3" angle and is bolted to the floor using 7/8" bolts. The governing failure mode is cantilevered bending of the angle legs. The HCLPF capacity is estimated to be 0.14g with the median capacity about 0.44g.

Piping and Valves

Based on the extensive PRA and experience data base, the HCLPF capacities of piping and valves were estimated to be in excess of 0.5g.

Table 5.1 gives a summary of equipment fragilities for the spent fuel pool cooling and makeup systems.

5.2 H. B. Robinson, Unit 2 (HBR2) Equipment

5.2.1 HBR2 Cooling and Makeup Systems

A list of components comprising these systems was prepared and shown in Table 4.3. The generic categories of components in this list include motor control centers, switch gear pumps, tanks, valves, heat exchangers, and instruments.

During a visit to the Robinson plant, some of these items were examined with the major focus on the spent fuel pool structure. Based on a plant walkdown, information available in the updated FSAR, and equipment anchorage drawings, most of the equipment items were screened out as having high seismic capacities. This was also guided by the seismic fragility parameters of component categories reported in [Budnitz et al., 1985] and [Campbell et al., 1985].

Fragility estimation were made for the following equipment items:

CCW Surge Tank

Demineralizer Tank

Refueling Water Storage Tank

480v MCC No. 1

480v MCC No. 8

Condensate Storage Tank

The equipment fragilities were estimated using generic information and based on applicable design codes. In the following, we describe the procedure used and the results of the fragility evaluation of these components; for components other than the ground mounted yard tanks, the deterministic capacity called the High Confidence Low Probability of Failure (HCLPF) capacity is estimated. Assuming the values of β_R and β_U to be 0.3 and 0.4 respectively, the median acceleration capacity, A_m, of the component is calculated.

CCW Surge Tank

This is a steel tank 4 ft in diameter and 14 ft long; it is mounted on the roof of the reactor auxiliary building using two saddle supports. The saddles are bolted down to the floor with two 3/4 in. bolts on each saddle. The weight of the tank including water is estimated to be 13 kips. The surge tank is judged to be rigid hence the maximum acceleration acting on it at the SSE is estimated to be 0.40g; at this load, the shear stress in the bolts is calculated as 4.1 ksi; comparing this stress with the allowable shear stress of 0.6 Sy = 21.6 ksi, the HCLPF capacity is estimated as 1.05 g. The median ground acceleration capacity A_m, is estimated to be 3.31g.

Demineralizer Tank

The demineralizer tank is located at Elevation 226'0" in the Auxiliary Building. It is a 32" diameter steel tank mounted on four legs of 4" angle and bolted to the floor using 1" bolts. The governing failure mode is the cantilevered bending of the angle legs. The HCLPF capacity is estimated to be 0.44g with the median capacity to be 1.41 g.

Tanks

Yard tanks which were identified by the systems analysis for the Robinson Unit 2 spent fuel pool risk analysis are the refueling water storage tank (RWST) and the condensate storage tank (CST). In the following, the evaluation of the CST is described in detail.

The condensate storage tank is a 35 ft diameter steel tank fabricated using 1/4 in. stainless steel (A 240 Type 304) plate; it is anchored to the foundation reinforced concrete ring wall with 12 anchor bolts of 1-3/4 in. diameter. Maximum depth of water is 28 ft 3 in. The median ground response spectrum used for this evaluation is NUREG/CR-0098. Since the tank is at grade on a soil site, a median damping is increased from 7% used typically for welded tanks founded on rock to 10% to account for soil structure interaction effects. Based on previous PRA studies, the critical failure mode of the tank is identified to be the overturning moment failure. The median overturning

moment capacity of the tank is estimated to be 20,930 ft-kips. This includes the resistance provided by the tank weight, fluid weight, base plate, shell buckling and anchor bolts. The median overturning moment at the 0.2 g SSE level is calculated to be 6,681 ft-kips resulting in a median strength factor equal to 20,930/6,681 = 3.1. The uncertainty in this strength factor is estimated taking into account the uncertainties in the shell buckling coefficient, location of the anchor bolt force, bottom plate holding force, yield strength of anchor bolts and modeling of the failure mode. This value is β_R = 0.18. This overturning moment failure is somewhat ductile and a median inelastic energy absorption capacity factor of 1.1 is estimated.

It is assumed that the average of the two horizontal components is used in specifying the median ground response spectrum. Because of the axisymmetry of the tank, no matter how the two horizontal components are oriented the tank maximum response will result from the larger of the two horizontal components rather than the average of the two. Therefore, a factor of 0.9 is estimated to reduce the tank capacity calculated on the basis of the spectrum averaged over two components.

The other safety factors are estimated both in terms of the median values and β_R and β_U values as explained for the spent fuel pool structure and are tabulated in Table 5.2.

The refueling water storage tank (RWST) at Robinson Unit 2 is a 42 ft diameter tank fabricated from 1/4 in steel plates; it is anchored to the ring wall using 20 anchor bolts of 1-3/4 in. diameter. The maximum water height in the tank is 34 ft 3 in. By comparing the overturning moment capacities of RWST and CST, the median ground acceleration capacity of the RWST is estimated to be 0.60g with β_R = 0.21 and β_U = 0.27.

Motor Control Centers

It was assumed that the motor control centers are all located at Elevation 275' 0". From the Updated FSAR, the maximum floor spectral acceleration in the auxiliary building is 2.19 g. This spectral acceleration was compared to the Generic Equipment Ruggedness Spectrum GERS [EPRI 1987] at 5% damping using a reduction factor of 1.3 as recommended in the EPRI Seismic Margins Methodology [NTS, 1987]. The HCLPF capacity corresponding to a non-recoverable failure mode was estimated to be 0.28 g. As a representative MCC, we reviewed the MCC No. 6; it has 10 cabinets in a line with a total of six 1/2" diameter shell anchors. The lineup is supported at the top through three struts made up of two equal 2 1/2" angles. The struts are bolted to the side wall using two anchor bolts of 1/2" diameter. This anchorage and lateral support are considered to be sufficiently rugged that the structural failure of the cabinets is not a critical mode. The median ground acceleration capacity of the MCCs is estimated to be 0.89 g based on the GERS discussed above.

Table 5.3 gives a summary of the equipment fragilities.

Table 5.1

Summary of Equipment Fragilities
for VYNPS SFP

Component	A_m (g)	β_R	β_U	HCLPF Capacity (g)	Notes
Motor Control Centers 7b,7c,8b,9b	0.50	0.30	0.40	0.16	1
Station Service Transformer 8	0.51	0.30	0.40	0.16	2
Station Service Transformer 9	0.89	0.30	0.40	0.28	5
4 kV Switchgear	0.44	0.30	0.40	0.14	3
RB CCW Surge Tank	0.29	0.30	0.40	0.09	4
SFP Demineralizer Tank	0.44	0.30	0.40	0.14	8
RB CCW Heat Exchanger	1.46	0.30	0.40	0.46	5
SFP Heat Exchanger	0.73	0.30	0.40	0.23	6
RHR Heat Exchanger	>2.00			>0.50	7
RHR Pump	>2.00			>0.50	7
Piping	>2.00			>0.50	7
Valves	>2.00			>0.50	7

1. Assumes 2 non-shell 1/2" bolts per cabinet
2. Anchor bolts in bending and shear
3. Assumes 4 non-shell 3/8" bolts per cabinet
4. One 3/8" bolt per leg from photographs; assumed non-shell expansion anchors
5. Bolt shear; all dimensions from photographs and notes
6. 3/4" diameter 4 bolts per field notes; assumed to be cast in place
7. Based on PRA results
8. Support leg bending

Table 5.2

Median Factors of Safety and Variabilities for HBR2 CST

Factor	Median	β_R	β_U
Strength	3.1	0	0.18
Inelastic Energy Absorption	1.1	0.02	0.02
Spectral Shape	1.0	0.20	0.00
Damping	1.0	0.03	0.14
Modeling	1.0	0	0.10
Soil-Structure Interaction	1.0	0.01	0.10
Modal Combination	1.0	0.03	0
Combination of EQ Components	1.0	0.01	0
Horizontal Component Direction		0.9	00
TOTAL	3.1	0.21	0.27

Median PGA capacity = 3.1 (0.20g) = 0.62 g

HCLPF Capacity = 0.62 exp (- 1.64 (0.21 + 0.27)) = 0.28 g

Table 5.3

Summary of HBR2 Equipment Fragilities

Component	A_m (g)	β_R	β_U	HCLPF Capacity (g)
CCW Surge Tank	3.31	0.30	0.40	1.05
Fuel Pool Demineralizer Tank	1.41	0.30	0.40	0.44
Refueling Water Storage Tank	0.60	0.21	0.27	0.27
Motor Control Centers No. 1 and 8	0.89	0.30	0.40	0.28
Condensate Storage Tank	0.62	0.21	0.27	0.28

6. RISK EVALUATION

6.1 Objective

The objective of this study is to estimate the probability of failure of the Spent Fuel Pool due to seismic events. Failure of the pool is defined to be gross rapid loss of pool contents that would empty all the cooling water and expose the fuel rods. It has been determined that the failure of cooling and make-up systems would not result in immediate uncovering of the fuel rods. There is a response time of at least 3 days, maybe as much as 7 days before fuel uncovery would occur. Thus, SFP failures attributed to these system failures and are not directly comparable to SFP failures caused by structured degradation leading to sudden loss of water. The damage to fuel racks in a seismic event are judged to be minor and fuel rack damage is not significant as long as there is water in the pool.

The estimation of probability of failure is accomplished by using the seismic probabilistic risk assessment (PRA) methodology, described earlier in Chapter 2.

Preliminary seismic hazard curves for the two sites are shown on Figures 6-1 and 6-2. These curves correspond to the confidence values of 15%, 50%, and 85%. Note that these preliminary curves have not been finally reviewed by the NRC and are used herein only to get a preliminary understanding of the seismic induced spent fuel failure. The hazard curves may change after NRC review and guidance for their proper use will be developed.

Using these hazard curves, a set of discrete hazard curves with associated subjective probability weights were generated. This was done by fitting a lognormal distribution to the uncertainty in the hazard at any peak ground acceleration value. This lognormal probability distribution was assumed to have the median value of the hazard (i.e. annual frequency of exceedance) given by the 50th percentile curve and the 95th percentile value given by the top most curve in the figure. This probability distribution was discretized into 11 ranges with probabilities of 0.03, 0.05, 0.07, 0.12, 0.15, 0.16, 0.15, 0.12, 0.07, 0.05, 0.03. Note that the lognormal probability distribution was cutoff at the 99th percentile value. By repeating this procedure at other accelerations, a family of hazard curves was generated.

6.2 VYNPS Analysis

6.2.1 VYNPS Assumptions

The following assumptions have been made in the seismic risk calculations reported herein:

Seismic fragility of the spent fuel pool structure was estimated earlier using detailed information on the structure. The median capacity with all high density racks is estimated to be 1.4 g with the HCLPF capacity of 0.50 g. For the existing fuel rack configuration, the HCLPF capacity is estimated to be 0.65g. Case 1 shows the annual failure frequencies of the pool structure.

Seismic fragilities of mechanical and electrical components have been estimated by using both site-specific information from walkdowns, as well as the walkdown notes and photographs, and generic information on the component categories from previous PRAs. The HCLPF capacities were estimated using deterministic methods and the median capacities were calculated assuming β_R and β_U to be 0.3 and 0.4, respectively.

6.2.2 VYNPS Accident Sequences and Failure States

Seismic fragilities and random failure rates of different components relevant to this analysis are shown in Table 6.1. Based on the systems analysis presented in Chapter 4, two pool states were developed, PS1 and PS2.

The Boolean expressions for these two pool states are given by:

PS1 = 12 + (7 + 11 + 1 * 2) * (5 * { 4 + 9 + 8 + 10 }

+ 4 * { 3 + 6 })

PS2 = 12 + (7 + 11 + 1 * 2) * (4 + 9 + 10)

The quantification of these Boolean expressions was accomplished using the component seismic fragilities and random failure rates given in Table 6.1. The fragilities were assumed to be perfectly independent both in the randomness and in the uncertainty aspects.

It may be noted that the components 1, 2, 7 and 11 are all in the non-safety electrical systems of the plant. As shown in Table 6.1, their low capacities seem to contribute significantly to the seismic induced failure of the spent fuel pool support systems.

6.2.3 VYNPS SFP Case Studies

Case studies 1, 2 and 3 were conducted using the seismic fragilities estimated as shown in Table 6.1, case definitions are given in Table 6.2. They also include the operator failure rates or random failures. The influence of random failures on the seismic system failure frequencies is shown in case studies 4 and 5.

The anchorage of the MCC cabinets could not be determined by the walkdown notes and photographs; therefore it was assumed in case studies 2 through 5 that the MCC cabinets were anchored using 2-1/2 in non-shell expansion anchors per cabinet and the seismic fragility parameters A_m and β_S were estimated. Sensitivity case studies 6 and 7 were conducted that assumed MCC cabinets had 4-3/8 in non-shell anchors per cabinet. The median capacity was estimated to be 0.82 g as contrasted with the earlier value of 0.50 g. There was not a large change in the failure probability because of the dominance of the cabinets as seen in Table 6.2.

6.2.4 Probability of VYNPS Spent Fuel Pool Failure

The total probability of pool failure is determined by combining the probabilities of the two Pool States, PS1 and PS2, based on the time the plant is in that mode of operation (normal operation or complete core discharge to the spent fuel pool). For this analysis, it was assumed that the plant could have a complete core discharge to the pool once every five years and that the full core could be in the pool for a duration of one month. The analysis is given below:
Let:

$P(PS1)$ = probability that fuel pool is in pool state 1, per year

$P(PS2)$ = probability that fuel pool is in pool state 2, per year

$P(f|PS1)$ = probability of fuel pool failure while in pool state 1, per year

$P(f|PS2)$ = probability of fuel pool failure while in pool state 2, per year

then, $P(f)$, the total probability of fuel pool failure is given by

$$P(f) = P(f|PS1)\ P(PS1) + P(f|PS2)\ P(PS2)$$

$P(PS1)$ and $P(PS2)$ have been estimated to be 59/60 and 1/60 respectively. The mean conditional probabilities for different failure states are given in Table 6.2. The results of this analysis indicate that for:

Case 2 & 3 $P(f) = 1.5\ E\text{-}4$
Case 4 & 5 $P(f) = 1.2\ E\text{-}4$
Case 6 & 7 $P(f) = 9.4\ E\text{-}5$

6.3 H. B. Robinson, Unit 2 (HBR2) Analysis

6.3.1 Probability of HBR2 Spent Fuel Pool Failure

Seismic fragilities and random failure rates of different components relevant to the HBR2 analysis are provided in Table 6.3.

Gross spent fuel pool structural failure results in loss of the pool liner integrity and complete loss of the pool water inventory in a short time leading to fuel damage, possible cladding fire and radioactivity release. The seismic fragility for this failure mode is discussed in Section 3.3.2

Fuel uncovery, damage and possible radioactivity release occurs from failure to cool the water in the pool resulting in water boil-off and failure to provide make-up water in the event cooling fails. If pool cooling is successful or the pool make-up systems are available, then SFP success is maintained. The Boolean expression is :

Pool Failure = 1 + (4 + 5 + 7 + 9) * (6 + 8 + 12)

The quantification of this Boolean expression was done using the component fragilities and random failure rates given in Table 6.3. The fragilities were assumed to be perfectly independent both in the randomness and in the uncertainty aspects. The results of the qualification are given in Table 6.4.

Table 6.1

Seismic Fragilities and Random Failure Rates for VYNPS

	COMPONENT FRAGILITIES	Am	β_R	β_U
#1	MCC 7b FAILS (SS TRANSFORMER 7)	0.50	0.30	0.40
#2	MCC 7c FAILS (SS TRANSFORMER 7)	0.50	0.30	0.40
#3	MCC 8B FAILS (SS TRANSFORMER 8)	0.50	0.30	0.40
#4	MCC 9B FAILS (SS TRANSFORMER 9)	0.50	0.30	0.40
#5	RBCCW SURGE TANK TK 7-1A FAILS	0.29	0.30	0.40
#6	SFP HEAT EXCHANGER E-9-1A FAILS	0.73	0.30	0.40
#7	STATION SERVICE TRANSFORMER	0.50	0.30	0.40
#11	SWITCHGEAR	0.44	0.30	0.40

	OPERATOR FAILURE RATES	RATE/DEMAND	ERROR FACTOR
#8	OPERATOR FAILS TO OPEN MOV V-89A	0.04	3.0
#9	OPERATOR FAILS TO OPEN MANUAL VALVE V-25	0.08	3.0
#10	OPERATOR FAILS TO OPEN MOV V-50a	0.08	3.0

Table 6.2

Results of the Analyses
of VYNPS SFP

Case	Annual Seismic Failure Frequencies (per reactor-yr)			
	Mean	5%	50%	95%
1. Pool Structure only Am= 1.4 g; HCLPF= 0.5 g				
(a) Cutoff at X= 1.0	3.8E-05	1.8E-11	7.7E-08	3.6E-05
(b) Cutoff at 99%	6.7E-06	3.1E-11	8.3E-08	1.9E-05
(c) Cutoff at 98%	4.9E-06	3.1E-11	8.0E-08	1.9E-05
(d) Cutoff at 97%	3.8E-06	3.1E-11	7.7E-08	1.4E-05
2. SFP Support Systems Failure State PS1	1.5E-04	2.0E-07	1.2E-05	6.7E-04
3. SFP Support Systems Failure State PS2	1.7E-04	2.3E-07	1.3E-05	6.7E-04
4. SFP Support Systems Failure State PS1 w/o random failures	1.2E-04	1.2E-07	9.5E-06	5.3E-04
5. SFP Support Systems Failure State PS2 w/o random failure	1.1E-04	7.1E-08	8.1E-06	4.6E-04
6. SFP Support Systems Failure State PS1 w/revised MCC fragilities	9.4E-05	1.0E-07	6.6E-06	3.9E-04
7. Pool State PS2 with revised MCC fragilities	9.0E-05	1.1E-07	6.2E-06	3.2E-04

Note: Cases 2 through 4 do not include alternate makeup.
Failure to align normal makeup is considered.

Table 6.3

Seismic Fragilities for HBR2

Component Fragilities	Am (g)	β_R	β_U	HCLPF (g)
#4 Fuel Pool Demineralizer Tank	1.41	0.30	0.40	0.44
#5 Refueling Water Storage Tank	0.60	0.21	0.27	0.27
#7 480v Motor Control Center No. 1	0.89	0.30	0.40	0.28
#8 480v Motor Control Center No. 8	0.89	0.30	0.40	0.28
#12 Condensate Storage Tank	0.62	0.21	0.27	0.28
OPERATOR FAILURE RATES		RATE/DEMAND		ERROR FACTOR
#6 Operator fail to align CST for pool makeup		0.08		3.0
#9 Operator fails to align RWST for pool makeup		0.08		3.0

Table 6.4

Results of the Analyses
of HBR2 SFP

Case	Annual Seismic Failure Frequencies (per reactor-yr)			
	Mean	5%	50%	95%
1. Pool Structure only A_m = 2.0 g; HCLPF = 0.65 g				
(a) Cutoff at X= 1.0	8.6E-06	6.1E-12	1.3E-08	8.6E-06
(b) Cutoff at 99%	1.8E-06	9.9E-12	1.5E-08	5.0E-06
(c) Cutoff at 97%	9.9E-07	9.5E-12	1.4E-08	3.5E-06
2. SFP Support Systems Failure	1.5E-04	5.5E-07	1.9E-05	6.0E-04

Note: Case 2 does not include alternate makeup.
Failure to align normal makeup is considered.

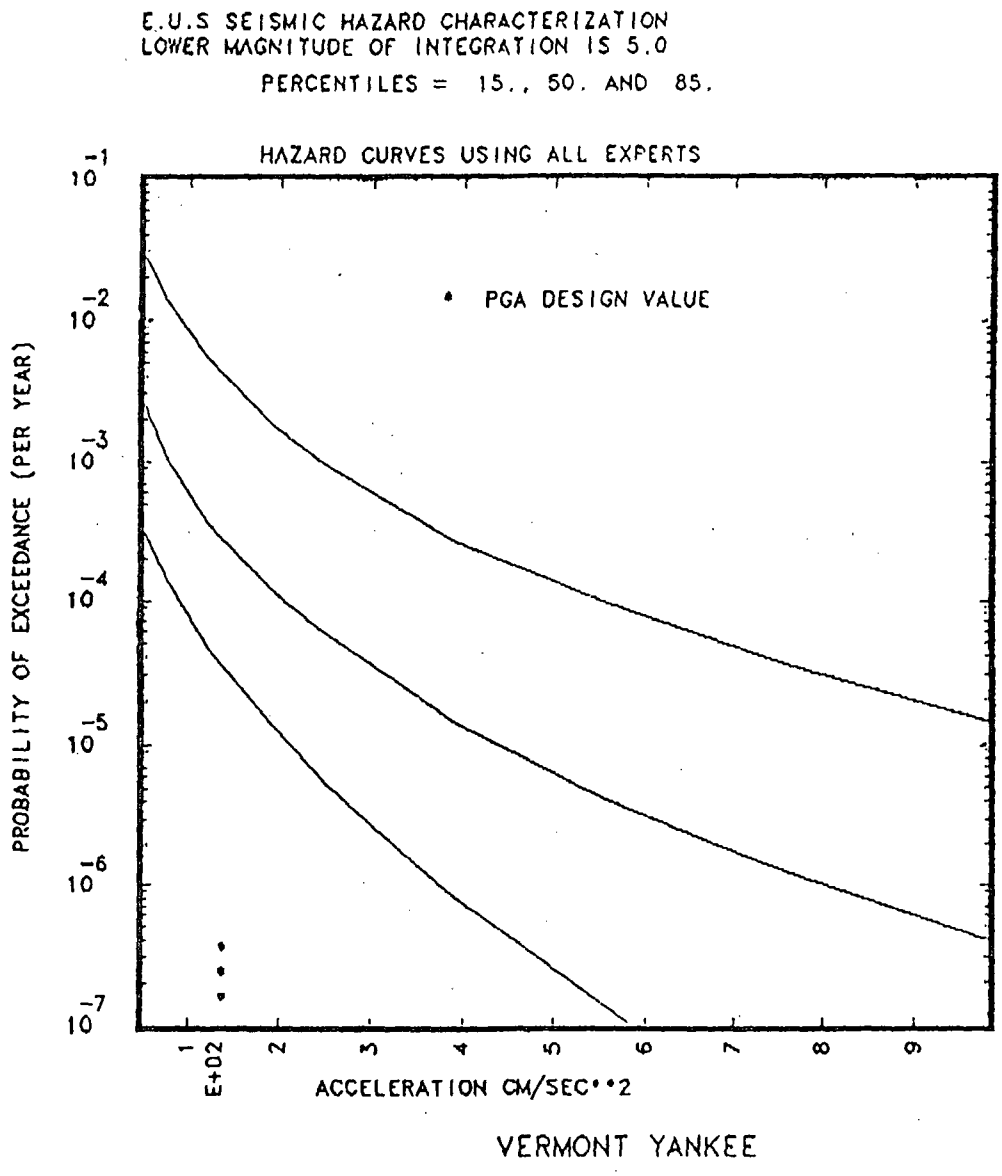

Figure 6-1: Seismic Hazard Curves for the VYNPS Site

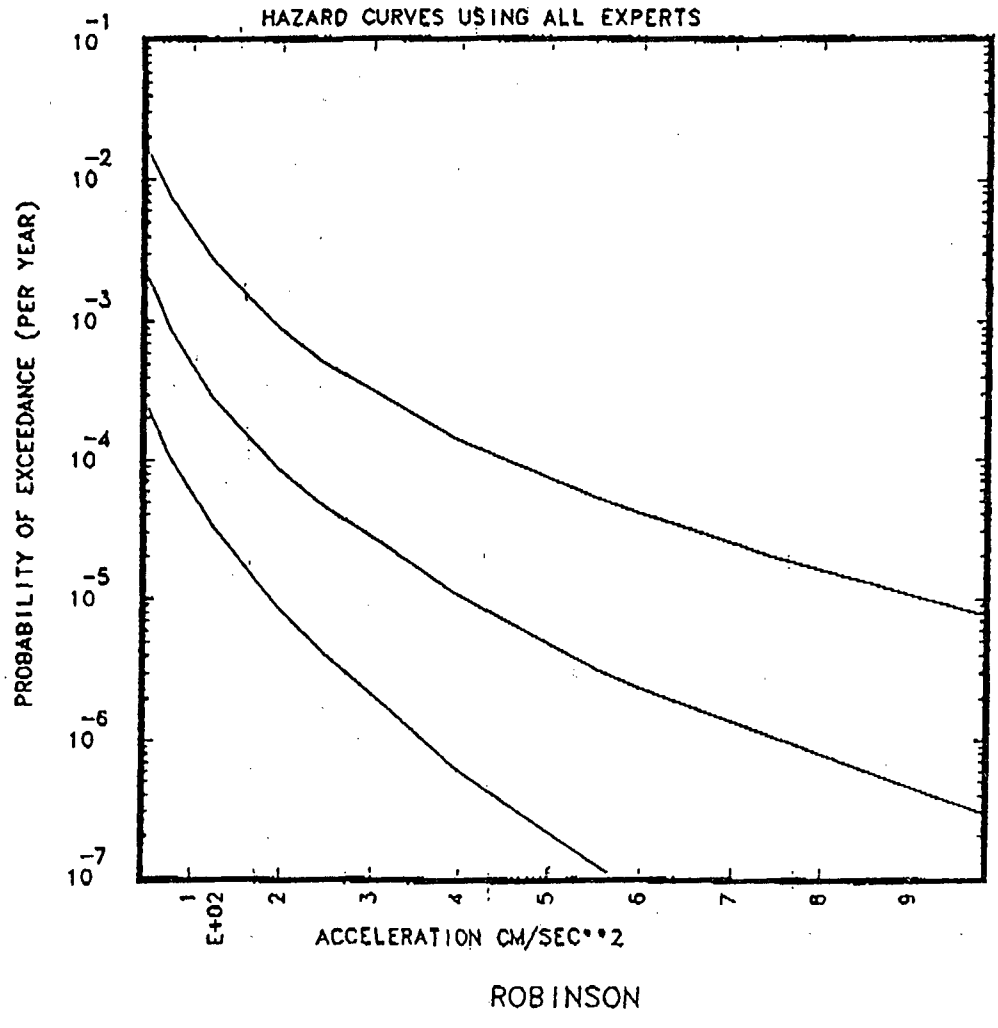

Figure 6-2: Seismic Hazard Curves for the HBR2 Site

7. CASK DROP ANALYSIS

7.1 Background

Cask drop analyses were performed as part of this study because the BNL study indicated sigificant uncertainty as to whether damage would occur. The spent fuel pools at Vermont Yankee and H.B. Robinson were analyzed for their response to cask drops. The purpose of this study is to assess the affects of a shipping cask drop on a spent fuel pool wall, assuming that the VY and HBR wall designs (thickness, strength and reinforcement) are typical. The walls selected for analysis were determined after discussion with the NRC and were based on the fuel pool configuration, and the path the casks would follow when crossing the pool. The cask weights and drop heights were obtained from actual plant operating criteria. The following cask drops were analyzed:

Vermont Yankee	-	40 ton	6" Drop
		110 ton	6" Drop
H. B. Robinson	-	68 ton	4' Drop

7.2 Analysis Methodology

Characterization of the nonlinear behavior of reinforced concrete is currently a topic of intense academic research. Attempts at analytically modeling the complicated interaction between reinforcing steel and concrete and the rate-dependence of concrete constitutive relationships have had limited success, and there is no one universally accepted model for nonlinear concrete finite element analysis. Efforts in this area have been hampered by the lack of an acceptable failure criteria for tri-axially loaded concrete. According to [Winter and Nilson 1979]:

"In spite of extensive and continuing research, no general theory of the strength of concrete under combined stress has yet emerged. Modifications of various strength theories, such as the maximum-tension stress, the Mohr-Coulomb, and the octahedral-stress theories, all of which are discussed in strength-of-materials texts, have been adapted with varying degrees of success to concrete".

These observations were made with regard to concrete under static, monotonic slow strain rate loading. In the case of extreme environmental loads (seismic, blast, impact), with resulting high strain rates, the difficulties are magnified. It is noted therefore that in absence of experimental testing, the estimation of damage in a reinforced concrete structure can be very subjective. Concrete design has necessarily been a mixed bag of structural mechanics fortified with empirical data from experimental tests. Predictive capabilities of the ultimate strength of typical reinforced concrete structures such as simple beams and columns is fairly well understood but more exotic or lesser used structural systems are difficult to design and analyze.

For the impact of the spent fuel cask on the wall, the load on the wall is in-plane and the configuration is essentially a deep beam subjected to transverse load. The American Concrete Institute [ACI 1977] has design formulas for deep reinforced concrete beams. The design formulas are based on standard Whitney stress block formulas. The underlying assumption of the ultimate strength formulas is that plane sections of the beam remain plane after loading. As a beam becomes very deep, the plane section assumption becomes less valid. The ACI code places limits on the aspect ratio (span/depth) outside the range of applicability of the ACI formulas, the code states that the beams shall be designed "taking into account the nonlinear distribution of strain", however, the code does not provide guidance on how this should be performed. The design profession has handled deep beams by utilizing elasticity solutions to estimate the stress distribution in very deep beams [L. Chow, et al., 1977 and Design of Deep Girders, 1977]. The stresses from elasticity solutions are integrated to determine the location and magnitude of stress resultants and steel is apportioned in order to supply tensile stress resultants. A check of the aspect ratio of a typical pool wall shows that they are very deep beams and are below the range of application of simple ACI formulas. In addition, from finite element impact analysis (discussed in detail below) the stress distribution is quite complex and changes continually during impact loading. Consequently, a simple application of ACI type formulas or use of elasticity solutions which have been derived for static loads is inadequate. Information on the experimentally determined strength of moderately deep reinforced concrete beams can be found in the literature [K. N. Smith et al., 1982, and H. A. Rawden et. al 1965] however, the data is restricted to static loadings and the aspect ratio of the tested beams are much shallower than the fuel pool walls. Work on impact loading of reinforced concrete beams has been conducted by Loo and Santos [Y. C. Loo and A. P. Santos, 1986]. The authors developed analytical expressions for beam response to an impact load at mid-span of a pinned-pinned beam. The results are only applicable in the linear response range and the derived expressions are for thin beams (i.e., transverse deflections dominated by flexure rather than shear) and consequently are not directly applicable to the current problem. Extensive effort has gone into developing empirical formulas for missile impact on reinforced concrete (an excellent summary is given by Sliter [G. E. Sliter, 1980]). These formulas deal primarily with impact of small missiles and local impact response such as cratering, crushing, etc., and do not address the global response of the structure.

All of these cited works and design formulas are not applicable to the particular geometry and loading of the spent fuel wall impact problem. Consequently one must resort to a numerical analysis to obtain estimates of the damage the wall sustains as a result of impact.

A numerical methodology which has been used by practicing engineers to approximate the behavior of concrete structures is to perform a finite element analysis in which the reinforced concrete structure is idealized as a linear elastic structure [A. Davito et al., 1978, and Personnel Communication 1979]. When this approach is used damage estimates under extreme loads can be made based on the stresses obtained from the linear analysis. It is

understood that this method does not account for stiffness degradation due to concrete/steel damage nor does it account for energy dissipation due to inelastic action. However, because of limitations on state-of-the-art nonlinear finite element techniques, more rigorous analysis may not be justified. For the current study it was decided to exploit the contact surface algorithms in existing nonlinear finite element codes in order to rigorously model the impact of the cask on the wall. The wall is taken as a homogenous, isotropic, linear elastic structure. Based on the stresses from the linear elastic analysis, judgements on wall damage can be made. All analyses were conducted with NIKE2D [J. Hallquist 1986], a nonlinear finite element program with the capability to model contact/impact problems. Further simplification of the problem is obtained by assuming the impacting cask is rigid.

7.3 Cask Drop Analysis of Vermont Yankee Fuel Pool

7.3.1 Finite Element Model

A two-dimensional finite element model was constructed for the south wall of the Vermont Yankee spent fuel pool (see Fig. 7-1). This wall was selected as a worst case example. The wall was treated as a plane stress structure with the appropriate thickness. Consideration of all possible load combinations was beyond the scope of the current study, thus dead weight, hydrostatic loads and thermal loads were not included in the analysis. Consideration of hydrostatic and thermal loads requires a full 3-D analysis and is more computationally intensive than the 2-D analysis which have been performed. The stresses caused by the cask impact are much larger than the stresses due to the self-weight of the wall, and the impact load stresses different regions of the wall than does the gravity load. In light of this, it is felt that inclusion of the gravity load component would not substantially change the damage estimates. The boundary conditions were taken as fixed at the outer corners of the wall where the north-south running beams support the pool structure. There is also an east-west running beam under the south wall. This beam was not included in the finite element model, which essentially neglects its stiffness. Because of the nature of the dynamic response, and the fact that the in-plane stiffness of the pool wall is so great, neglecting the beam for impact loading is acceptable. The ends of the wall in the finite element model are left free and thus any stiffening provided by the north-south walls and floor diaphragms is neglected. For the finite element analysis, the wall is taken as a linear elastic material with an elastic modulus of $57000\ (f'_c)^{1/2}$. The original design strength of the concrete was f'_c = 4000 psi (12). In-situ testing of the concrete in the pool bottom showed present day strength of about 7000 psi. Because of uncertainty in wall concrete strength (it was unclear if the concrete in the floor was the same as the wall concrete), the 4000 psi value was used for conservatism. Two cask weights were considered, the first cask was taken to be 110 tons, the second cask was 40 tons. Both casks were assumed dropped from a height of 6 inches (the operating criteria dictates this as the maximum height the cask can be lifted (7)). The cask is modeled as a solid steel body with a width of 8 feet.

The geometrically nonlinear portion of the problem (i.e., the impact in which the contact surface is changing) was modeled with the NIKE2D contact algorithm. The equations of motion were integrated at a time step of .0005 seconds, based on some limited sensitivity analyses this time step appears sufficiently short to capture the problem dynamics.

7.3.2 110 Ton Cask Drop

The displacement of the system during impact is summarized in Fig. 7-2 which shows the vertical displacement of a point at mid-span and mid-depth of the wall. Also shown is the displaced shape of the wall from initial impact until the cask rebounds. In order to estimate the damage which the wall incurs, the contours of principal stresses and vertical and horizontal strains were plotted for each time step in the response. The principal stress values were used to estimate regions of potential concrete cracking. While a tri-axial failure criteria for concrete is not currently available, a bi-axial failure envelope has been established. This failure envelope is shown in Fig. 7-3. In the region where both principal stresses are compressive, the failure criteria is simply the exceedance of the concrete compressive stress by either stress component (i.e., quadrant iii in Fig. 7-3). From Fig. 7-3 it is observed that if either principal stress component is positive and greater than the modulus of rupture of the concrete (taken as $4\,(f'_c)^{1/2}$) then a tension crack will develop. Figure 7-4 shows regions of the wall in which the principal stress is positive and larger than the modulus of rupture at some time during the impact analysis. This figure indicates that virtually the entire wall is subject to tensile cracking at some point during the response. Minor cracking is generally not a significant problem and this does not necessarily indicate any catastrophic failure or even loss of water from the pool. The pool has a thin metal liner which provides containment of the pool water. If the liner remains intact, the water will be contained despite concrete cracking. Another indicator of wall damage is the possibility of yielding of the reinforcing steel. In order to estimate the regions in which the reinforcing steel might yield during impact loading, contour plots of the vertical and horizontal strains at each time step were used. The contour values were set equal to the yield strain values of the steel which allowed a direct view of yield regions at each time step. The contour plots for each time step were then superimposed, to show cumulative damage as indicated in Fig. 7-5 and Fig. 7-6. The results of these overlays are shown in Fig. 7-7 and Fig. 7-8. These plots indicate the regions of the wall where the horizontal and vertical strains exceed the strain which reinforcing steel would have at initial yield at some time during the impact response (yielding in different regions does not occur simultaneously). These plots allow an estimation of areas in which the reinforcing steel yields and thus significant structural damage may occur.

7.3.3 40 Ton Cask Drop

The impact analysis was repeated for a 40 ton cask, all other parameters remained the same. The response time history of the wall is shown in Fig. 7-9, where the displacements are significantly less than the 110 ton cask

case (Fig. 7-2). As with the 110 ton cask the maximum principal tensile stress exceeds the modulus of rupture throughout the wall and thus concrete cracking potentially occurs throughout the wall. The estimated regions of reinforcing steel yielding are indicated in Fig. 7-10 and Fig. 7-11. For the 40 ton cask the vertical steel region of yield is still substantial, but the region of yield of horizontal steel is greatly reduced from the 110 ton case. The reason for the significant reduction in the horizontal steel yielding appears to be due to the fact that the wall does not experience such large overall deflections for the 40 ton case (compare displaced shape plots in Fig. 7-9 and Fig. 7-2 at the maximum response times) and the yielding of the horizontal steel occurs as a result of the global or overall deflections of the wall. The vertical steel yielding, on the other hand, occurs in the early stages of impact as the impact stresses propagate through the depth of the wall, prior to the overall response of the wall.

7.4 Cask Drop Analysis of H.B. Robinson Fuel Pool

7.4.1 Finite Element Model

A 68 ton cask was considered dropped from a height of 4 feet onto the reinforced concrete pool wall. A plane stress finite element model was constructed for both the cask and the pool wall (see Fig. 7-12). The hole in the wall is the entrance to the waste gas decay tank area. Dead weight, hydrostatic, and thermal loads were not included in the analysis. The cask was given an initial velocity equal to that which would be attained in a four foot drop.

7.4.2 Results of Analysis

The time history response of the wall/cask system, expressed in terms of the vertical displacement of a node on the wall directly under the cask, is shown in Fig. 7-13. Also shown in Fig. 7-13 are the displaced shapes of the wall at selected time steps. The wall is observed to "crush" directly under the cask. In the last displaced shape plot, the cask has bottomed out and is in the process of rebounding. As with the Vermont Yankee pool, cumulative damage estimates of the concrete and reinforcing steel were obtained by superimposing strain plots from each time step (see Fig. 7-14 and 7-15). The strain contours which were plotted were set equal to yield strain values for steel. The stress values in the wall exceed that required for concrete cracking throughout the wall. The wall is observed to suffer significant damage as a result of the 4 foot drop. Based on the previous results for the Vermont Yankee pool (drop height of 6 inches) it is clear that the relatively high drop height has dramatically increased the damage.

7.5 Summary of Observations

The dynamic response of the walls resulting from cask impact loading is more like an elastic half space than a deep beam. The stresses from impact propagate through the wall radially from the point of impact prior to the overall transverse displacement of the wall. As a result, the deformed shape

of the wall at any given time is a combination of global transverse displacement (like a shear beam) and deflections caused by propagation and reflections of stress waves in the wall. The resulting displaced shapes are quite complex and do not resemble the simple transverse deflection one would expect from a shear beam. Because of the dimensions of the walls (i.e., the walls would be classified as "very deep beams" by the ACI code) and the observed complex dynamic response, simple classical methods of strength estimation such as ACI code formulas are inadequate. In addition, estimation of cracked sections for more rigorous analysis is essentially impossible.

The finite element analysis which was performed had the desirable feature of rigorously modeling the impact between the cask and wall with the NIKE2D impact algorithm, however a number of simplifying assumptions had to be made to conduct the analysis in a timely fashion. The most significant simplifications were the assumptions of homogeneous, isotropic linear elastic material behavior for both the cask and the wall. Obviously as the walls incur damage the material does not remain elastic. It is also noted that the assumption of a rigid cask results in higher stresses than if the cask flexibility is included. The analysis included only the planar load due to impact and did not address added the load due to thermal, wall gravity or pool water loads. Based on the stress distributions from the impact analyses, it appears that hydrostatic loading would have the most interaction with impact loads. A simulation of hydrostatic and impact load combination would require a three-dimensional modeling effort.

The results of the idealized analyses indicate that pool walls similar to those of both the Vermont Yankee and Robinson plants would suffer severe damage as a result of the worst-case cask drops. The indicated regions of potential reinforcing steel yield are quite extensive. While the integrity of the pool liner is difficult to predict, it seems likely that the liners could be severely damaged (tearing, cracking of welds, and pull-out of anchors). Based on these results, loss of pool water certainly cannot be ruled out.

Even with the most advanced nonlinear finite element techniques, it would be difficult to obtain a very high level of confidence in the complete accuracy of the impact analysis of the wall. A definitive estimate of wall damage would require full scale drop tests on a wall. However, the simple linear analysis which has been performed gives insight into both the level of damage, and for the Vermont Yankee plant, the relative damage between the 110 ton and 40 ton casks.

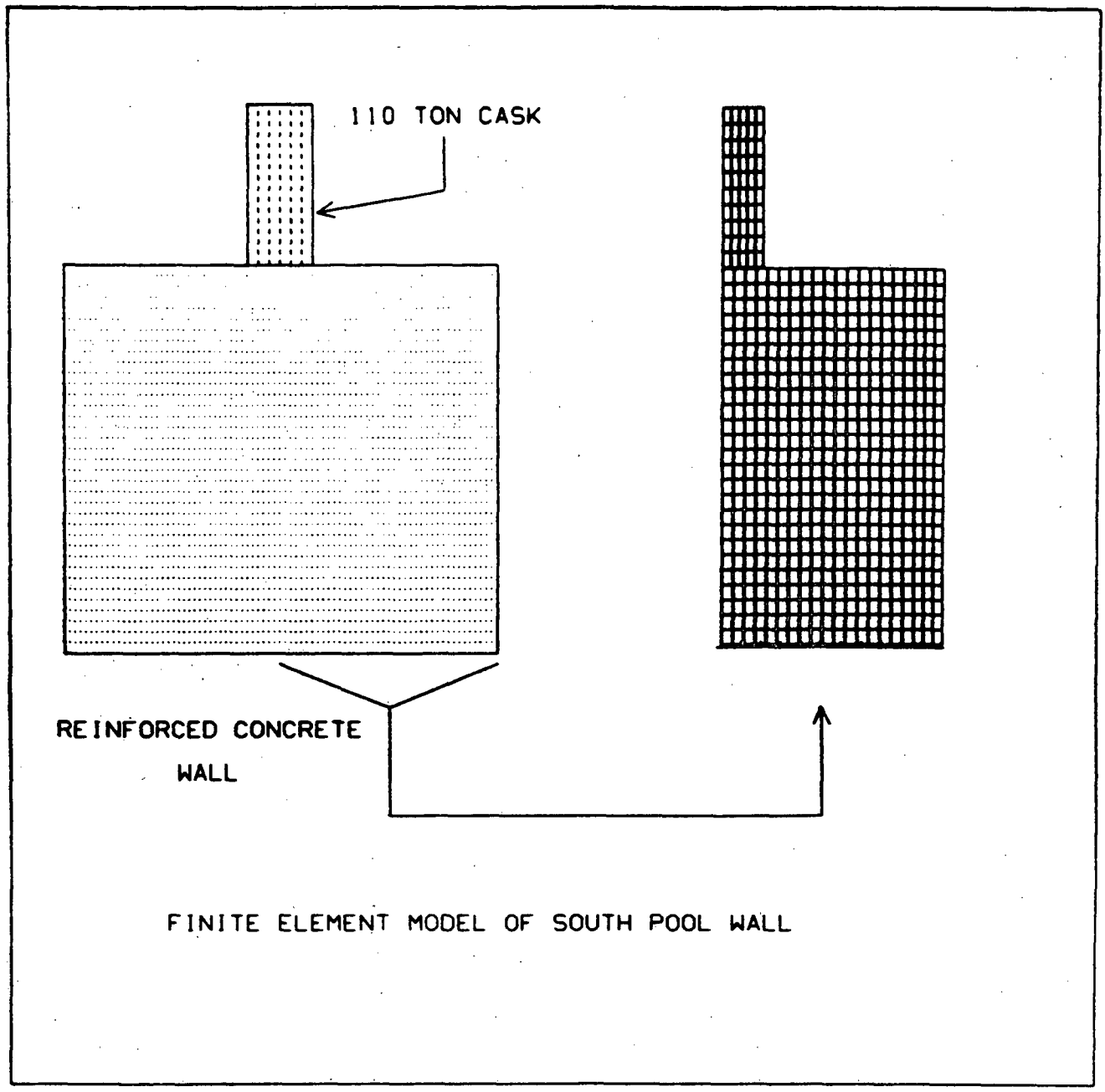

Figure 7-1: Finite Element Model of Wall and Cask

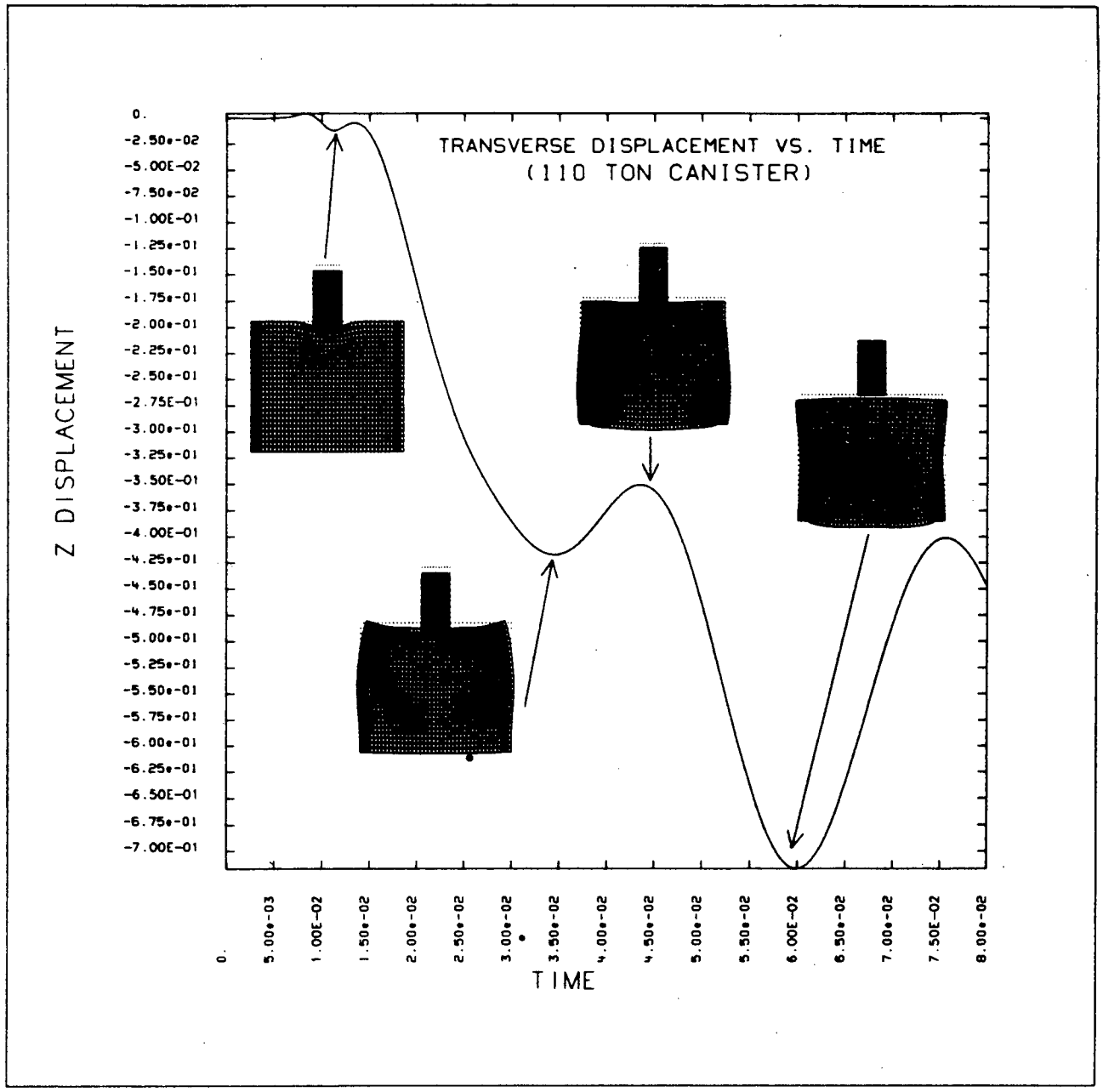

Figure 7-2: Dynamic Response Resulting From Impact

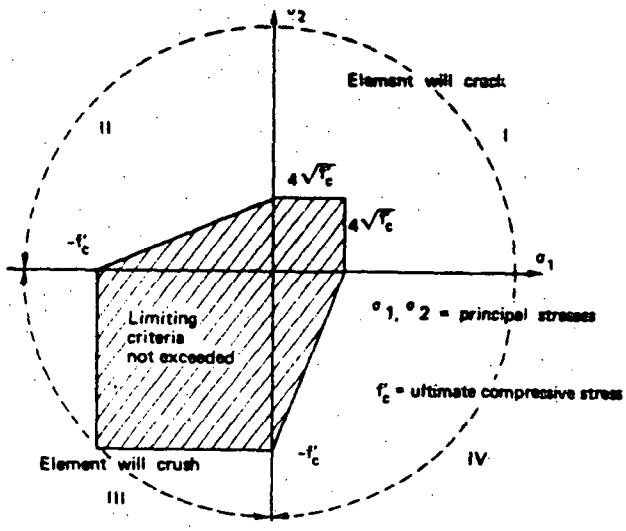

Figure 7-3: Bi-Axial Failure Envelope for Concrete

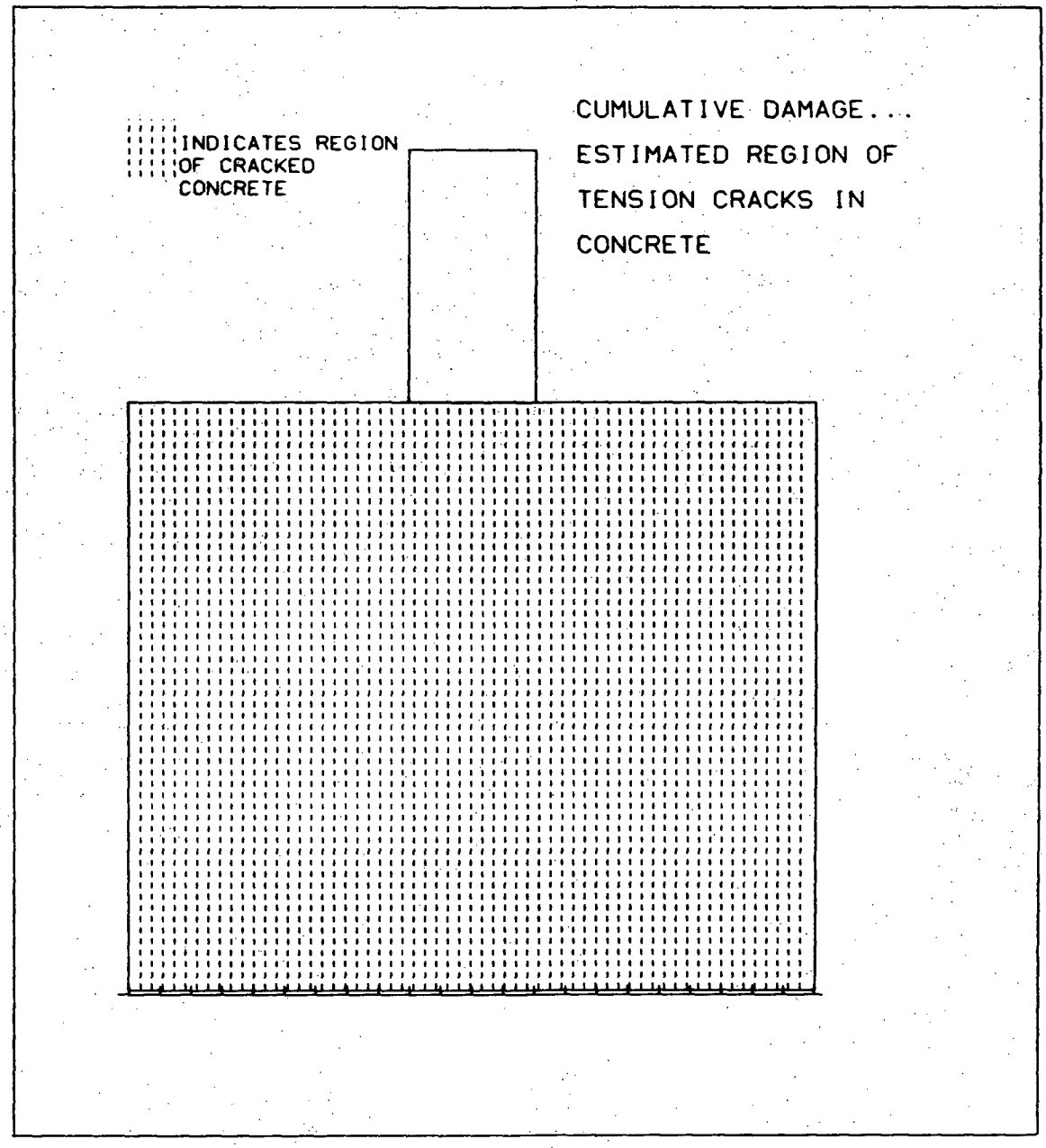

Figure 7-4: Estimated Region of Tensile Cracking in Concrete

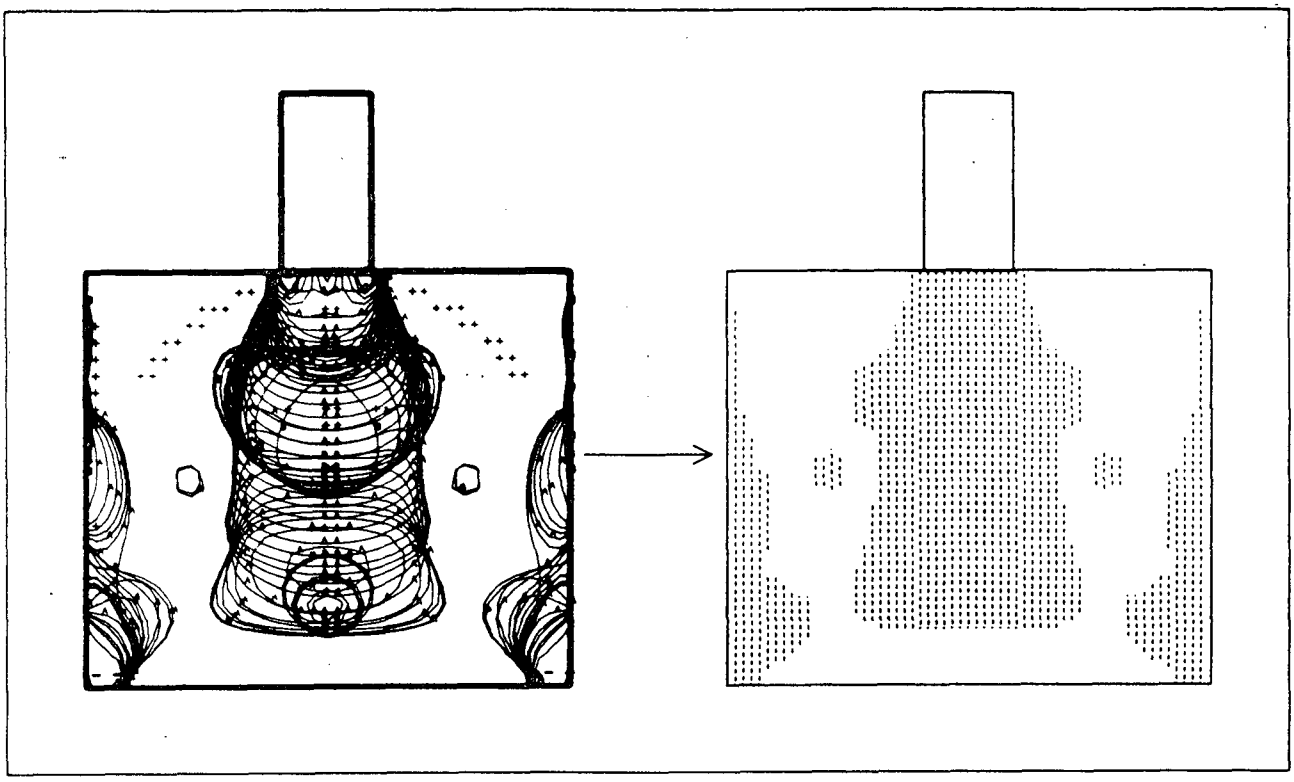

Figure 7-5: Estimating Region of Vertical Steel Yielding

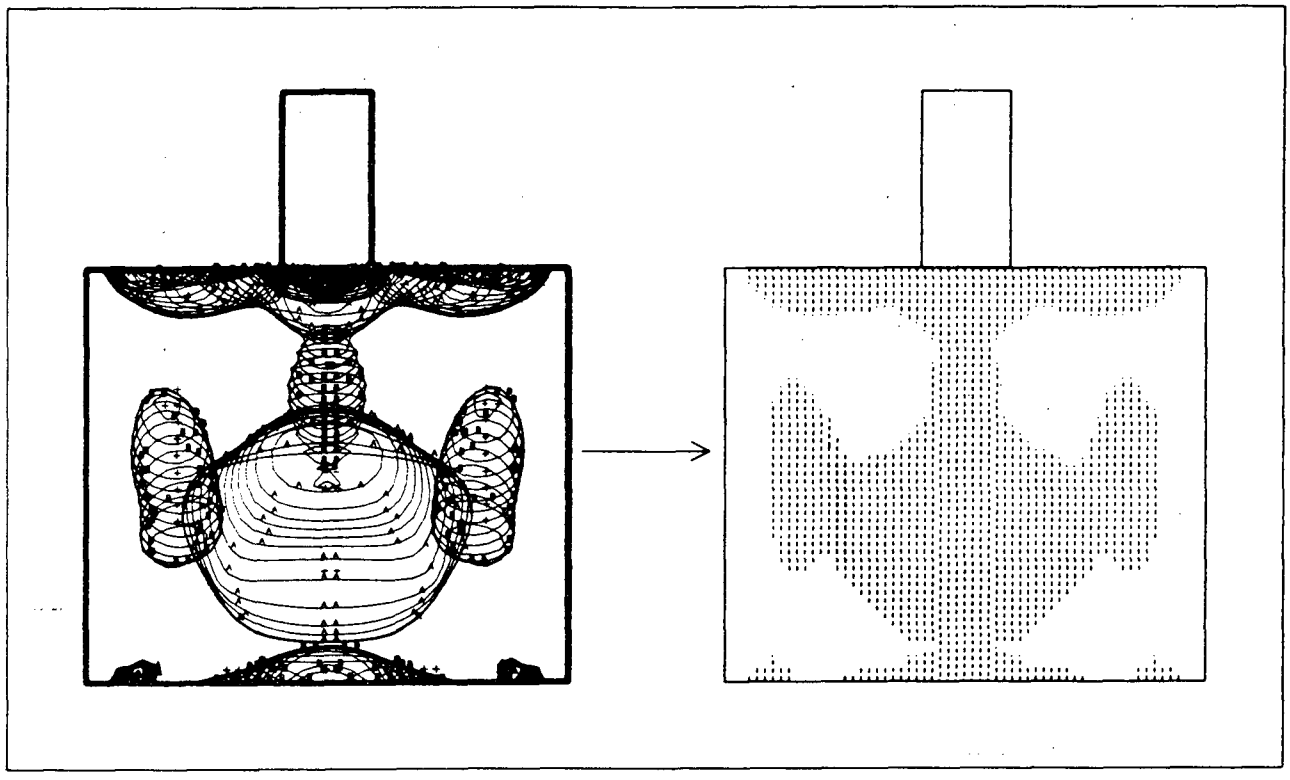

Figure 7-6: Estimating Region of Horizontal Steel Yielding

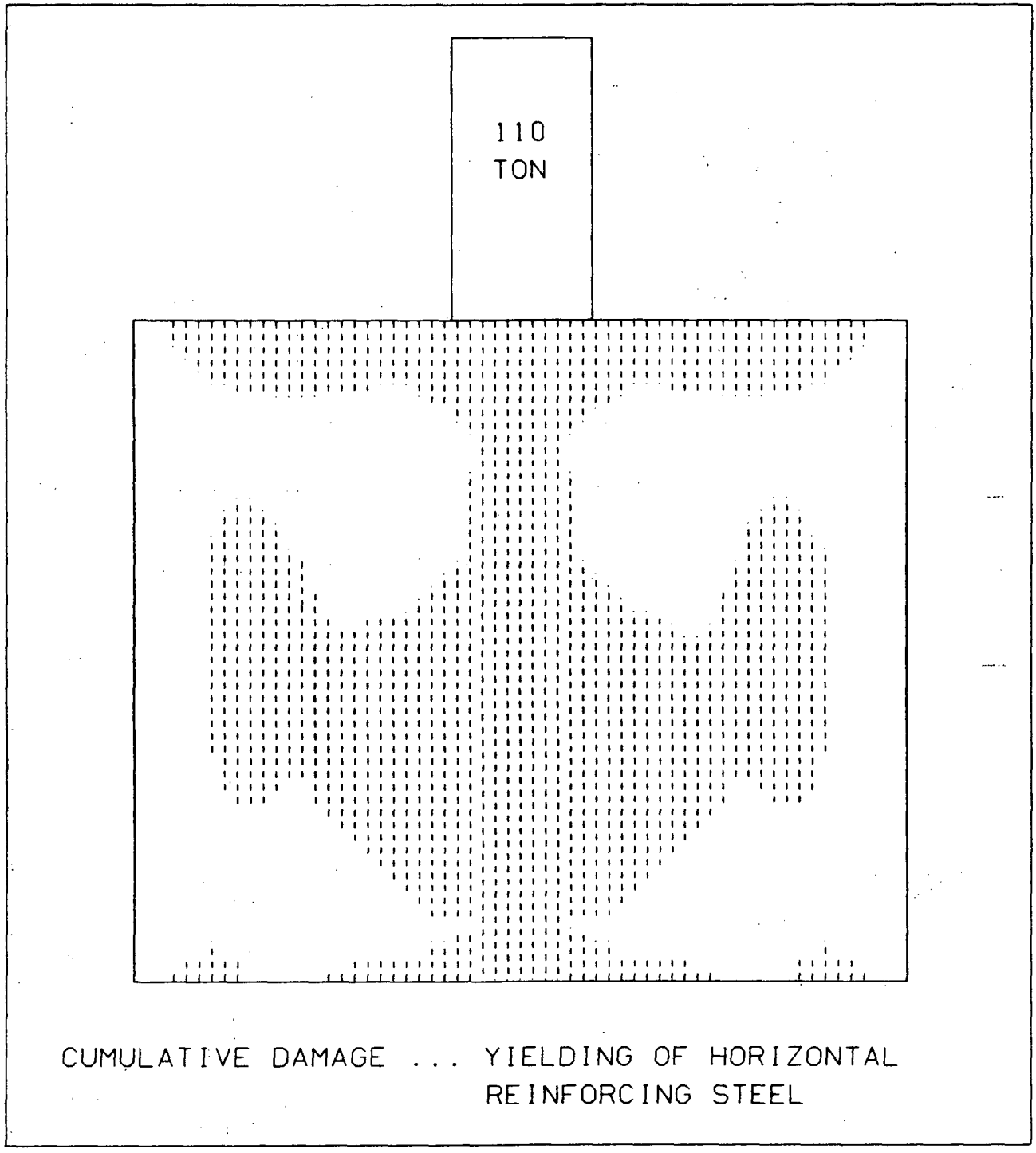

Figure 7-7: Yielding of Horizontal Steel

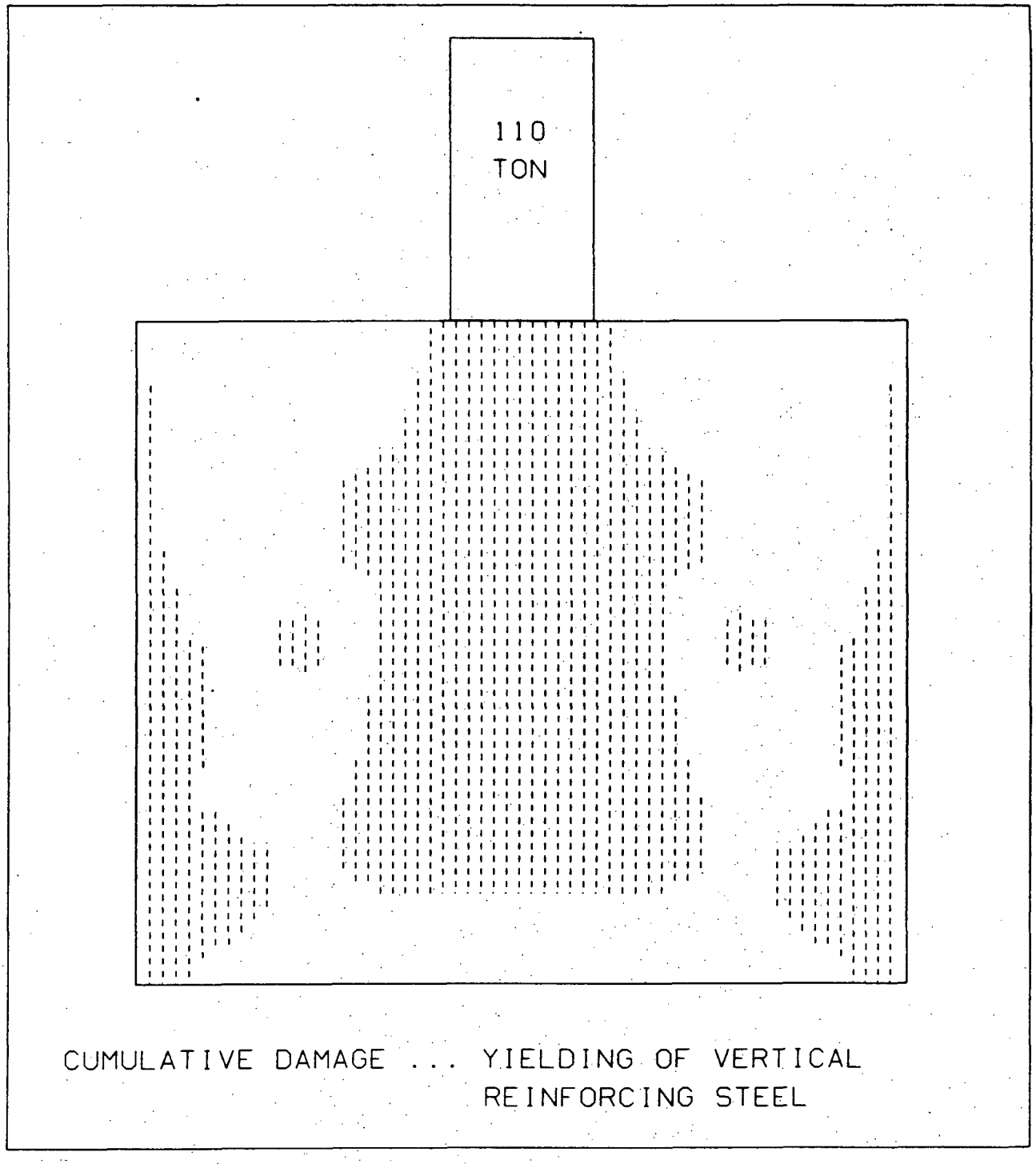

Figure 7-8: Yielding of Vertical Steel

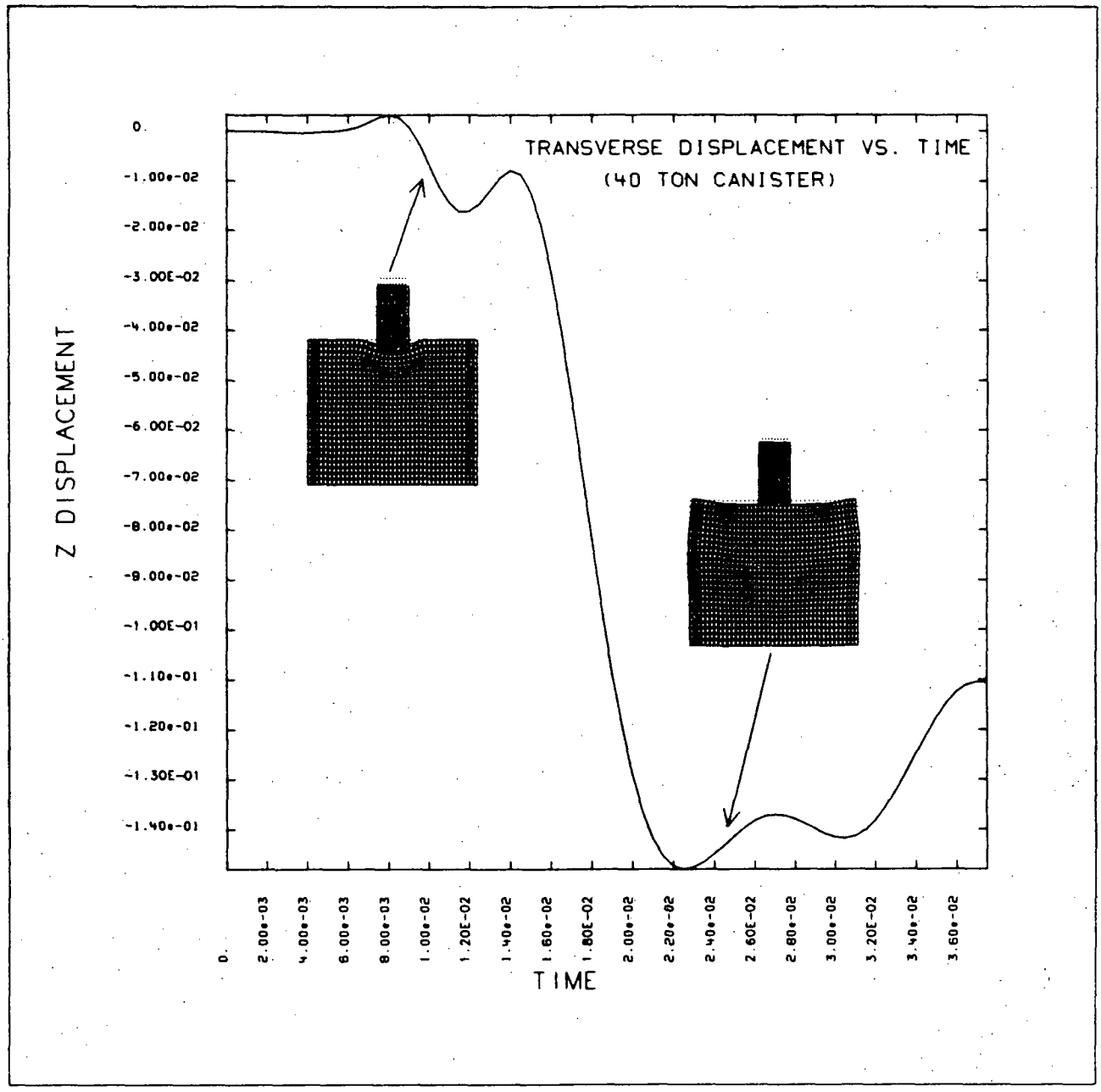

Figure 7-9: Dynamic Response Resulting From Impact

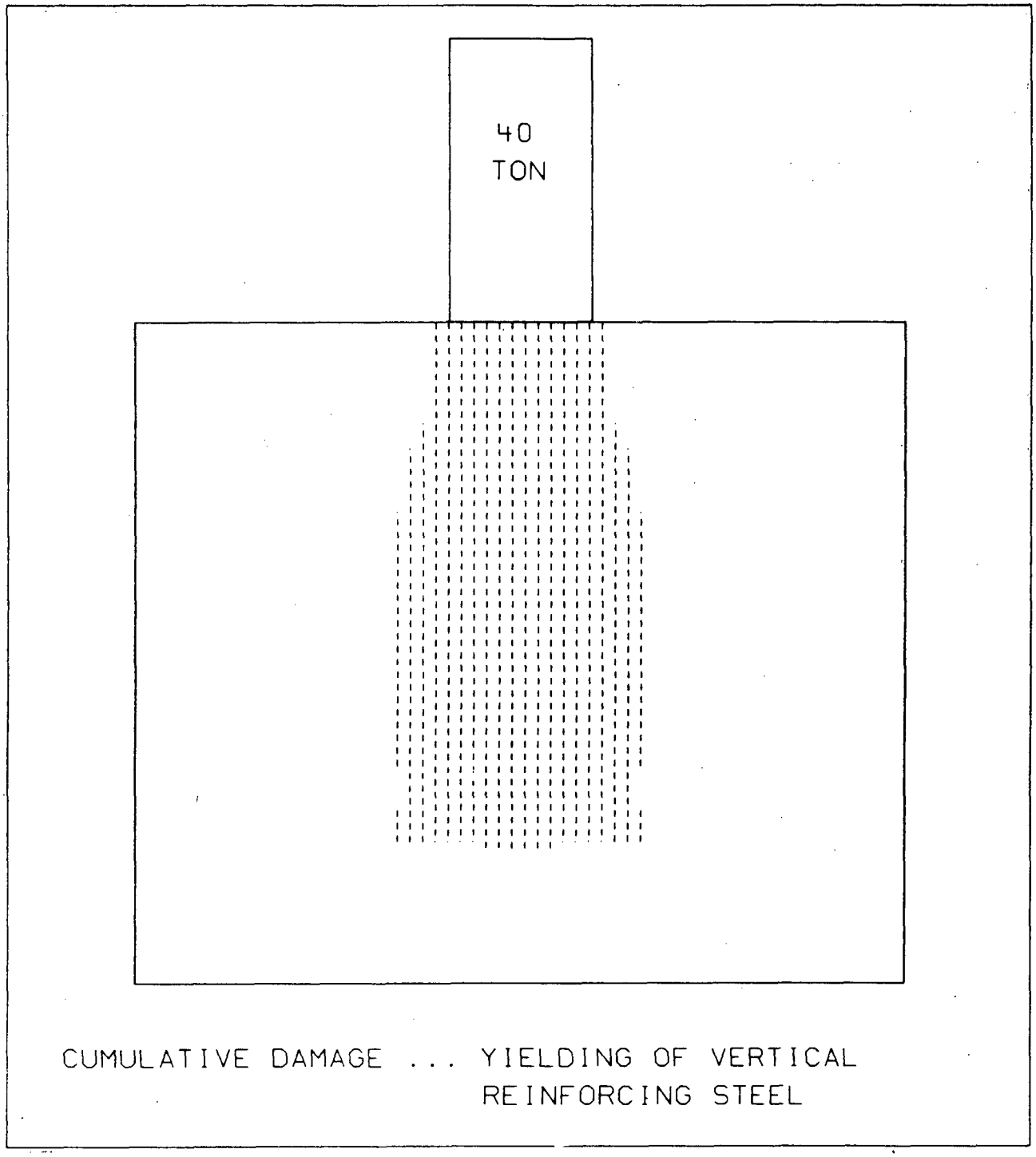

Figure 7-10: Yielding of Vertical Steel

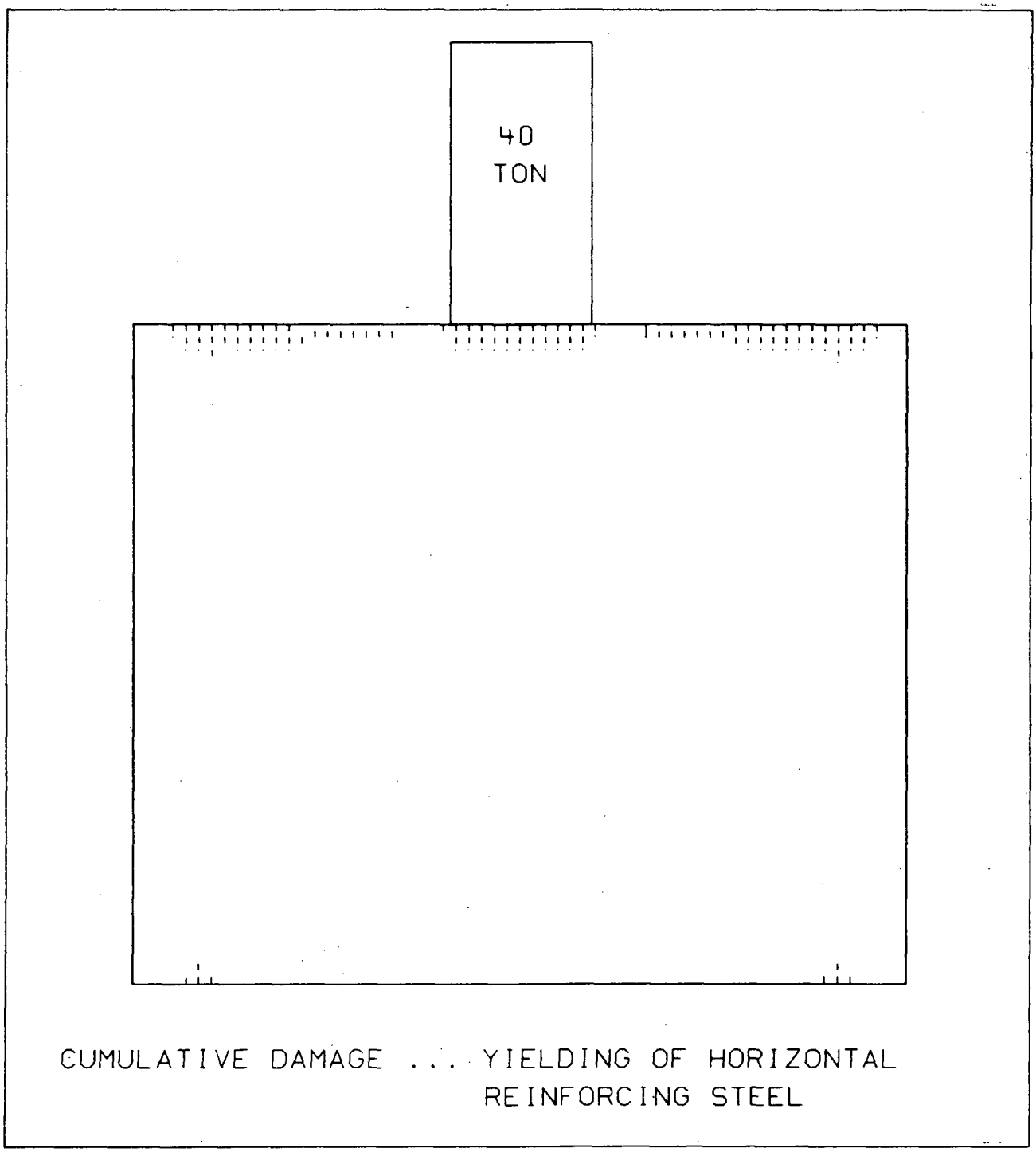

Figure 7-11: Yielding of Horizontal Steel

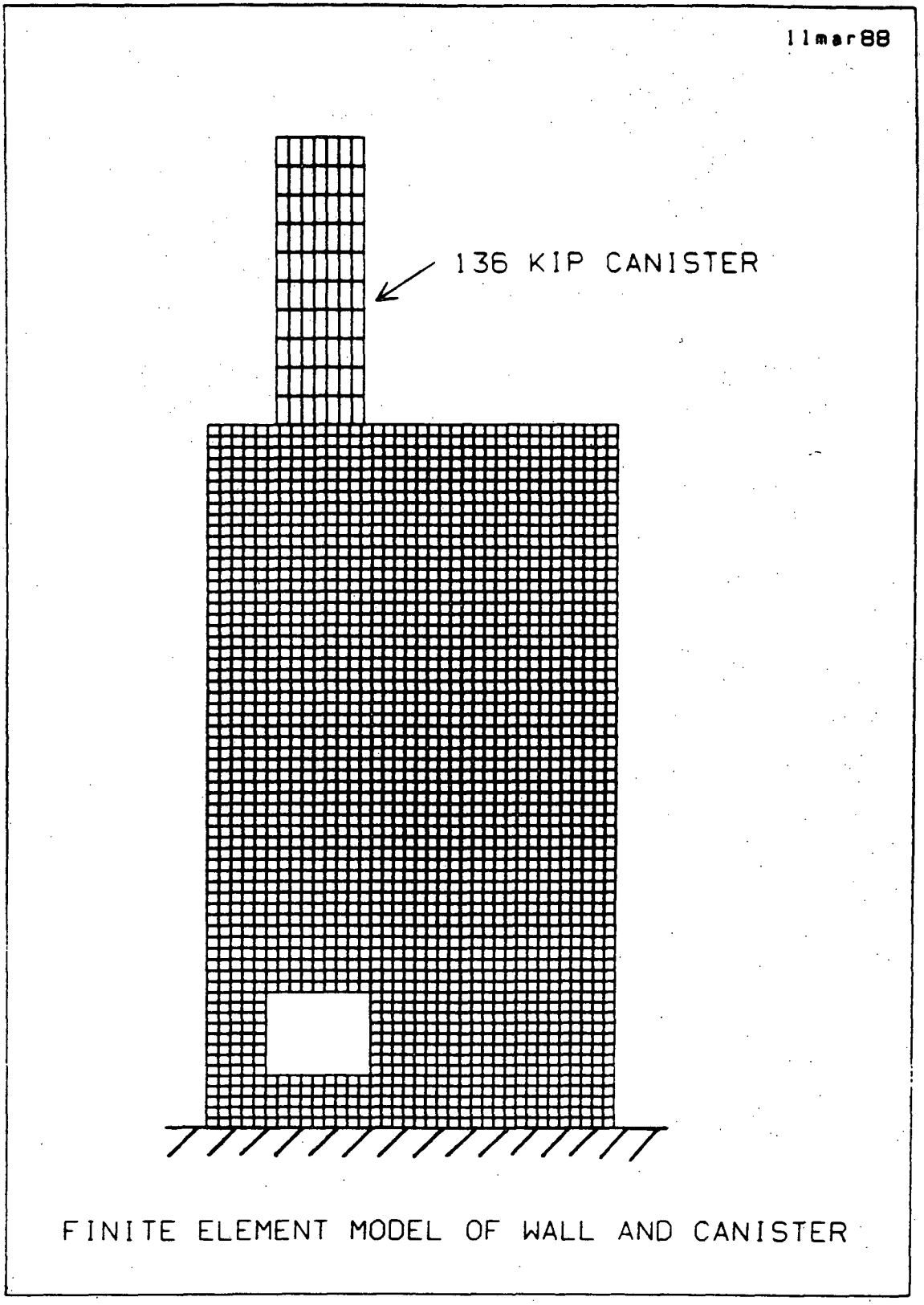

Figure 7-12: Finite Element Model of the Cask and Wall System

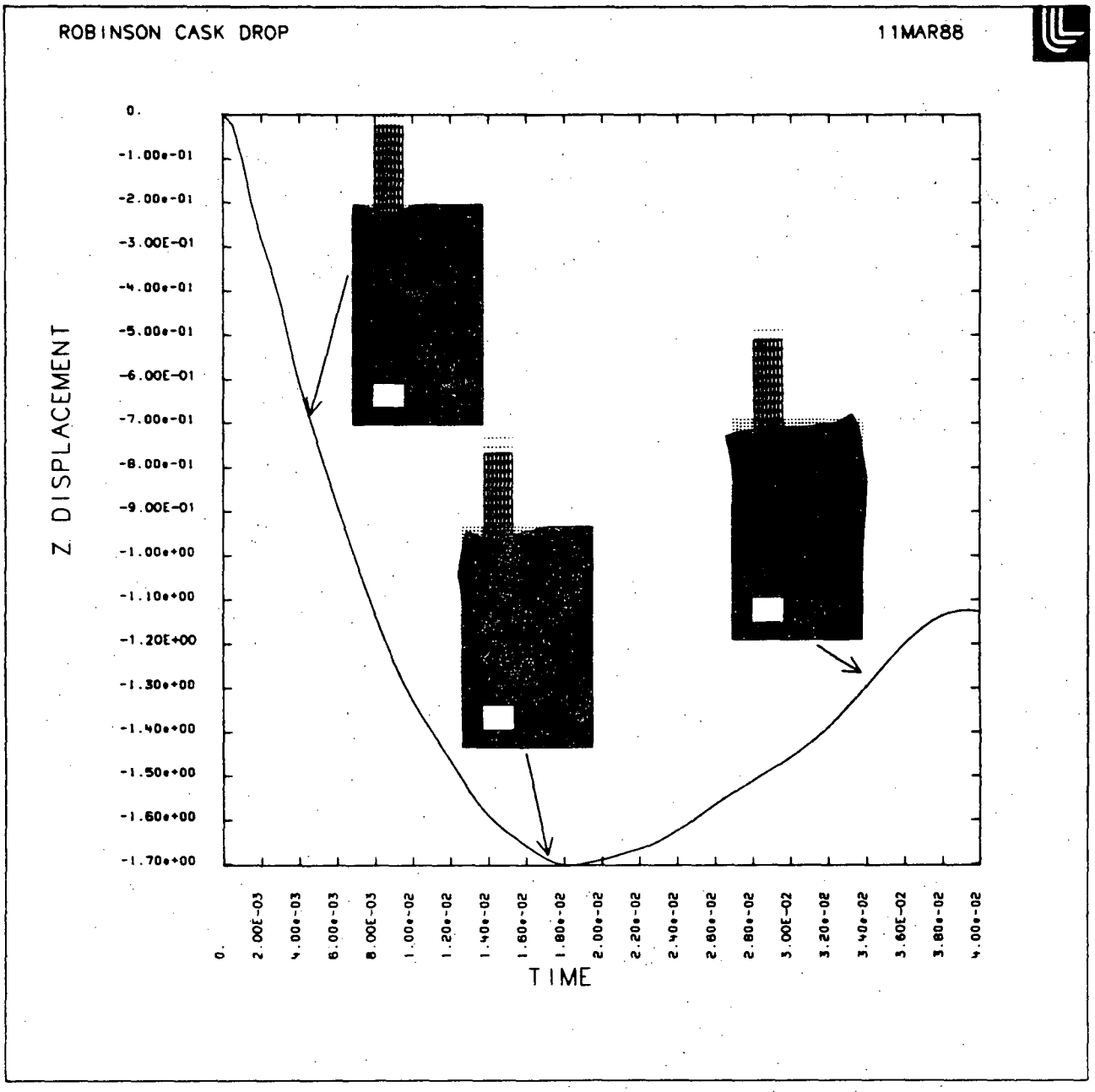

Figure 7-13: Time History Response of the Wall

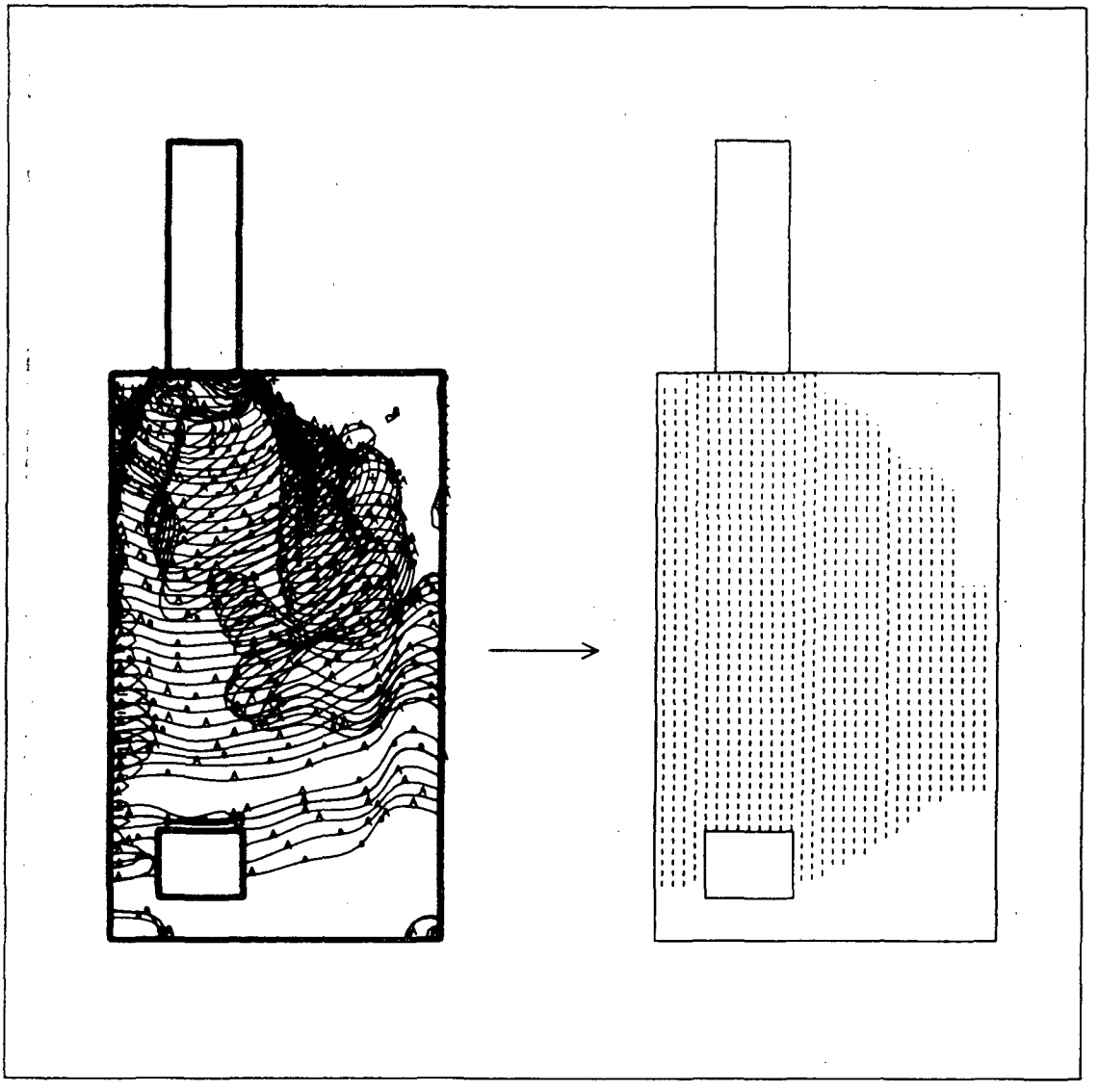

Figure 7-14: Estimating Damage to Vertical Reinforcing Steel

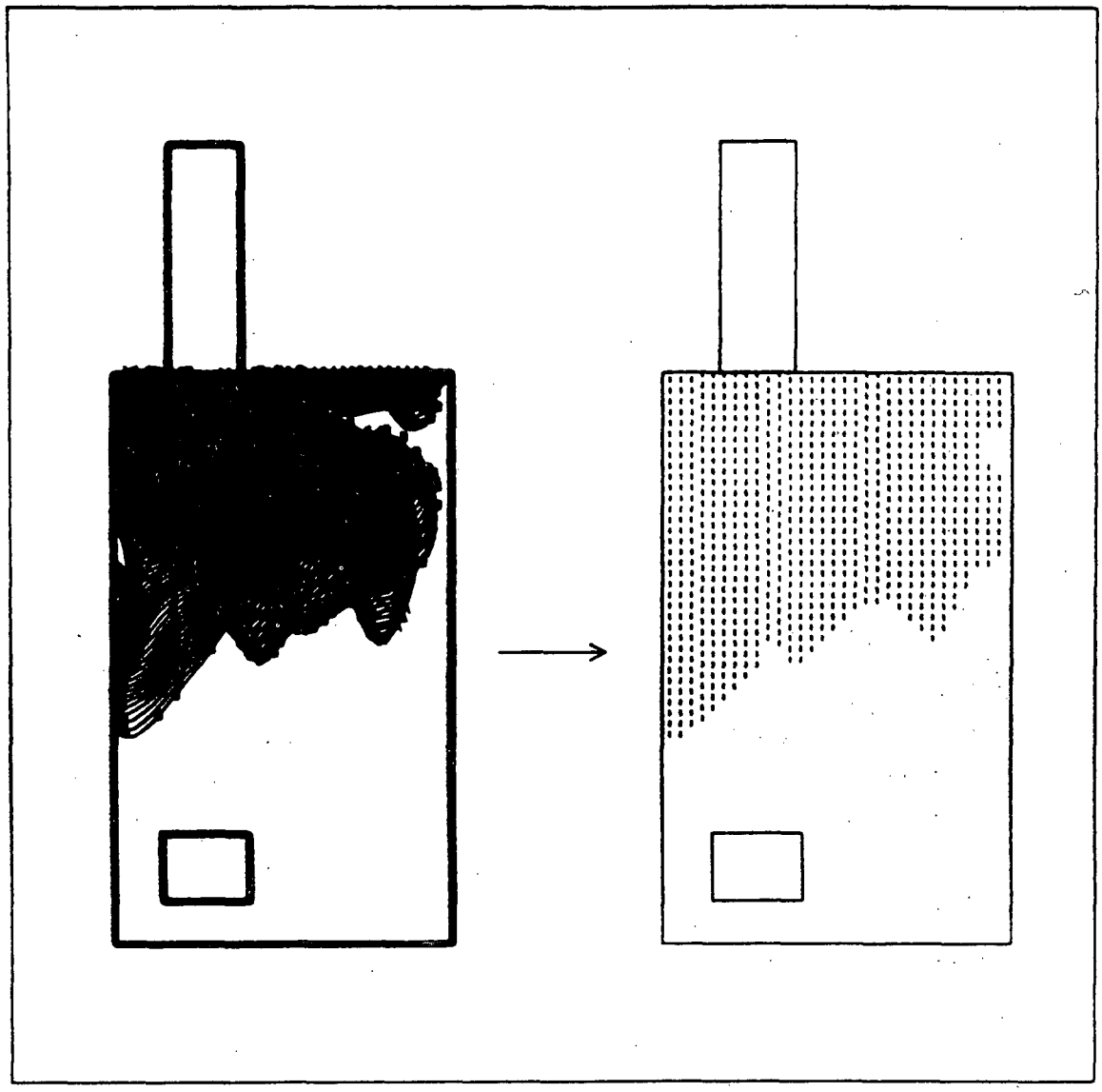

Figure 7-15: Estimating Damage to Horizontal Reinforcing Steel

8. SUMMARY AND CONCLUSIONS

8.1 Summary

The objective of this study was to provide technical assistance to the NRC concerning the Generic Issue - 82, "Beyond Design Basis Accidents in Spent Fuel Pools". The realistic seismic capacity of spent fuel pools at two representative plants was estimated and the spent fuel pool's seismic failure probability was assessed and site specific information was used for this analysis. For this purpose, the spent fuel pools at Vermont Yankee (BWR) and H. B. Robinson Unit 2 (PWR) were studied. The seismic PRA and margins approach was used in this study to assess the seismic risks from spent fuel pool failures.

The failure modes for the spent fuel pools were: 1) loss of liner integrity precipitated by gross structural failure of the spent fuel pool, 2) loss of function of the fuel pool support system (e.g., pool cooling and make-up water capacity) resulting in loss of water inventory, 3) damage to fuel racks and 4) cask drop accidents. Gross structural failure of the pool was analyzed by identifying the potential locations for gross failure. In the Vermont Yankee spent fuel pool, the out-of-plane shear failure of the pool slab was determined to be the controlling failure mode. In the Robinson spent fuel pool, the controlling failure mode was identified to be the out-of-plane bending of the pool wall. The fragility of the pool structures under these failure modes was estimated taking into account the seismic margins inherent in design along with the uncertainties. The so-called High Confidence of Low Probability of Failure capacity of the pool structure from seismic motion was estimated to be 0.50g for Vermont Yankee and 0.65g for H. B. Robinson Unit 2. The higher capacity for the Robinson fuel pool may have resulted from structure and fuel rack modifications included with installation of the high density fuel racks.

The cooling and make-up water systems for the two pools were reviewed; event and fault trees were constructed to identify the accident sequences that result from failure of these systems. For the components appearing in these accident sequences, seismic fragilities were estimated based on the design information and plant walkdowns. Boolean equations developed from the fault tree analysis were quantified using the seismic fragilities and hazard curves. The dominant components to spent fuel pool systems failure are similar to component that have been found to contribute to seismic risk in several PRAs; poorly anchored electrical equipment and tanks. The consequences of the cooling and make-up water system failure on the spent fuel pool system were assessed by performing a thermal analysis. It was concluded that the fuel assembly uncovery would occur only after 3 to 7 days from the time of failure of the cooling and make-up water systems; this response time is considered to be sufficiently long for any recovery action.

The free-standing high density fuel racks at Vermont Yankee were reviewed for potential failure under seismic loads. It was concluded that crushing of fuel and assemblies and the flexural failure of the rack are not credible failure

modes. Therefore, the fuel assemblies cannot be compressed into a critical mass; no serious effects can result as long as the fuel is covered.

In this study, preliminary site-specific seismic hazard curves developed by LLNL for the NRC under the Eastern United States Seismicity Program were used.

The mean annual frequency of seismic failure for the spent fuel pool structure was estimated to be 6.7E-06 for Vermont Yankee and 1.8E-06 for H. B. Robinson Unit 2. The 5% to 95% confidence range for these frequencies was about 3.0E-11 to 2.4E-05. The mean annual frequency of failure of cooling and make-up water systems in the two spent fuel pool systems was about 1.5E-04/reactor-yr. As explained before, the consequence of this failure is not significant because of the long response time available to recover cooling or provide alternate makeup.

The effect of a spent fuel cask drop on spent fuel pools was studied by performing a nonlinear two-dimensional finite-element analysis of the impact problem using Vermont Yankee and HBR as representative designs. For Vermont Yankee, two cask drops were considered: 40 ton and 110 ton both dropping from 6 inches. For Robinson, a 68 ton cask dropping from 4 feet was considered. The results of the analyses indicate that the pool walls would suffer severe damage as a result of cask drop. The indicated regions of potential reinforcing steel yield are quite extensive and while the integrity of the pool liner in difficult to predict, it seems likely that the liner would be severely damaged. Based on these results, loss of pool water certainly cannot be ruled out. The probability of this event is not estimated in this study; it is a function of the rate of spent fuel shipping, amount of storage available in the plant, handling equipment, reliability and human error in the handling of the cask. In the BNL report, the estimated cask drop probability was less than E-8 per reactor-yr which is consistent with the implementation of A-36 requirements.

8.2 Conclusions

Based on the insights and results obtained in this study the following conclusions can be drawn:

1. The spent fuel pool structure which is designed to retain large amounts of water and to withstand gravity and lateral loads from the fuel racks has a relatively high seismic capacity (the HCLPF capacity of the pool structure is estimated to be more than 3 times the SSE value); this is true for both the BWR spent fuel pool which is mounted high in the reactor building and the PWR pool which is generally at the ground level. Therefore, seismic risk contribution from spent fuel pool structural failures is negligibly small.

2. The assessment of potential failure modes of the fuel pool racks and fuel assemblies has indicated that the fuel rack design is such that the assembly cannot be compressed into a critical mass thereby leading to a severe accident.

3. Parts of the cooling and makeup systems for spent fuel pools are not designed as seismic class 1 systems and as such their failure is expected at relatively low seismic levels. However, the failure of cooling and makeup systems would not uncover the spent fuel assemblies for about 3 to 7 days; it is expected that some recovery action could be taken in this time period.

4. This study has shown that the use of plant-specific and site-specific information would reduce the uncertainty bands on the seismic risk estimates; previous BNL study using generic information had estimated the annual frequency of gross structural failure of the pool to vary from 1.6E-10 to 2.6E-04 for PWR; the current study shows this range to be 3.1E-11 to 1.4E-05. Similar results are obtained for the BWR spent fuel pool. Note that the reduction in the uncertainty on the higher end is more significant. The range of uncertainty in the risk estimate is governed by the range of uncertainty in the seismic hazard at the site. Note that the hazard curves used in this study are preliminary and subject to change following NRC and peer reviews. It is expected that the uncertainty range in hazard curves will be reduced, thereby reducing the uncertainty in the risk estimates.

5. This study used two representative spent fuel pools- a PWR and a BWR. These pools have been designed to the seismic design criteria existing in the late 1960s. Their large seismic capacities lead us to conclude that the pools designed to current seismic standards should have higher seismic capacities and should not contribute significantly to seismic risk.

9. REFERENCES

American Concrete Institute, Building Code Requirements for Reinforced Concrete, ACI 318-77, Detroit, Michigan, 1977.

American Nuclear Society, "Design Objectives for Light Water Reactor Spent Fuel Storage Facilities at Nuclear Power Stations", ANSI N210-1976/ANS-57.2, April 1976.

American Society of Civil Engineers, Design of Structures to Resist Nuclear Weapons Effects", Manual and Report on Engineering Practice No. 42, 1985.

Bernreuter, D. L., Savy, J. B., and Mensing, R. W., UCID-20421, Seismic Characterization of the Eastern United States, Volume 1: Methodology and Results for Ten Sites, April 1985.

Bernreuter, D. L., Savy, J. B., and Mensing, R. W., NUREG/CR-4885, UCID-20696, Seismic Hazard Characterization of the Eastern United Stated: Comparative Evaluation of the LLNL and EPRI Studies, May 1987.

Biggs, J.M., Introduction to Structural Dynamics, McGraw-Hill Book Company, 1964.

Chow, L., Conway, H., and Winter, G., Stresses in Deep Beams, Proceedings of the American Society of Civil Engineers No. 127, May 1952.

Davito, A., Murray, R., Nelson, T., and Bernreuter, D., Seismic Analysis of High Level Neutralized Liquid Waste Tanks at the Western New York State Nuclear Service Center West Valley New York, Lawrence Livermore National Laboratory, UCRL-52485, 1978.

Dong, R.G., "Effective Mass and Damping of Submerged Structures", UCRL-52342, Lawrence Livermore National Laboratory, April 1978.

EPRI, 1987a, "Seismic Verification of Nuclear Plant Equipment Anchorage", EPRI NP-5228, Prepared by URS Corp., May.

EPRI, 1987b, "Generic Seismic Ruggedness, of Power Plant Equipment", EPRI NP-5223, Prepared by ANCO Engineers for EPRI, May.

Habedank, G., Habip, L.M., and Swelim, H., "Dynamic Analysis of Storage Racks for Spent Fuel Assemblies", Nuclear Engineering and Design, 54(1979) 379-383.

Hallquist, John O., NIKE2D--A Vectorized Implicit, Finite Deformation Finite Element Code for Analyzing the Static and Dynamic Response of 2-D Solids with Interactive Rezoning and Graphics, Lawrence Livermore National Laboratory, UCID-19677, Rev. 1, December, 1986.

Hashimoto, P.S., and Ravindra, M.K., Seismic Evaluation of the Vermont Yankee Spent Fuel Pool, EQE, Incorporated, Newport Beach, California, FIN A-0816, September, 1987.

H. B. Robinson SEG Plant, APP-036-13 - Spent Fuel Pit High Temp., Rev. 6, Page 15.

H. B. Robinson SEG Plant, APP-036-14 - Spent Fuel Pit Hi. Lvl., Rev. 6, Page 16.

H. B. Robinson SEG Plant, APP-036-15 - Spent Fuel Pit Lo. Lvl., Rev. 6, Page 17.

H. B. Robinson SEG Plant, Operating Procedure OP-910 - Spent Fuel Pit Cooling and Purification System, April 23, 1985.

H. B. Robinson SEG Plant, System Description SD-013 - Component Cooling Water, June 4, 1987.

H. B. Robinson SEG Plant, System Description SD-014 - Spent Fuel Pit Cooling and Purification System, November 11, 1986.

H. B. Robinson SEG Plant, System Description SD-016 - Electrical System, February 3, 1988.

H. B. Robinson Unit 2 Nuclear Power Plant, "Final Safety Analysis Report", Section 3. - Design of Structures, Components, Equipment, and Systems, Section 9. - Fuel Storage and Handling, Section 15 - Spent Fuel Cask Drop Accidents.

Kaplan, S, "On The Method Of Discrete Probability Distribution in Risk and Reliability Calculations", Risk Analysis, Vol. 1, 1981.

Kennedy, R.P., and Ravindra, M.K., "Seismic Fragilities for Nuclear Power Plant Risk Studies", Nuclear Engineering and Design, Vol. 79, No. 1, pp 47-68, May 1984.

Kennedy, R.P., et al, "Engineering Characterization of Ground Motion - Task 1: Effects of Characteristics of Free-Field Motion on Structural Response", NUREG/CR-3805, May, 1984.

Kennedy, R.P., et al, "Probabilistic Seismic Safety Study of an Existing Nuclear Power Plant", Nuclear Engineering and Design, 59, 1980.

Loo, Y.C., and Santos, A.P., Impact Deflection Analysis of Concrete Beams, ASCE Journal of the Structural Division, November 1986.

Newmark, N.M. and W.J. Hall, "Development of Criteria For Seismic Review of Selected Nuclear Power Plants", NUREG/CR-0098, May, 1978.

NTS, 1987, "Evaluation of Nuclear Power Plant Seismic Margin", NTS Engineering, RPK Structural Mechanics Consulting, Pickard Lowe and Ganick and Woodward Clyde Consultants for EPRI, August.

Nuclear Energy Services, "At-Reactor Storage Expansion Engineering Evaluation", Report prepared for U.S. Department of Energy, Savannah River Operations Office, September 1981.

Park, R. and T. Paulay, Reinforced Concrete Structures, John Wiley and Sons, 1975.

Personal communication between Dr. William Hall and Dr. A. T. Clark discussing the methodology of LLNL analysis of West Valley Facility, Nathan M. Newmark Consulting Engineering Services, 1979.

Personal communication between R. Murray (LLNL) and E. Throm (NRC) regarding the Vermont Yankee Pool Analysis, 1987.

Portland Cement Association, Design of Deep Girders, Concrete Information No. ST 66, 1966.

Prassinos, P.G., M.K. Ravindra, and J.B. Savy, "Recommendations to the Nuclear Regulatory Commission on Trial Guidelines for Seismic Margin Reviews of Nuclear Power Plants", NUREG/CR-4482, March, 1986.

Ravindra, M. K., Sues, R. H., Kennedy, R. P., and Wesley, D. A., "A Program to Determine the Capability of the Millstone Nuclear Power Plant to Withstand Seismic Excitation above the Design SSE", draft report prepared for Northeast Utilities, Berlin, CT, November, 1984.

Ravindra, M.K., et al, "Seismic Margin Review of the Maine Yankee Atomic Power Station - Fragility Analysis", NUREG/CR-4826, Volume 3, March, 1987.

Rawden de Paiva, H.A., and Seiss, C.P., Strength and Behavior of Deep Beams in Shear, ASCE Journal of the Structural Division, October 1965.

R. R. Wylie Computer Aided Fault Tree Analysis, Operation Research Center, University of California, August 1978.

Sailor, V.L., et al, "Severe Accidents in Spent Fuel Pools in Support of Generic Safety Issue 82", NUREG/CR-4982, July, 1987.

Sailor, V.L., K.R. Perkins, H. Connell, and J. Weeks, "Beyond Design-Basis Accidents in Spent Fuel Pools (Generic Issue 82)", Draft Report for Division of Safety Review and Oversight, Office of Nuclear Reactor Regulation, U.S. NRC by Brookhaven National Laboratory, January 1987.

Sliter, G.E., Assessment of Empirical Concrete Impact Formulas, ASCE Journal of the Structural Division, May 1980.

Smith, K.N., and Vantsiotis, A.S., Deep Beam Test Results Compared with Present Building Code Models, ACI Journal, July 1982.

Soler, A.I., and Singh, K.P., "Dynamic Coupling in a Closely Spaced Two-Body System Vibrating in a Liquid Medium: The Case of Fuel Racks",

U.S. Atomic Energy Commission, "Nuclear Reactors and Earthquakes", TID-7024, August, 1963.

USNRC "PRA Procedures Guide", Chapter 11, Seismic Risk Analysis, NUREG/CR-2300, January 1983.

USNRC "Proposed Revision 2 to Regulatory Guide 1.13: Spent Fuel Storage Facility Design Basis", December 1981.

USNRC "Reactor Safety Study, An Assessment of Accident Risk in U.S. Nuclear Power Plants", NUREG/CR-75/014, WASH-1400, October 1975.

USNRC, Safety Evaluation by the Office of Nuclear Reactor Regulation Relating to the Modification of the Spent Fuel Storage Pool, Facility Operating license No. DPR-23, Carolina Power and Light Company, H. B. Robinson Steam Electric Plant Unit 2, Docket No. 50-261, attachments and amendments, 1982.

Vermont Yankee Nuclear Power Corporation, "Vermont Yankee Spent Fuel Storage Rack Replacement Report", April, 1986.

Vermont Yankee Nuclear Power Station, "Final Safety Analysis Report (FSAR), Section 4.8 - Residual Heat Removal System, Section 8. - Station Electrical Power Systems, Section 9.2 - Liquid Radwaste System, Section 10. - Station Auxiliary Systems, Section 10.5 - Fuel Pool Cooling and Demineralizer System, Section 10.7 - RHR Service Water System, Section 10.9 - Reactor Building Closed Cooling Water System, Section 10.13 - Station Makeup Water System, Section 10.14 - Station Instrument and Service Air System.

Vermont Yankee Nuclear Power Station, Licensed Operator Training Program, Instructors Guide/Student Handout, "Cond/Demin Water Transfer System", Lot-05-108, Rev. 0, October 1985.

Vermont Yankee Nuclear Power Station, Licensed Operator Training Program, Instructors Guide/Student Handout, "Fuel Pool Cooling and Cleanup System", Lot-05-407, Rev. 0, October 1985.

Vermont Yankee Nuclear Power Station, Licensed Operator Training Program, Instructors Guide/Student Handout, "Reactor Building Closed Cooling Water System (RBCCW)", Lot-05-304, Rev. 0, September 1985.

Vermont Yankee Nuclear Power Station, Licensed Operator Training Program, Instructors Guide/Student Handout, "Residual Heat Removal System", Lot-03-306, Rev. 0, December 1985.

Vermont Yankee Nuclear Power Station, Licensed Operator Training Program, Instructors Guide/Student Handout, "480 VAC Electrical Distribution System".

Vermont Yankee Nuclear Power Station, Operation Procedure - ON3147, Loss of RBCCW, November 4, 1985.

Vermont Yankee Nuclear Power Station, Operation Procedure - ON3157, Loss of Fuel Pool Level, August 1, 1986.

Vermont Yankee Nuclear Power Station, Operation Procedure - R.P. 2184, Fuel Pool Cooling System, Rev. 12, August 1, 1986.

Vermont Yankee Nuclear Power Station, Operation Procedure - R.P. 2185, Condensate/Demineralized Water Transfer System, Rev. 11, March 6, 1987.

Winter, G., and Nilson, A., Design of Concrete Structures, McGraw-Hill, 9th Edition, 1979.

Appendix A

Vermont Yankee Nuclear Power Station
Spent Fuel Pool

Thermal Analysis

Mass of water in fuel pool

Fuel pool volume

26'0" x 40'0" x 39'3/4"

FSAR Sec. pg. 10.3–3 10.3.4

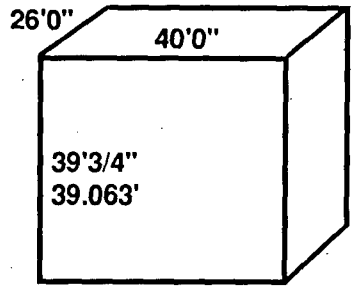

$$26' \times 40' \times 39.063' = 40625\ ft^3 \cdot \frac{1\ gal}{0.13368\ ft^3}$$

$$= 303{,}897.4\ gal$$

From FSAR pg 10.5–7, Table 10.5–1

Vol = 41,600 ft^3

Use 40625 ft^3

Specific volume of water @ 1 atm pressure, T = 150°F (Tech Spec limit) from Keenan, Keyes, Hill & Moore Steam Tables

T = 150°F	T = 212°F
$\upsilon_f = 0.016343\ \frac{ft^3}{lbm}$	$\upsilon_f = 0.016716\ \frac{ft^3}{lbm}$
$\upsilon_g = 96.99\ \frac{ft^3}{lbm}$	$\upsilon_g = 26.80\ \frac{ft^3}{lbm}$

$$m = \frac{V}{\upsilon_f} = \frac{40625\ ft^3}{0.016343\ \frac{ft^3}{lbm}} = 2{,}485{,}774\ lbm$$

Time required to heat fuel pool water to boiling temperature

Failure state 1

$Q = 6.54 \times 10^6 \frac{Btu}{hr}$ heat input from FSAR, pg 10.5–8, Table 10.5.2

Energy increase = heat input – heat loss

Energy increase = $\frac{(m\ Cp\ \Delta T)}{t}$

m = mass of fuel pool water, lbm

Cp = specific heat of water

$\cong 1.0 \frac{Btu}{lbm\ °F}$

ΔT = temperature rise

= (212°F – 150°F) = 62°F

t = time for temperature rise

Heat loss = heat conduction through walls and floor of fuel pool + heat convection from fuel pool water surface

Assume = 0 $= \dot{m}\ h\ \Delta T_{air}$

$\frac{(m\ Cp\ \Delta T)}{t} = \dot{Q} - \dot{m}\ h\ \Delta T_{air}$, for 1st cut calculation assume heat convective loss = 0

$$t = \frac{m\ Cp\ \Delta T}{\dot{Q}} = \frac{2{,}485{,}774\ lbm \left(\frac{1\ Btu}{lbm\ °F}\right) 62°F}{6.54 \times 10^6 \frac{Btu}{hr}}$$

$$= 23.57\ hrs$$

Rate of water elevation drop due to boil-off of fuel pool

Failure state 1

$\dot{Q} = \dot{m}\, h_{fg}$ where $\dot{m}$ = water mass loss rate

h_{fg} = heat of vaporization

$= 970.3 \frac{Btu}{lbm}$, water, T = 212°F, P = 1 atm, from Keenan, Keyes, Hill and Moore Steam Tables

$$\dot{m} = \frac{\dot{Q}}{h_{fg}}$$

$$= \frac{6.56 \times 10^6 \frac{Btu}{hr}}{970.3 \frac{Btu}{lbm}} = 6760.8 \frac{lbm}{hr}$$

$$\dot{V} = \dot{m}\, \upsilon_g = 6760.8 \frac{lbm}{hr}\ 0.016716 \frac{ft^3}{lbm}$$

$$= 113 \frac{ft^3}{hr}$$

From Keenan, Keyes, Hill and Moore Steam Tables

$\upsilon_g = 0.016716 \frac{ft^3}{lbm}$, T = 212°F

$$\dot{H} = \frac{\dot{V}}{A} = 113 \frac{ft^3}{hr}\ (26.40)\ ft^2$$

$$= 0.109 \frac{ft}{hr}$$

$$= 1.3 \frac{in.}{hr}$$

Time required to heat fuel pool to boiling temperature

Failure state 2

$\dot{Q} = 15.56 \times 10^6 \frac{Btu}{hr}$ heat input from FSAR, pg 10.5-9, Table 10.5.3

$$t = \frac{m\ Cp\ \Delta T}{\dot{Q}} = \frac{2{,}485{,}774\ lbm \left(\frac{1\ Btu}{lbm\ °F}\right) 62°F}{15.56 \times 10^6 \frac{Btu}{hr}}$$

$$= 9.91\ hrs$$

Rate of water elevation drop due to boil-off of fuel pool

Failure state 2

$$\dot{Q} = \dot{m}\, h_{fg}$$

$$\dot{m} = \frac{\dot{Q}}{h_{fg}} = \frac{15.56 \times 10^6 \ \frac{Btu}{hr}}{970.3 \ \frac{Btu}{lbm}} = 16036.3 \ \frac{lbm}{hr}$$

$$\dot{V} = \dot{m}\, \upsilon_g = 16036.3 \ \frac{lbm}{hr} \ 0.016716 \ \frac{ft^3}{lbm}$$

$$= 268.1 \ \frac{ft^3}{hr}$$

$$\dot{H} = \frac{\dot{V}}{A} = 268.1 \ \frac{ft^3}{hr} \ \frac{1}{(26 \times 40)\ ft^2}$$

$$= 0.258 \ \frac{ft}{hr}$$

$$= 3.09 \ \frac{in.}{hr}$$

Appendix B

Vermont Yankee Nuclear Power Station
Spent Fuel Pool

Fault Trees

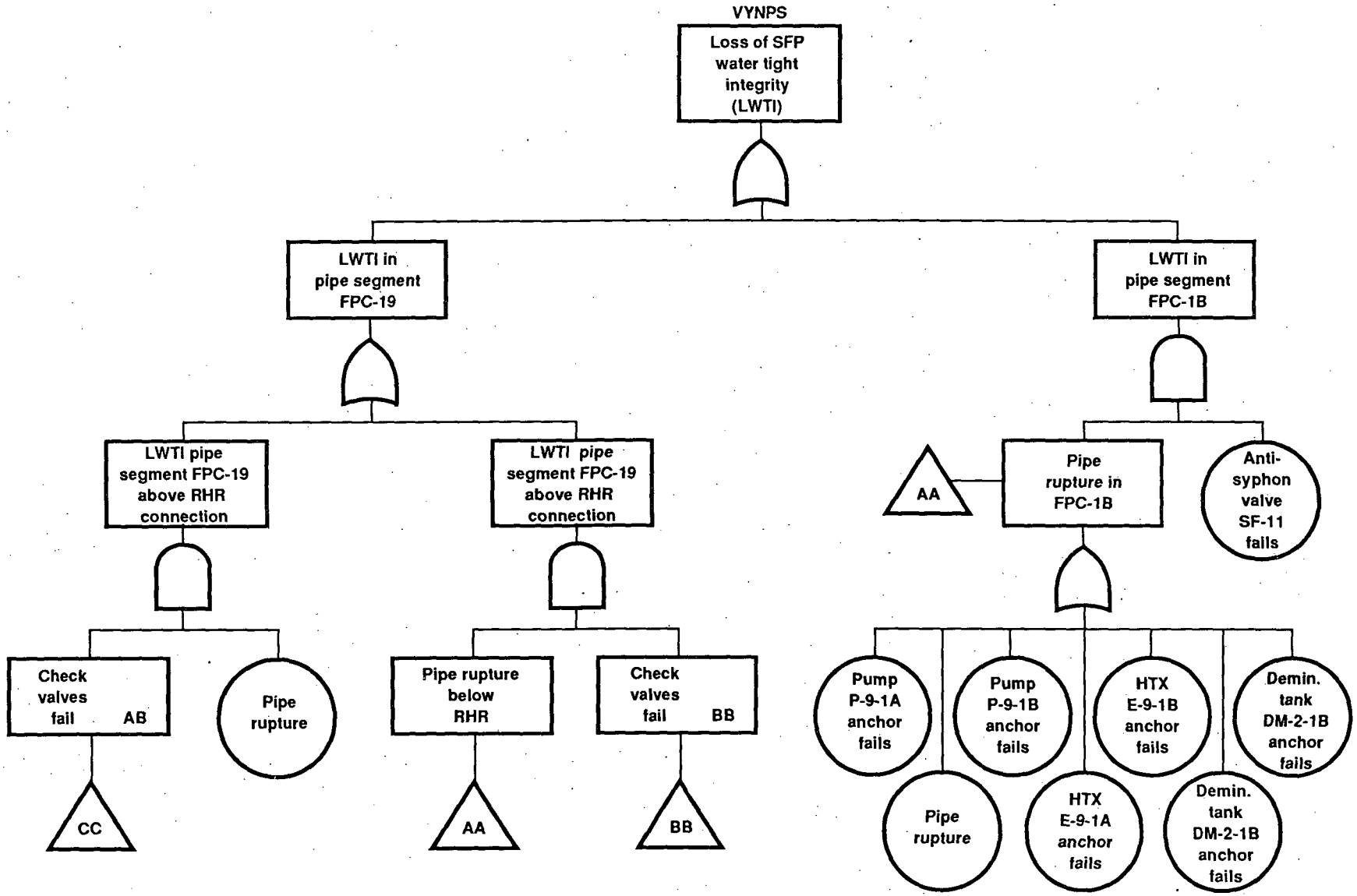
VYNPS
Loss of SFP water tight integrity (LWTI)
LWTI in pipe segment FPC-19
LWTI in pipe segment FPC-1B
LWTI pipe segment FPC-19 above RHR connection
LWTI pipe segment FPC-19 above RHR connection
AA
Pipe rupture in FPC-1B
Anti-syphon valve SF-11 fails
Check valves fail AB
Pipe rupture
Pipe rupture below RHR
Check valves fail BB
Pump P-9-1A anchor fails
Pump P-9-1B anchor fails
HTX E-9-1B anchor fails
Demin. tank DM-2-1B anchor fails
CC
AA
BB
Pipe rupture
HTX E-9-1A anchor fails
Demin. tank DM-2-1B anchor fails

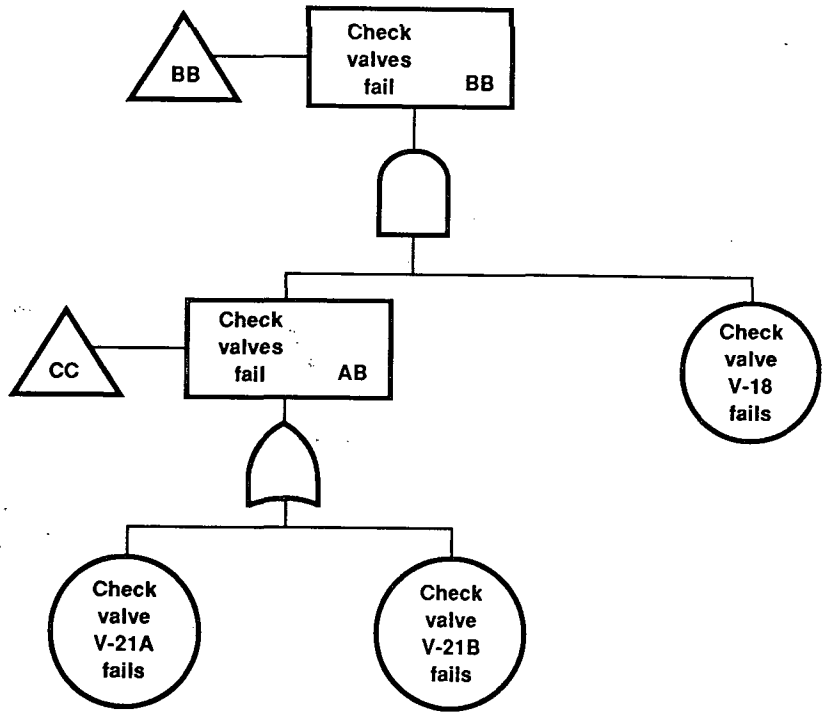
BB
Check valves fail BB
CC
Check valves fail AB
Check valve V-18 fails
Check valve V-21A fails
Check valve V-21B fails

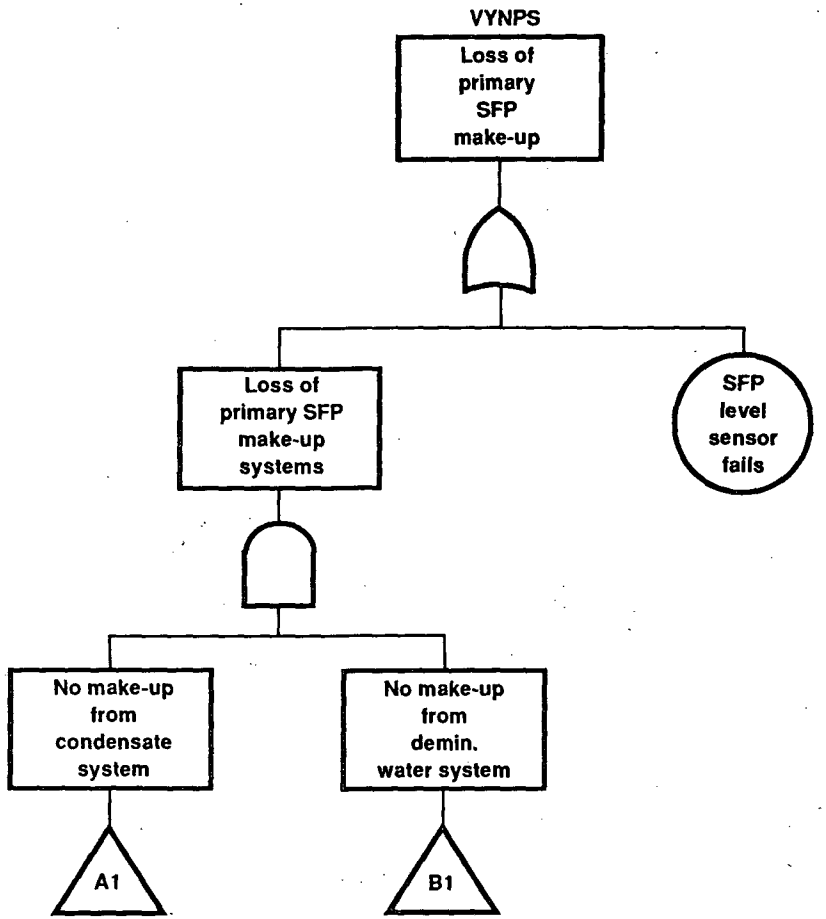
VYNPS
Loss of primary SFP make-up
Loss of primary SFP make-up systems
SFP level sensor fails
No make-up from condensate system
No make-up from demin. water system
A1
B1

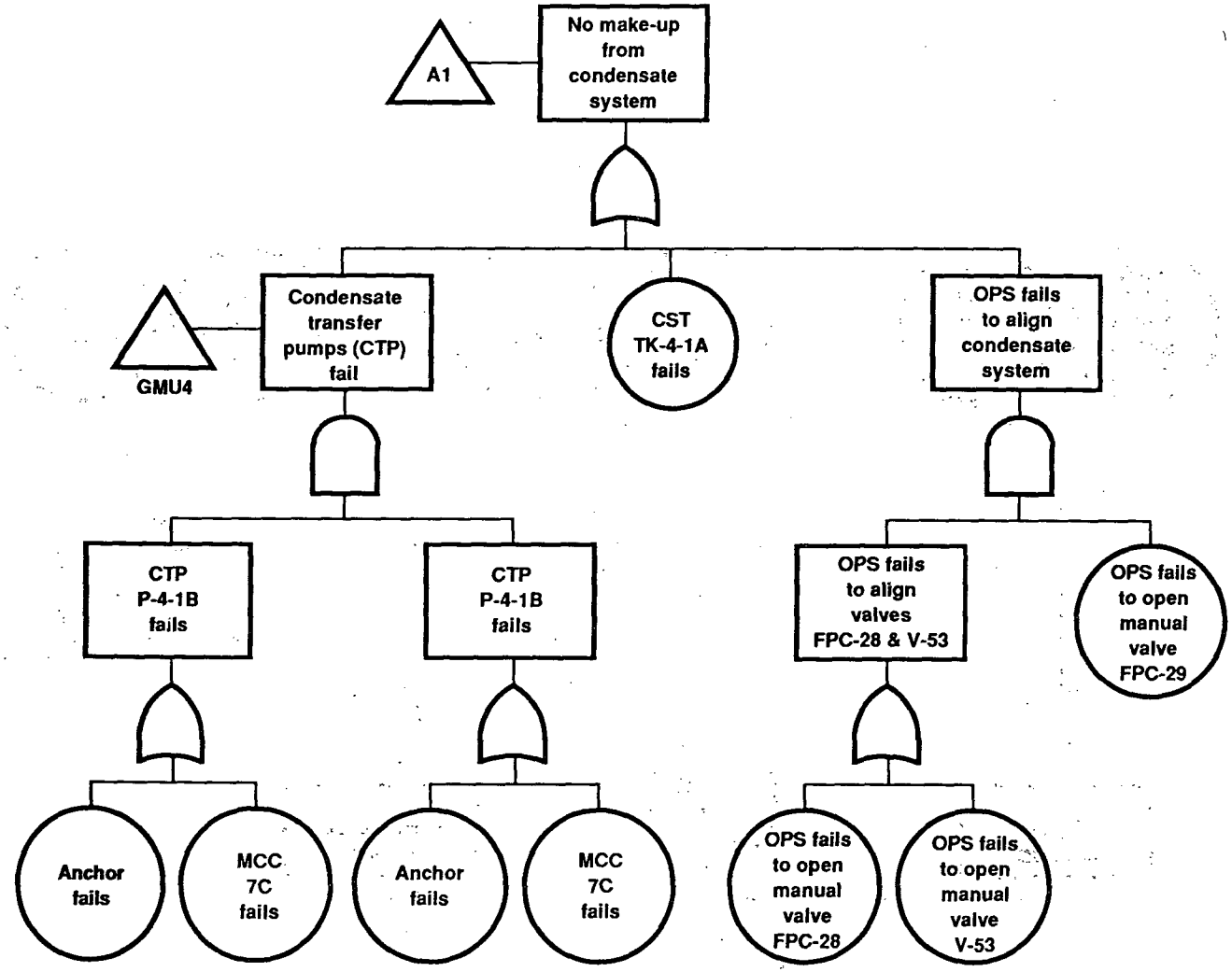
A1
No make-up from condensate system
GMU4
Condensate transfer pumps (CTP) fail
CST TK-4-1A fails
OPS fails to align condensate system
CTP P-4-1B fails
CTP P-4-1B fails
OPS fails to align valves FPC-28 & V-53
OPS fails to open manual valve FPC-29
Anchor fails
MCC 7C fails
Anchor fails
MCC 7C fails
OPS fails to open manual valve FPC-28
OPS fails to open manual valve V-53

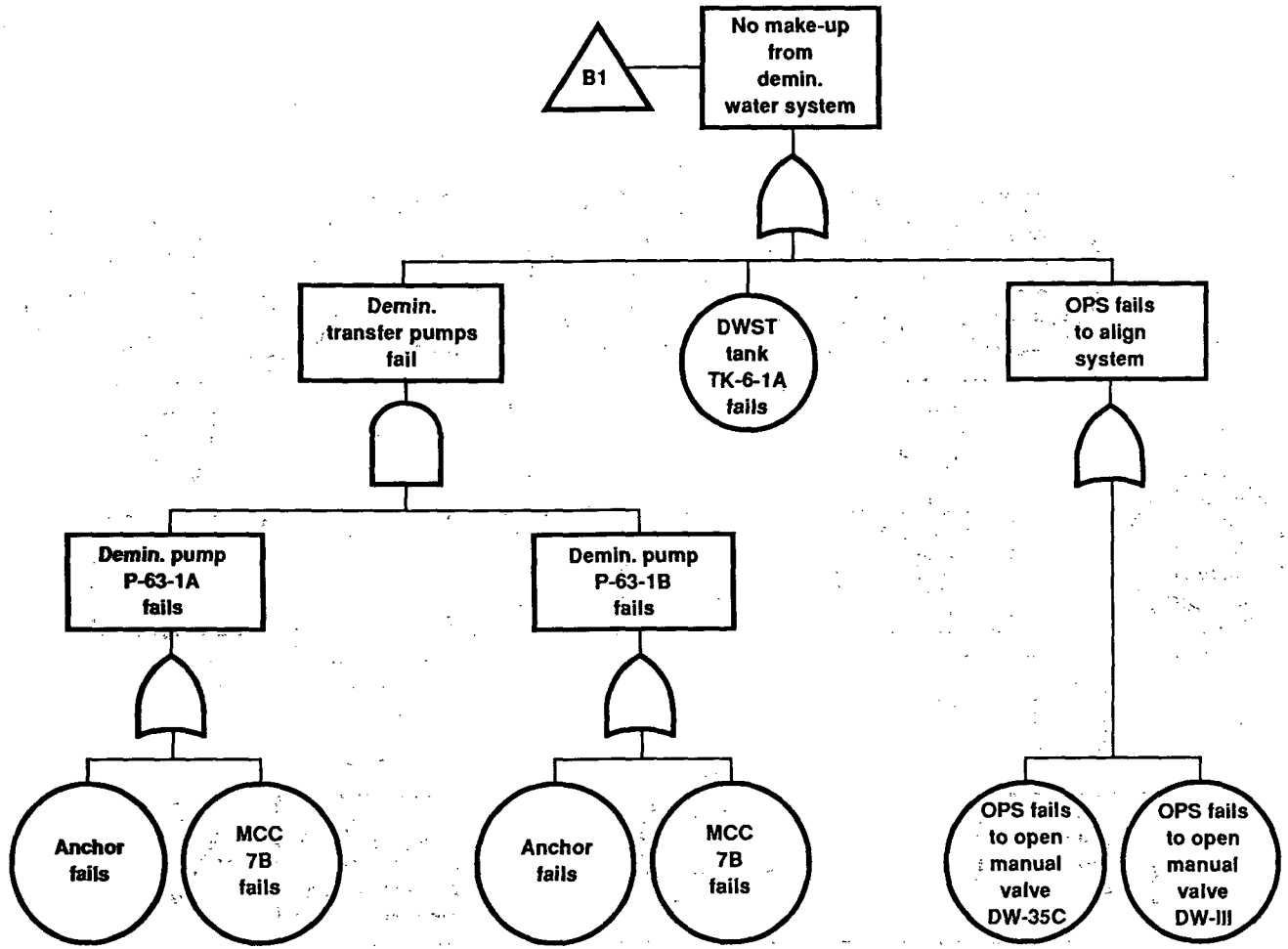
B1
No make-up from demin. water system
Demin. transfer pumps fail
DWST tank TK-6-1A fails
OPS fails to align system
Demin. pump P-63-1A fails
Demin. pump P-63-1B fails
Anchor fails
MCC 7B fails
Anchor fails
MCC 7B fails
OPS fails to open manual valve DW-35C
OPS fails to open manual valve DW-III

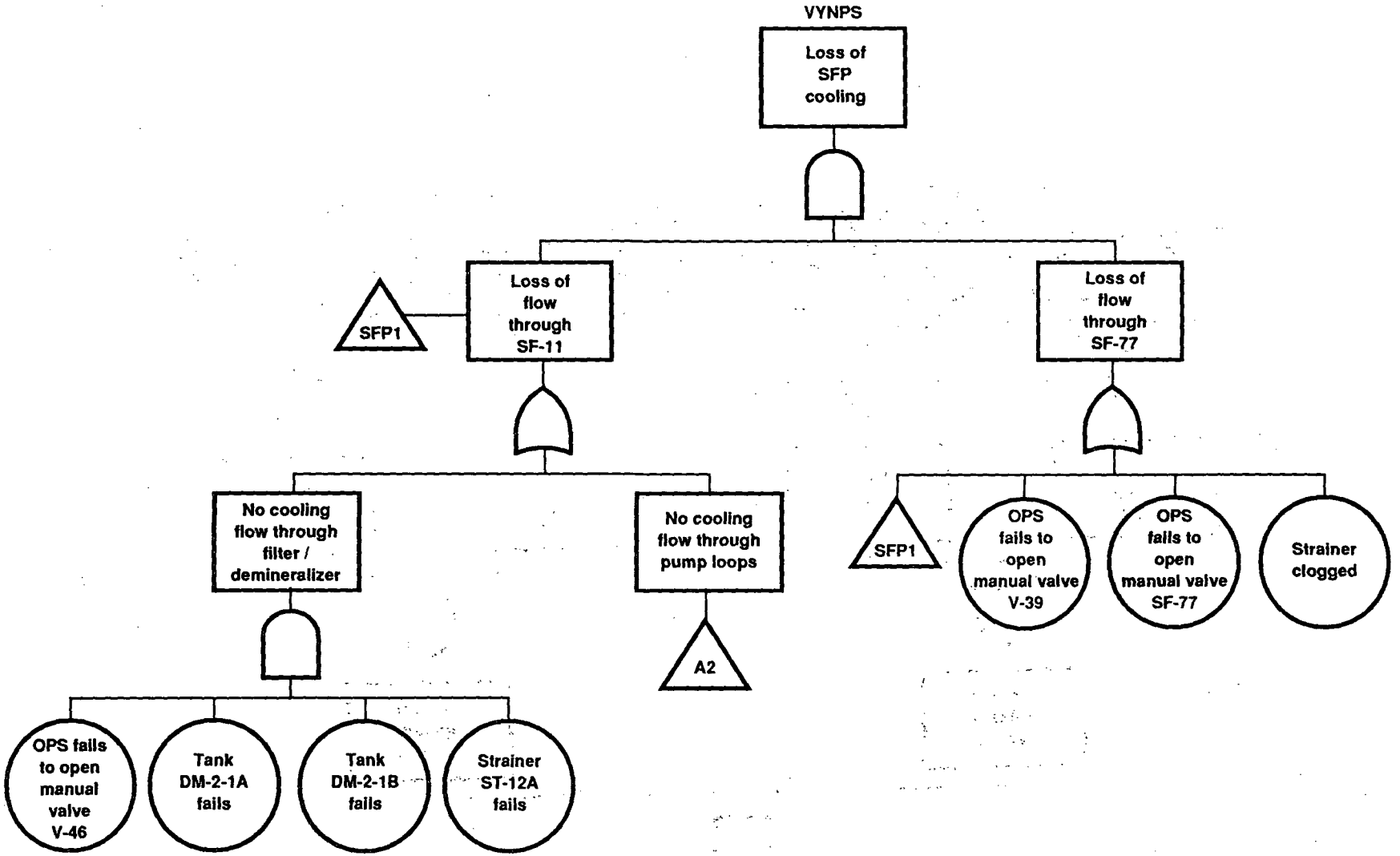
VYNPS
Loss of SFP cooling
Loss of flow through SF-11
SFP1
Loss of flow through SF-77
No cooling flow through filter / demineralizer
No cooling flow through pump loops
SFP1
OPS fails to open manual valve V-39
OPS fails to open manual valve SF-77
Strainer clogged
A2
OPS fails to open manual valve V-46
Tank DM-2-1A fails
Tank DM-2-1B fails
Strainer ST-12A fails

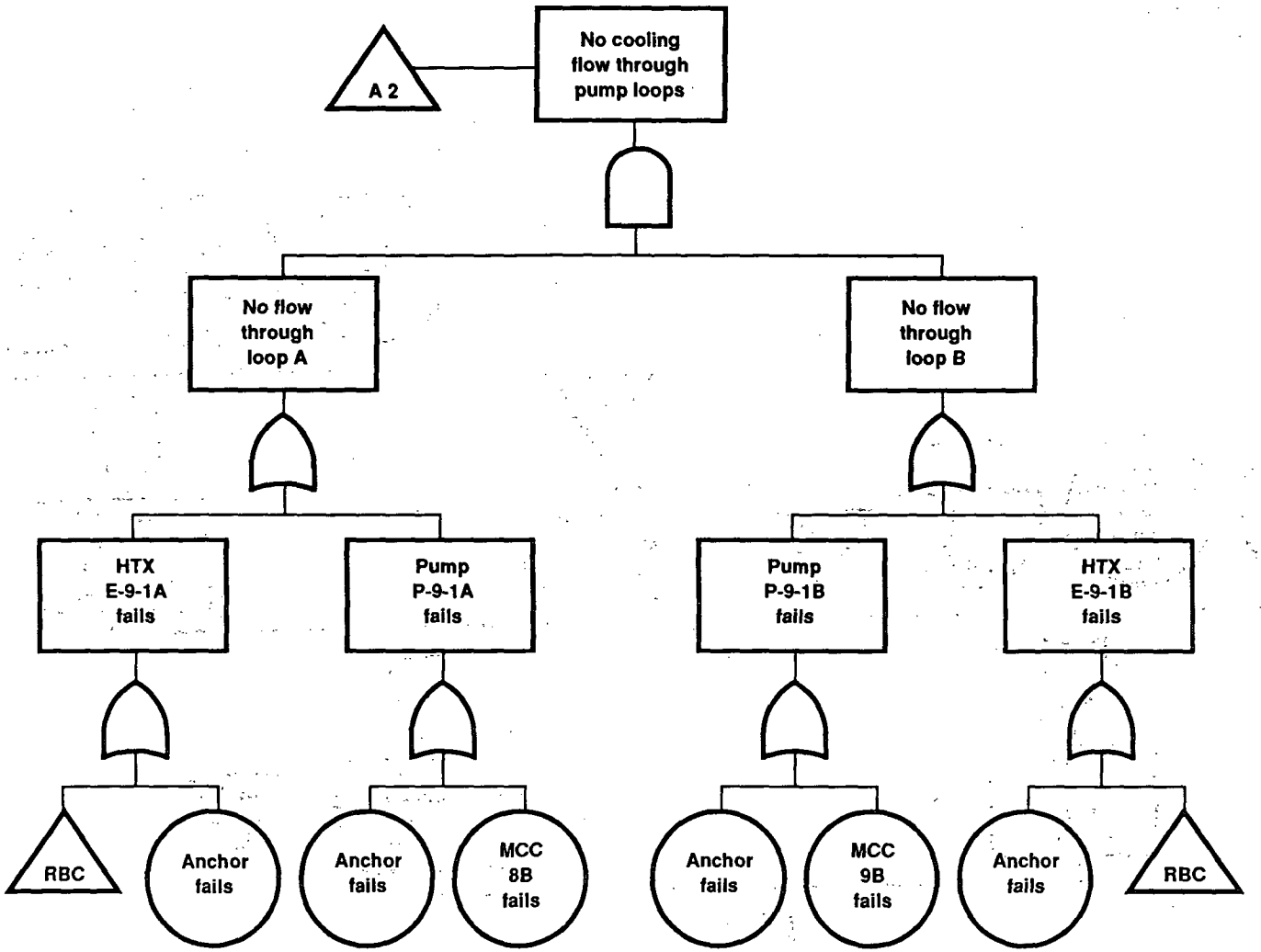
A 2
No cooling flow through pump loops
No flow through loop A
No flow through loop B
HTX E-9-1A fails
Pump P-9-1A fails
Pump P-9-1B fails
HTX E-9-1B fails
RBC
Anchor fails
Anchor fails
MCC 8B fails
Anchor fails
MCC 9B fails
Anchor fails
RBC

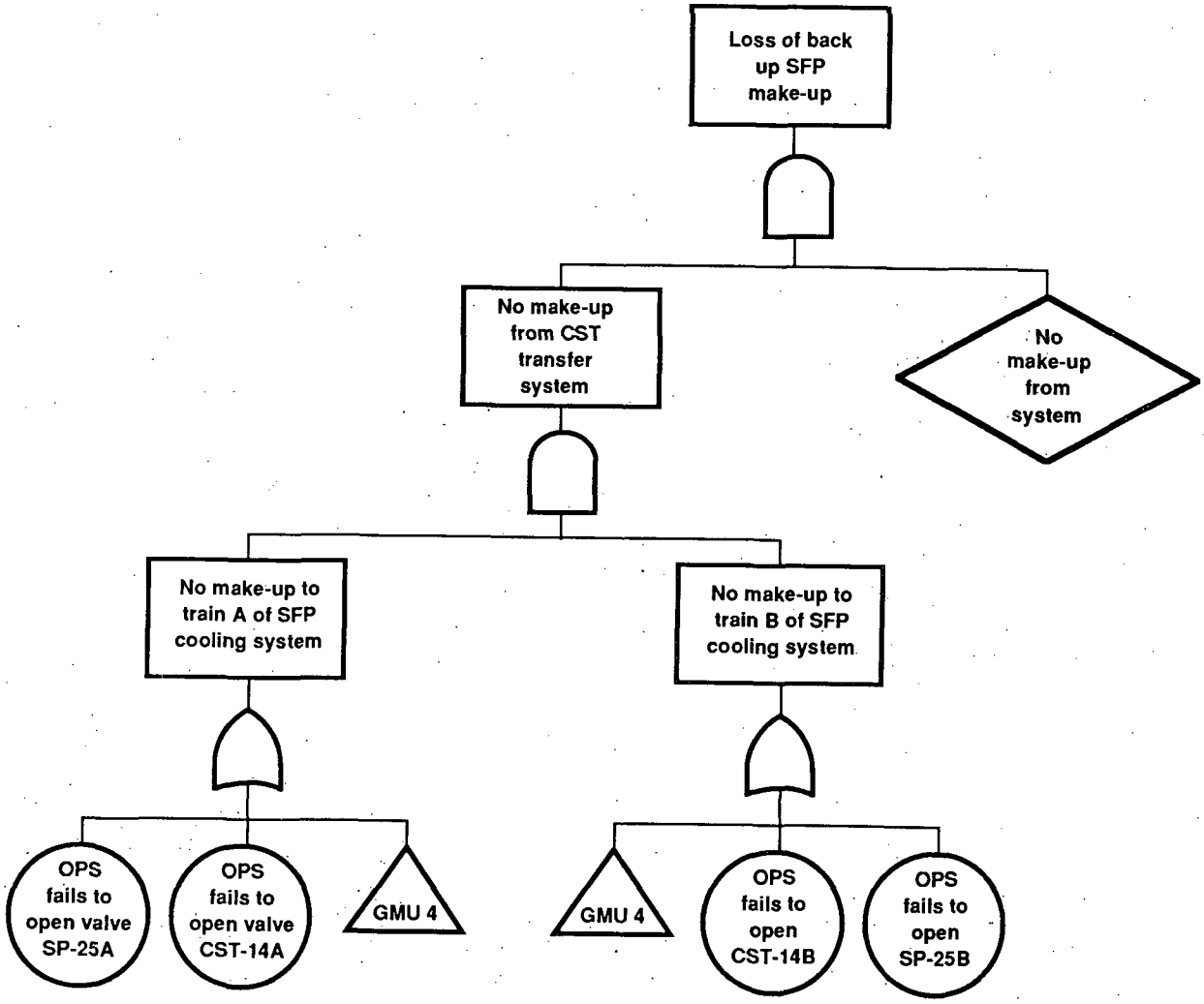
Loss of back up SFP make-up
No make-up from CST transfer system
No make-up from system
No make-up to train A of SFP cooling system
No make-up to train B of SFP cooling system
OPS fails to open valve SP-25A
OPS fails to open valve CST-14A
GMU 4
GMU 4
OPS fails to open CST-14B
OPS fails to open SP-25B

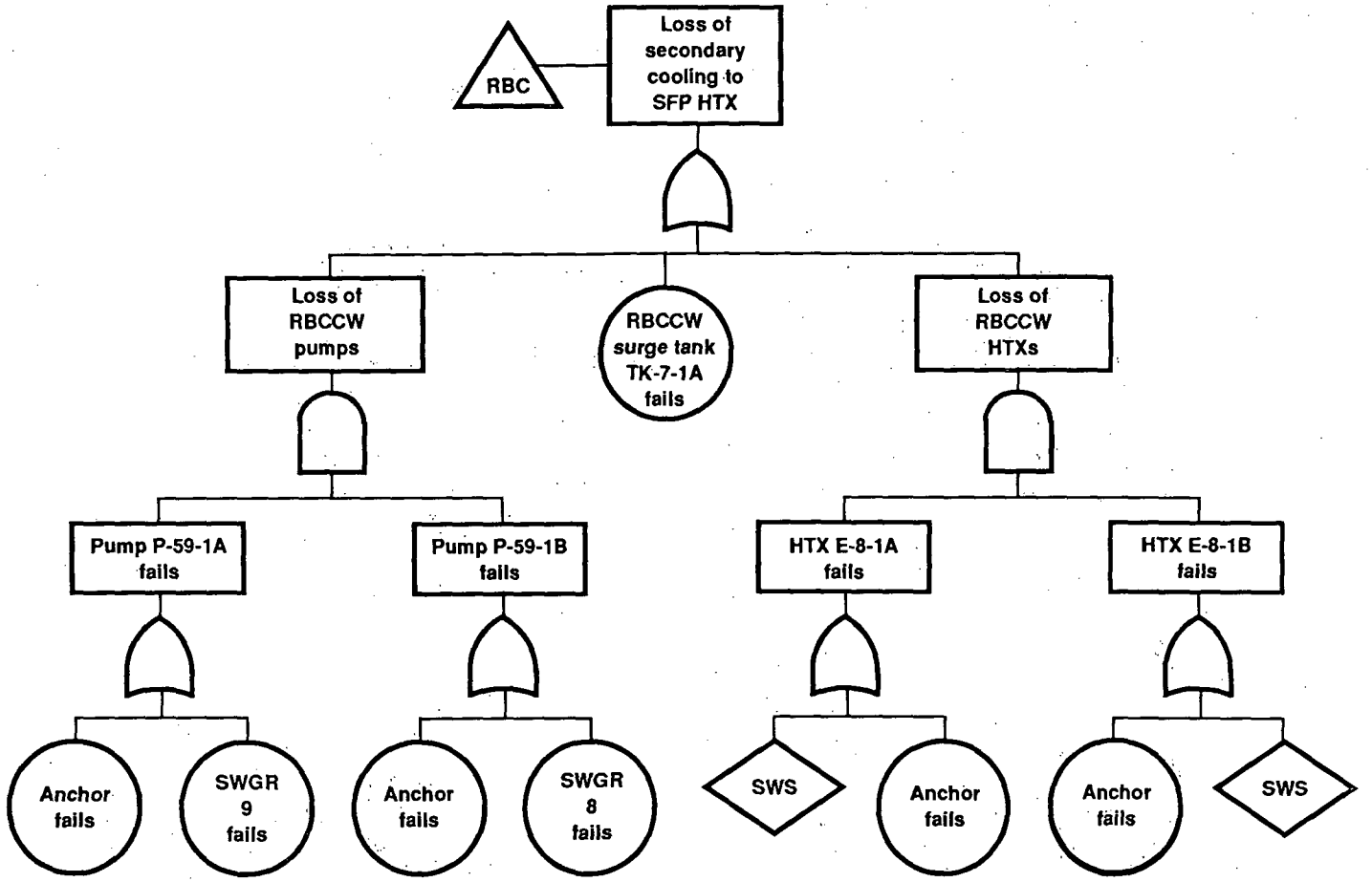
RBC
Loss of secondary cooling to SFP HTX
Loss of RBCCW pumps
RBCCW surge tank TK-7-1A fails
Loss of RBCCW HTXs
Pump P-59-1A fails
Pump P-59-1B fails
HTX E-8-1A fails
HTX E-8-1B fails
Anchor fails
SWGR 9 fails
Anchor fails
SWGR 8 fails
SWS
Anchor fails
Anchor fails
SWS

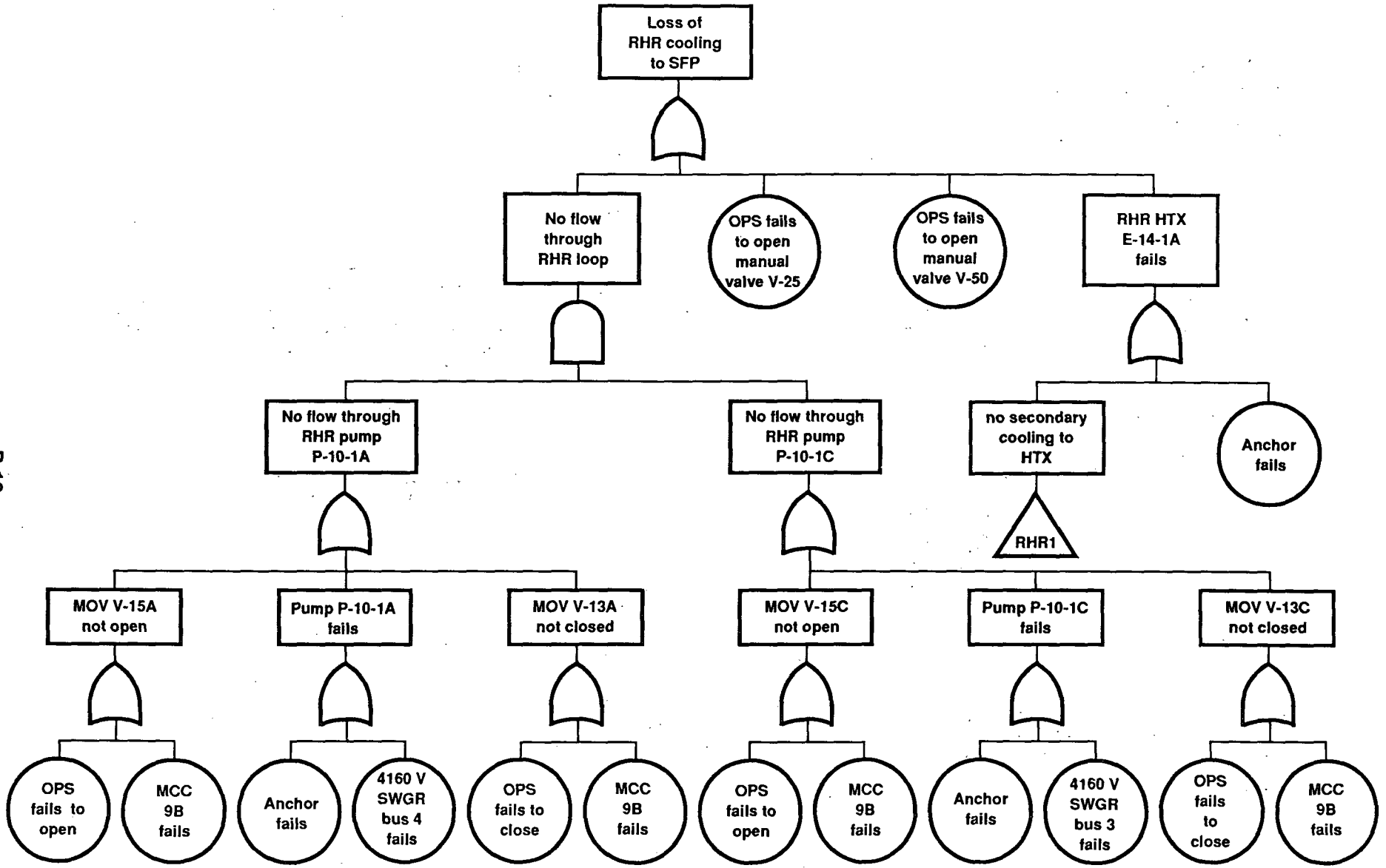
Loss of RHR cooling to SFP
No flow through RHR loop
OPS fails to open manual valve V-25
OPS fails to open manual valve V-50
RHR HTX E-14-1A fails
No flow through RHR pump P-10-1A
No flow through RHR pump P-10-1C
no secondary cooling to HTX
Anchor fails
RHR1
MOV V-15A not open
Pump P-10-1A fails
MOV V-13A not closed
MOV V-15C not open
Pump P-10-1C fails
MOV V-13C not closed
OPS fails to open
MCC 9B fails
Anchor fails
4160 V SWGR bus 4 fails
OPS fails to close
MCC 9B fails
OPS fails to open
MCC 9B fails
Anchor fails
4160 V SWGR bus 3 fails
OPS fails to close
MCC 9B fails

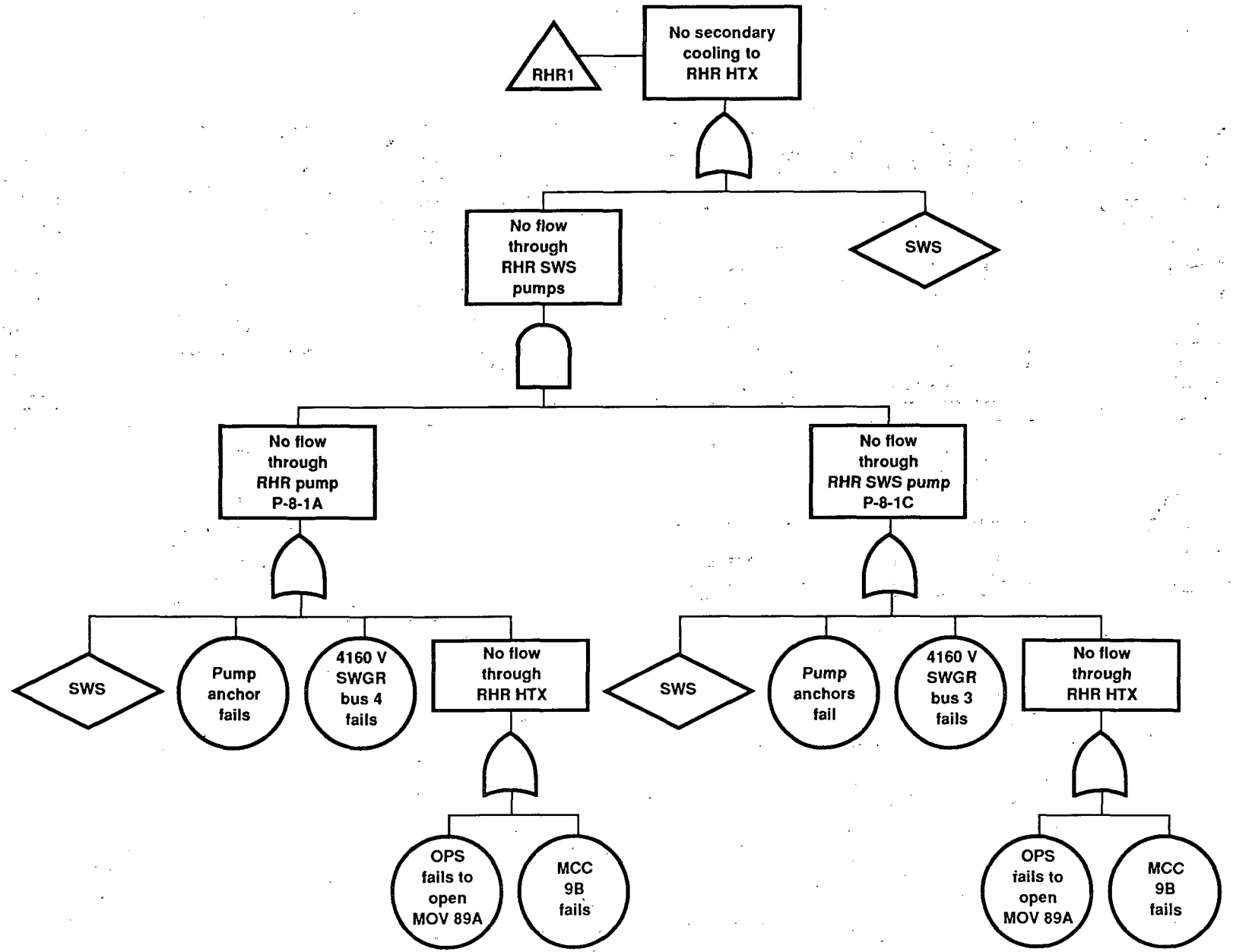
RHR1
No secondary cooling to RHR HTX
No flow through RHR SWS pumps
SWS
No flow through RHR pump P-8-1A
No flow through RHR SWS pump P-8-1C
SWS
Pump anchor fails
4160 V SWGR bus 4 fails
No flow through RHR HTX
SWS
Pump anchors fail
4160 V SWGR bus 3 fails
No flow through RHR HTX
OPS fails to open MOV 89A
MCC 9B fails
OPS fails to open MOV 89A
MCC 9B fails

Appendix C

H.B. Robinson Unit 2
Spent Fuel Pool

Fault Trees

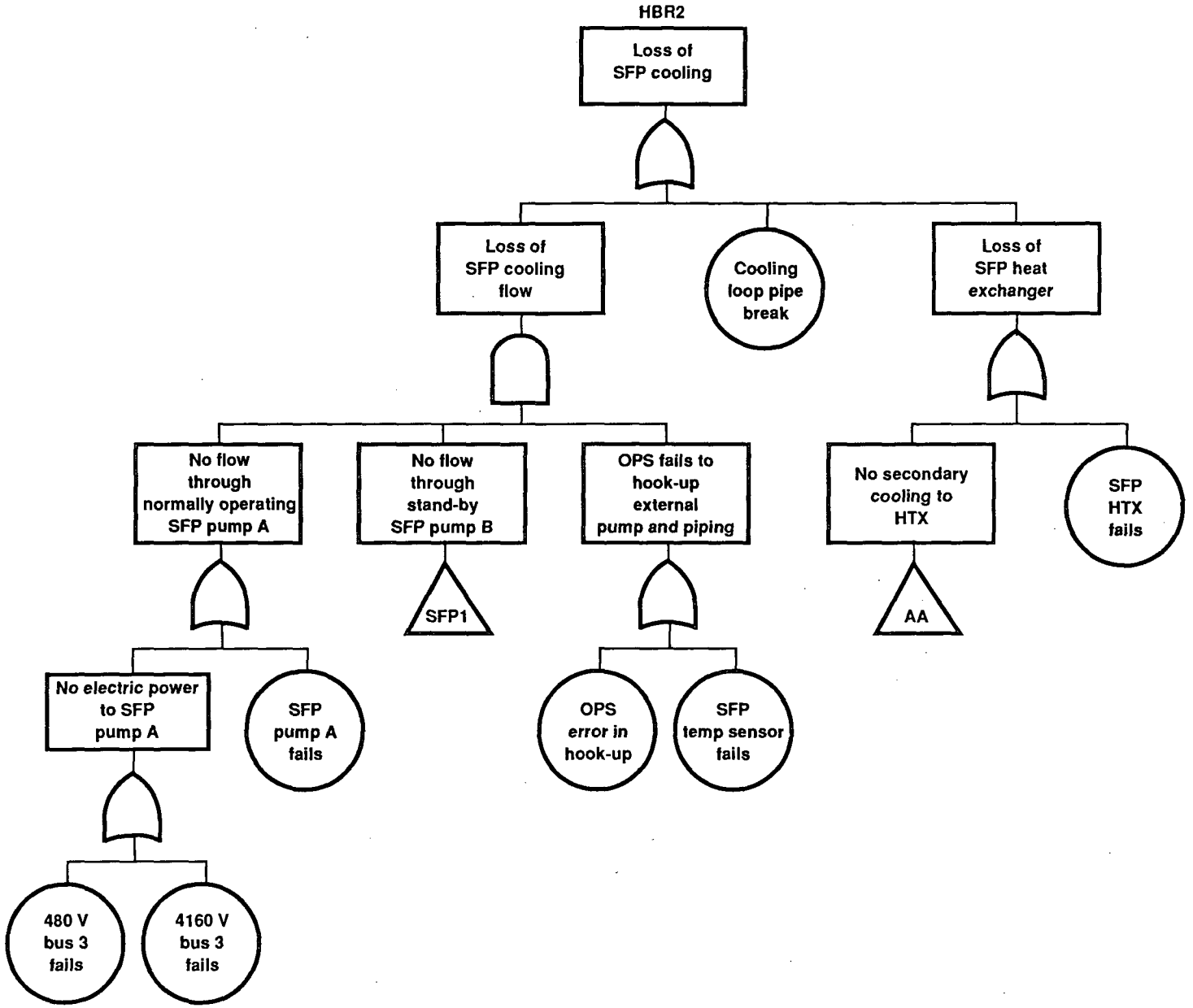
HBR2
Loss of SFP cooling
Loss of SFP cooling flow
Cooling loop pipe break
Loss of SFP heat exchanger
No flow through normally operating SFP pump A
No flow through stand-by SFP pump B
OPS fails to hook-up external pump and piping
No secondary cooling to HTX
SFP HTX fails
SFP1
AA
No electric power to SFP pump A
SFP pump A fails
OPS error in hook-up
SFP temp sensor fails
480 V bus 3 fails
4160 V bus 3 fails

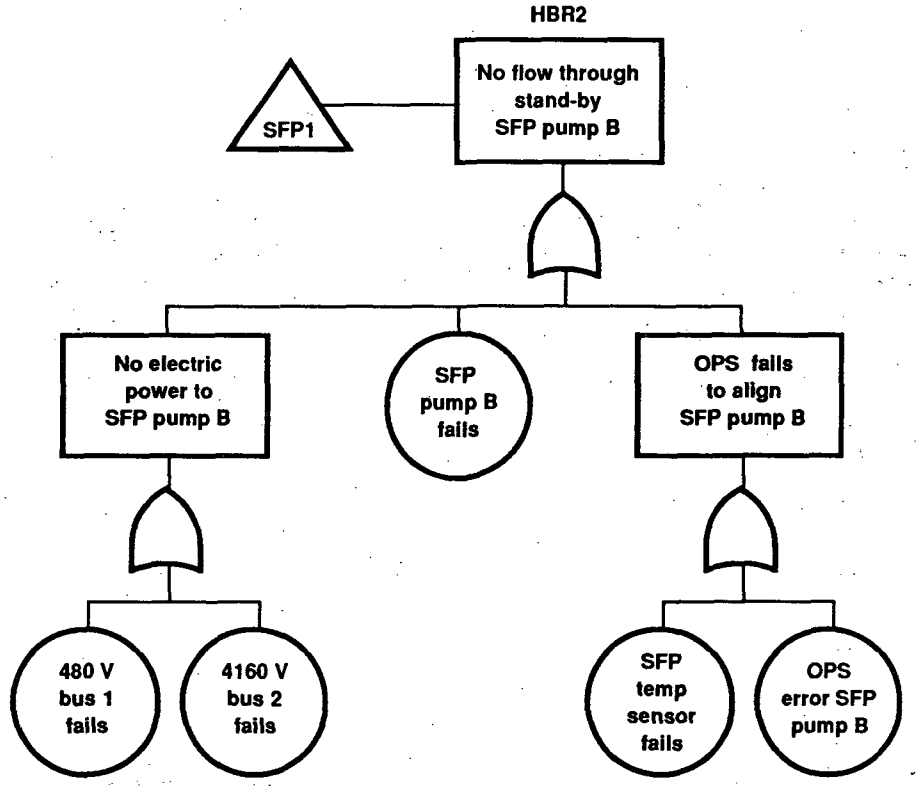
HBR2
No flow through stand-by SFP pump B
SFP1
No electric power to SFP pump B
SFP pump B fails
OPS fails to align SFP pump B
480 V bus 1 fails
4160 V bus 2 fails
SFP temp sensor fails
OPS error SFP pump B

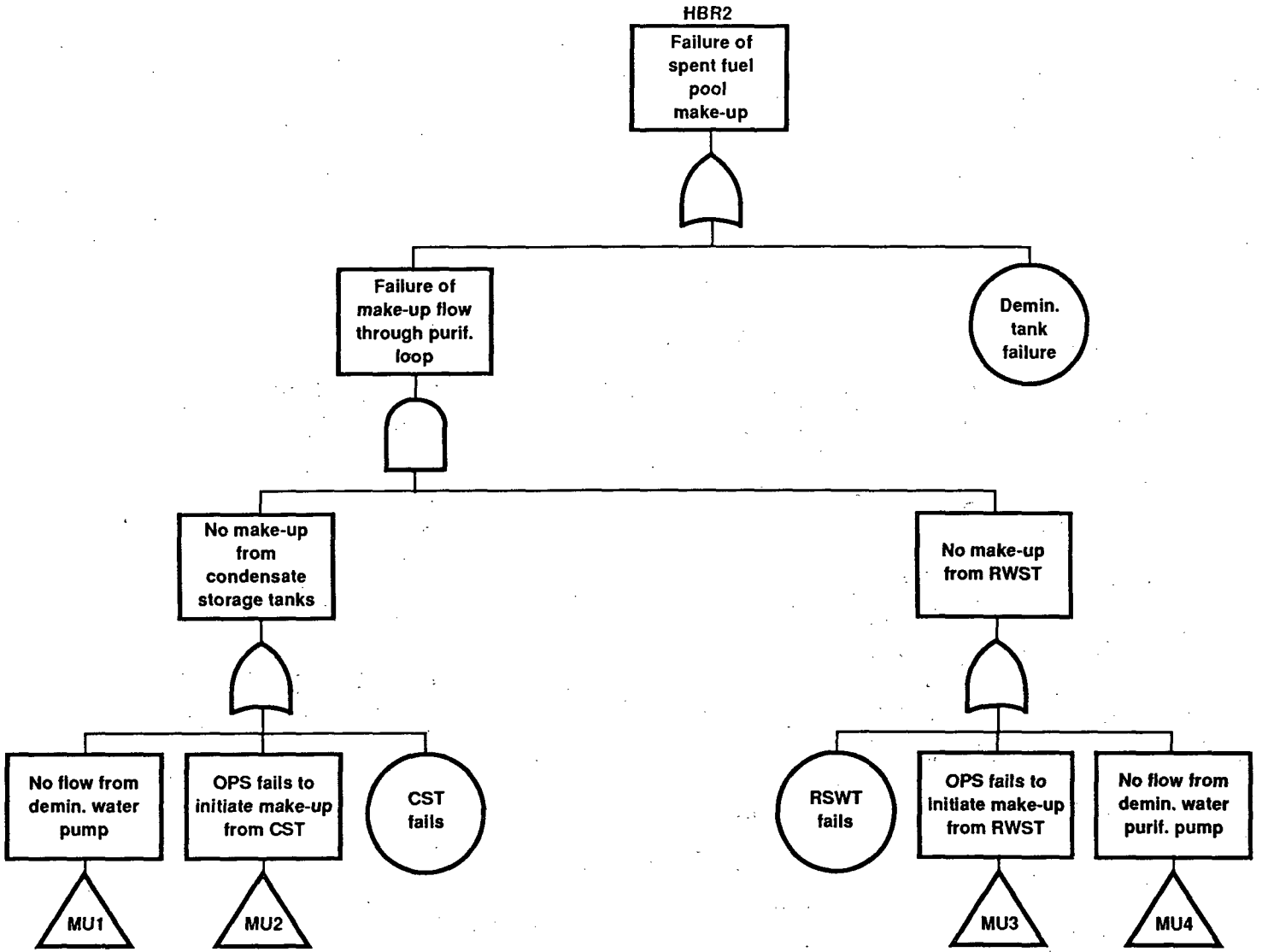
HBR2
Failure of spent fuel pool make-up
Failure of make-up flow through purif. loop
Demin. tank failure
No make-up from condensate storage tanks
No make-up from RWST
No flow from demin. water pump
OPS fails to initiate make-up from CST
CST fails
RSWT fails
OPS fails to initiate make-up from RWST
No flow from demin. water purif. pump
MU1
MU2
MU3
MU4

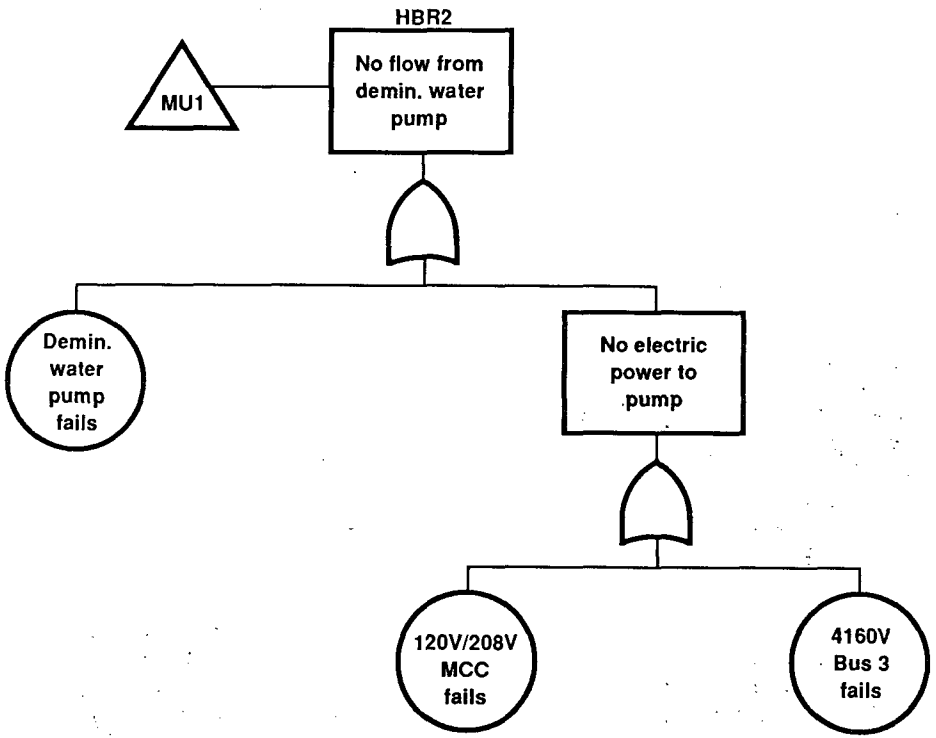
HBR2
No flow from demin. water pump
MU1
Demin. water pump fails
No electric power to pump
120V/208V MCC fails
4160V Bus 3 fails

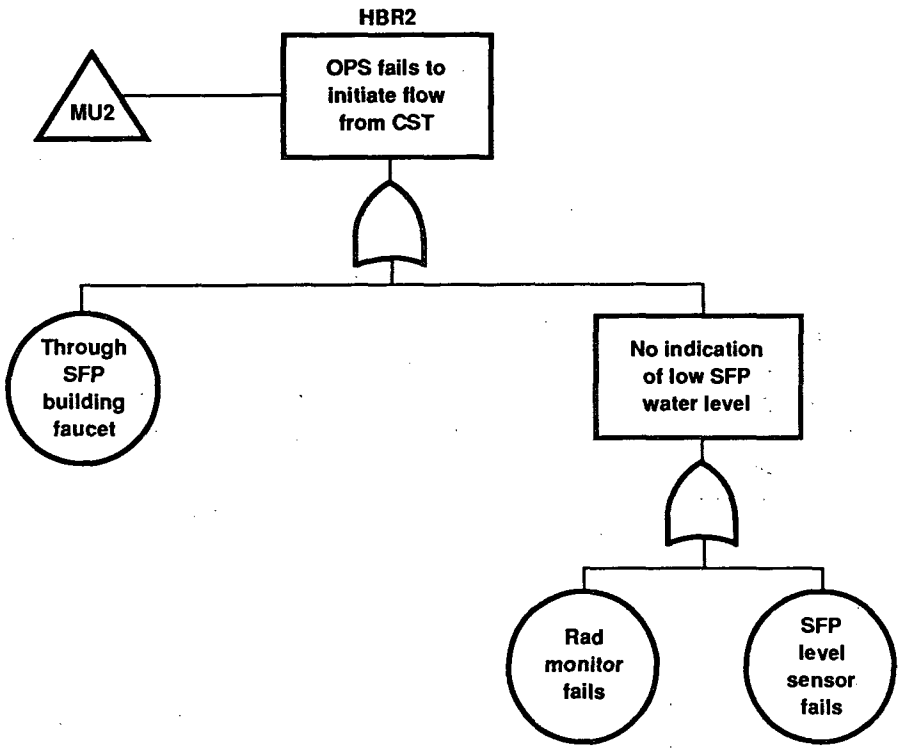
HBR2
MU2
OPS fails to initiate flow from CST
Through SFP building faucet
No indication of low SFP water level
Rad monitor fails
SFP level sensor fails

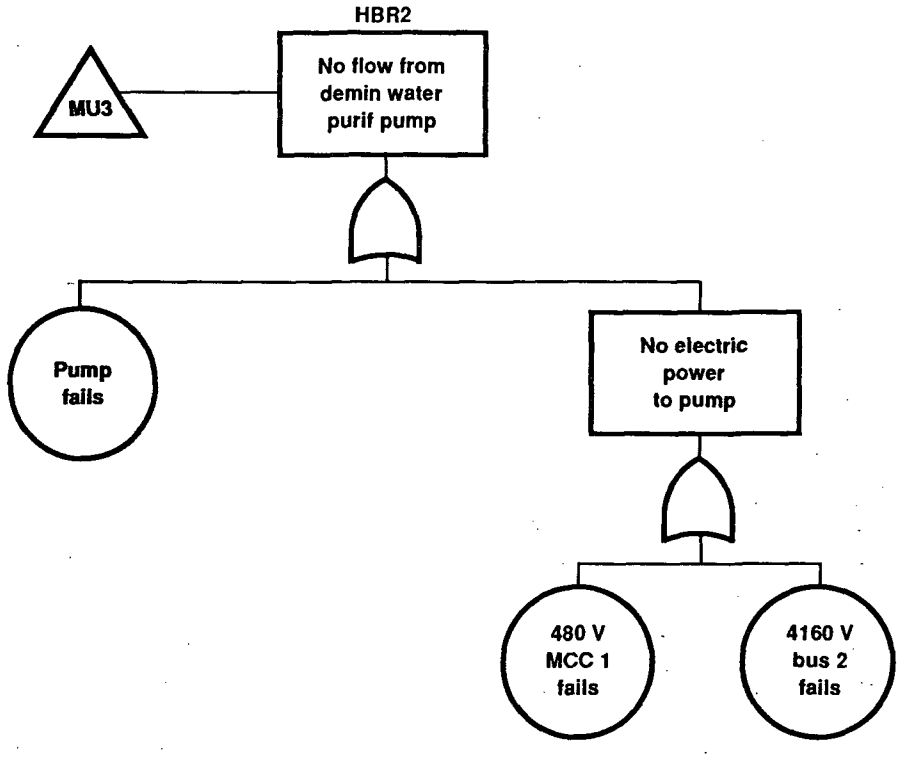
HBR2
No flow from demin water purif pump
MU3
Pump fails
No electric power to pump
480 V MCC 1 fails
4160 V bus 2 fails

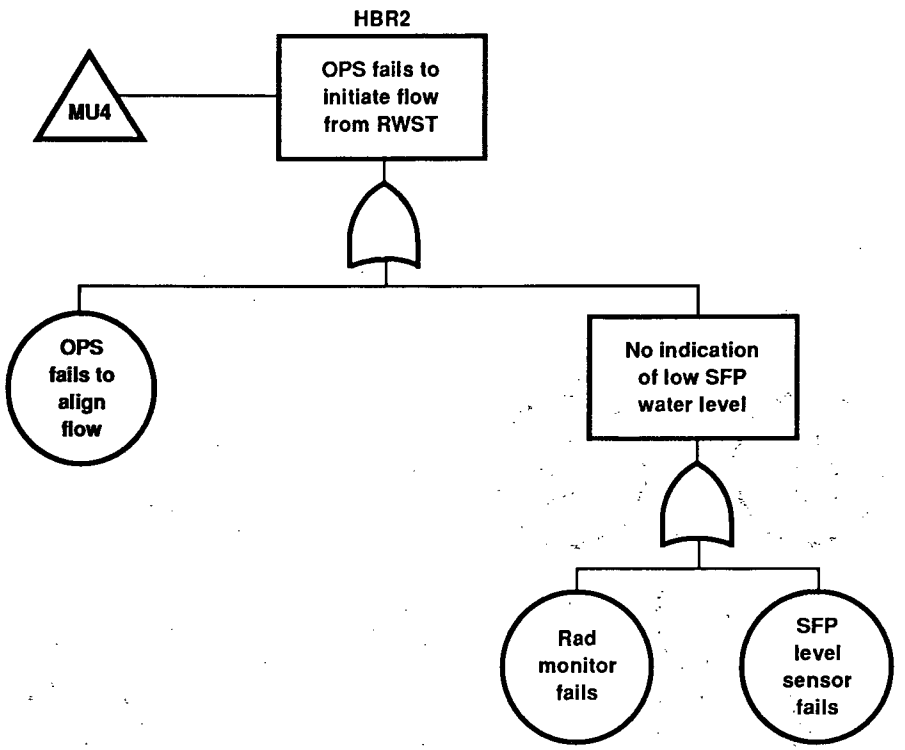
HBR2
MU4
OPS fails to initiate flow from RWST
OPS fails to align flow
No indication of low SFP water level
Rad monitor fails
SFP level sensor fails

NRC FORM 335 (8-87) NRCM 1102, 3201, 3202

U.S. NUCLEAR REGULATORY COMMISSION

BIBLIOGRAPHIC DATA SHEET

SEE INSTRUCTIONS ON THE REVERSE

1. REPORT NUMBER (Assigned by PPMB: DPS, add Vol. No., if any)
NUREG/CR-5176
UCID-21425

2. TITLE AND SUBTITLE
Seismic Failure and Cask Drop Analyses of the Spent Fuel Pools at Two Representative Nuclear Power Plants

3. LEAVE BLANK

4. DATE REPORT COMPLETED
MONTH: June YEAR: 1988

5. AUTHOR(S)
P. G. Prassinos, C. Y. Kimura, D. B. McCallen, R. C. Murray, LLNL
M. K. Ravindra, R. D. Campbell, P. S. Hashimoto, A. M. Nafday, W. H. Tong, EQE Engineering

6. DATE REPORT ISSUED
MONTH: January YEAR: 1989

7. PERFORMING ORGANIZATION NAME AND MAILING ADDRESS (Include Zip Code)
Lawrence Livermore National Laboratory
7000 East Avenue
Livermore, CA 94550

Subcontractor:
EQE Engineering, Inc.
3150 Bristol, Suite 350
Costa Mesa, CA 92626

8. PROJECT/TASK/WORK UNIT NUMBER

9. FIN OR GRANT NUMBER
FIN A-0814

10. SPONSORING ORGANIZATION NAME AND MAILING ADDRESS (Include Zip Code)
Division of Safety Issue Resolution
Office of Nuclear Regulatory Research
U. S. Nuclear Regulatory Commission
Washington, D. C. 20555

11a. TYPE OF REPORT
Technical

b. PERIOD COVERED (Inclusive dates)

12. SUPPLEMENTARY NOTES

13. ABSTRACT (200 words or less)

This report discusses work done in support of the resolution of Generic Issue-82, "Beyond Design Basis Accidents in Spent Fuel Pools". Specifically the probability of spent fuel pool failure due to earthquakes was determined for the pools at the Vermont Yankee Nuclear Power Station (BWR) and the H. B. Robinson S. E. Plant, Unit 2 (PWR). The dominant failure mode for each pool was gross structural failure caused by seismic motion resulting in the loss of pool liner integrity. The resulting sudden loss of water was then assumed to lead to a self-propagating cladding failure and fission product inventory release from the spent fuel elements in the pool. The mean annual frequency of failure due to this failure mode was found to be 6.7E-06 at Vermont Yankee and 1.8E-06 at H. B. Robinson. Other earthquake induced failure modes studied but found to be less important were loss of pool cooling and make-up capability, fuel rack damage and loss of liner integrity due to a cask drop accident.

14. DOCUMENT ANALYSIS - a. KEYWORDS/DESCRIPTORS
Spent Fuel Pools, Generic Safety Issue, Probabilistic Risk Assessment, PWRs, BWRs Seismic Hazard, Fragility, Vermont Yankee Nuclear Power Station, H. B. Robinson S. E. Plant

b. IDENTIFIERS/OPEN-ENDED TERMS

15. AVAILABILITY STATEMENT
Unlimited

16. SECURITY CLASSIFICATION
(This page) Unclassified
(This report) Unclassified

17. NUMBER OF PAGES

18. PRICE

*U. S. GOVERNMENT PRINTING OFFICE:1989-241-590:80298

UNITED STATES
NUCLEAR REGULATORY COMMISSION
WASHINGTON, D.C. 20555

A75162-00002 2
BILL JONES
T4A9
WASHINGTON DC 20555